Chebyshev Spectral Method for Singular Moving Boundary Problems with Application to Finance

Thesis by

Andrei Greenberg

In Partial Fulfillment of the Requirements

for the Degree of

Doctor of Philosophy

California Institute of Technology

Pasadena, California

2003

(Defended September 4, 2002)

“ ‘Странно... – думает он, ероша волосы и краснея. – Как же она решается? Гм!.. Это задача на неопределённые уравнения, а вовсе не арифметическая...’

Учитель глядит в ответы и видит 75 и 63.

‘Гм!.. странно... <...> ’

– Решайте же! – говорит он Пете.

– Ну, чего думаешь? Задача-то ведь пустяковая! – говорит Удодов Пете. – Экий ты дурак, братец! Решите уж вы ему, Егор Алексеич!

Егор Алексеич берет в руки грифель и начинает решать. Он заикается, краснеет, бледнеет.

– Это задача, собственно говоря, алгебраическая, – говорит он. – Ее с иксом и игрэком решить можно. Впрочем, можно и так решить. Я вот разделил... понимаете? Теперь вот надо вычесть... понимаете? Или вот что... Решите мне эту задачу сами к завтраму... Подумайте...

<...>

– И без алгебры решить можно, – говорит Удодов, протягивая руку к счетам и вздыхая. – Вот, извольте видеть...

Он щелкает на счетах, и у него получается 75 и 63, что и нужно было.

– Вот-с... по-нашему, по-неученому. ”

А.П. Чехов, “Репетитор.”[1]

[1]“ ‘How queer!’ he thinks, ruffling his hair and flushing. ‘How should it be done? H'm – this is an indeterminate equation and not a sum in arithmetic at all –’ The tutor looks in the back of the book and finds that the answer is 75 and 63. ‘H'm – that's queer. <...> ’ ‘Come, do the sum!’ he says to Pete. ‘What's the matter with you? That's an easy problem!’ cries Udodoff to Peter. ‘What a goose you are, sonny! Do it for him, Mr. Ziboroff!’ Gregory takes the pencil and begins figuring. He hiccoughs and flushes and pales. ‘The fact is, this is an algebraical problem,’ he says. ‘It ought to be solved with x and y. But it can be done in this way, too. Very well, I divide this by this, do you understand? Now then, I subtract it from this, see? Or, no, let me tell you, suppose you do this sum yourself for to-morrow. Think it out alone!’ <...> ‘That sum can be done without the help of algebra,’ says Udodoff, sighing and reaching for the counting board. ‘Look here!’ He rattles the counting board for a moment, and produces the answer 75 and 63, which is correct. ‘That's how we ignorant folks do it.’ ” – Anton Chekhov, “The Tutor.” *Translated by Marian Fell. From* Russian Silhouettes: More Stories of Russian Life, *by Anton Tchekoff, New York: Charles Scribner's Sons, 1915.*

Acknowledgements

The completion of such strenuous a task as Ph.D. thesis research is impossible without adequate support, with which I was definitely blessed. First and foremost, I wish to thank my advisor, Professor Oscar Bruno, who managed to find the perfect balance between independence and supervision, trust and test, support and challenge, best suited for guiding me down this long road. Oscar could be – and was – a mentor, an authority, a colleague, or a friend, depending on what a particular situation demanded. The excellent working relationship that we have developed over the last four years is, in my opinion, something to be truly proud of.

There is another person, without whom this research would not have even started, let alone completed. It was Professor Peter Bossaerts who introduced me to finance, and pointed out the remarkable opportunities to be pursued by someone with a math background. I have learned a great deal from Peter's inspiring, open-minded, often critical presentations, both in class and in private conversations, of various challenges in the modern finance.

I would certainly like to thank Professor Dan Meiron and Dr.Niles Pierce for providing their comments and thus contributing towards shaping up this work, as well as for patiently putting up with more than a fair share of organizational "issues."

The whole environment of the Applied and Computational Mathematics option at Caltech deserves a special note of gratitude. I am privileged to have been part of such a brilliant, stimulating and fun group of people as this one, which has done a lot to foster my creative growth. I would like to specifically thank Professor Don Cohen, who has served as an invaluable source of support and positive criticism on numerous occasions; Dr.Alexei Novikov, whose discussions have benefited this work on many counts; all my co-inhabitants, of various times, in 210 Firestone: Mike Louie, Bogdan Craciun, Razvan Fetecau and Laurent Demanet, who helped create an atmosphere of friendly cooperation in the office; Sheila Shull, who is one of the most efficient, most helpful and, quite simply, nicest people I have

ever met; Chad Schmutzer, who has many a time saved my technologically challenged self from (computer) panic attacks; and many, many other colleagues at the Department, each of whom deserves lots of kind words. I would also like to mention my good friend and math Ph.D., Andrei Khodakovsky, from whose expertise in mathematical physics I was able to benefit on several important occasions.

I would also like to thank all the people – instructors, peers and friends, both from inside and outside of Applied Math, whom I have met at Caltech and who made my stay here a fruitful and enjoyable experience. Tom Hou, Uri Keich, John Pelesko, Leonid Kunyansky, Patrick Guidotti, McKay Hyde, Jason Kastner, Maya Tokman, Gang Hu, Danny Petrasek, Christiane Orcel, Shuki Bruck, Ulyana Dyudina, Serge Makarov, Vadym Kapinus, George Shapovalov and wife Kira, Alexei Dvoretskii, Rustem Shaikhutdinov, Konstantin Matveev and wife Anna, Anton Ivanov and wife Olga, Alexey Pankine, Eric Severin, Ricardo Hassan, Sergey Pekarsky, Anna Kashina, Dmitry Kossakovsky, Vincent Bohossian, Michael Ol, Yuri Solomatine – the list of the wonderful personalities I have come to know and personal friends I have made here could go on and on.

I would be amiss not to mention the place where I have discovered the world of both pure and applied mathematics; the school that gave me the education, taught me the culture and developed the skills for independent research in this area. I could truly appreciate all that I received as an undergraduate at the Mechanics and Mathematics department of the Moscow State University during my graduate studies at Caltech.

Finally, last but not least, I want to thank my family for their generous part in making me who I am, without whom I would not have had all that it takes to succeed. I wish to thank my grandparents, who saw me grow and believed in me; my in-laws, notably, my father-in-law, Boris Yakovlevich Lokshin, himself a top applied mathematician, whose advice and help I could always rely on; my elder brother Tony (Anton), my closest friend and always an inspiring example; my parents, Tatyana Borisovna Ilyina and Jacob (Yakov Haskelevich) Greenberg, whose love, support, comfort, advice, hearts and souls were with me, literally, each step of the way, and whose presence I always feel, despite the physical distance separating us; and of course, my dearest wife, Galina, who made some important sacrifices to follow me to a new place, bore the cross of a graduate student's wife with stoicism, took care of me, loved, endured and supported me through all ups and downs of our five years at Caltech. It is to her that this thesis is most affectionately dedicated.

Abstract

In the simulation of the inherently nonlinear processes involving moving boundaries, accurate solutions only result from use of sophisticated, high-quality numerical algorithms. Much work has been devoted to the design of such algorithms; unfortunately, the most general approaches in existence are usually not very accurate, while those that produce the most accurate results for restricted classes of problems are hard to generalize. In this work we attempt to bridge this gap by proposing a general method for the solution of parabolic moving boundary problems – a method which, in particular, can accurately treat the notoriously difficult Stefan-like problems with singular initial conditions.

Our method is based on a front-fixing change of variables, followed by the solution of the resulting nonlinear partial differential equation via expansion in Chebyshev series, with the use of an appropriate *convergent smooth approximations* in singular cases. This approach provides a unified framework for arbitrary parabolic operators. For problems with smooth initial data, our method is competitive with any available technique in both speed and accuracy. At the same time, our method is able to produce accurate numerical solutions in the most general setting, whenever existence theorems for moving boundary problems hold. We establish convergence of these numerical solutions to the true solution for a large class of possibly singular initial conditions.

In addition to the general method mentioned above, we also introduce a number of additional computational techniques, which enable us to improve the performance of the method for singular problems. These include derivative evaluations with Padé approximations; smoothing the problem via prior integration in time; and domain decomposition.

We demonstrate the performance of our method with a number of well-known regular and singular problems. We compare our solutions to those obtained by other methods and show that our algorithms generally produce significantly more accurate results. The additional techniques mentioned above, which we introduce for greater efficiency and which

do not use smoothing approximations, give rise to substantial gains in computing times and still produce reasonably accurate solutions.

In the last part of this work we present a systematic study of the mathematical finance problem of pricing American options on a dividend-paying asset from the point of view of partial differential equations. A symmetry result, which is obtained via a simple change of variables, allows us to reduce any American option problem to one of the two canonical cases, depending on the relation between the interest rate and the dividend yield. Each of these cases is equivalent to a singular Stefan problem, which can be solved by the methods introduced in this text. We present several model calculations, including the classical problem of an American put on a single stock, as well as more complicated examples, such as index options and foreign currency options, thus demonstrating the remarkable practical scope of the proposed approach.

Contents

List of Tables

List of Figures

Chapter 1

Introduction

The age of chivalry is gone. That of sophisters,
economists and calculators has succeeded.
(Edmund Burke, 1729–1797)

Boundary value problems are ubiquitous in applied mathematics. Physical quantities which depend on several variables and are studied within a certain region (e.g., the whole space or a body) are usually modelled as solutions of differential equations satisfying a set of boundary conditions. In most cases the contours of the region are known in advance and remain fixed throughout the solution process. However, there is a class of phenomena which require mathematical models allowing for domains whose boundaries are partially or completely unknown and must be determined as a part of the solution. Examples of such processes are ample in physics; the two best known of them probably are those relating to the simultaneous flow of two non-mixing fluids and melting or solidification of materials. In either case, an unknown quantity (the velocity profile in the former and the temperature in the latter) is studied on both sides of an interface (fluid-fluid and liquid-solid, respectively), which is not specified and needs to be found. Mathematically, this is usually expressed by a partial differential equation valid away from the interface plus boundary conditions on it. Since the boundary is unknown, one more boundary condition than would be necessary on a fixed domain, must be specified.

Problems involving unknown boundaries are thus inherently nonlinear, even for linear differential equations, and thus, distinctly complex – and interesting. In the literature, they are known by the name of free or moving boundary problems. We adopt the terminology of [27], where steady state problems on unspecified domains are called "free boundary," while the term "moving boundary" is associated with time-dependent settings, notably those governed by parabolic equations. The latter are the sole subject of this work, even though

the same ideas can be applied to elliptic and even hyperbolic problems. Throughout this work, we use the terms "moving boundary," "moving front," "interface," "moving end," etc., interchangeably, to refer to the unknown part of the boundary of the domain where the problem is posed.

Problems with moving boundaries have received much attention for both their wide practical relevance and the mathematical challenges they present. The original model, which was developed by J. Stefan in the late 1880s in his study of melting and freezing processes, can be expressed as follows

$$\begin{aligned} &u_t = \kappa u_{xx}, && 0 < x < s(t),\ t > 0 \\ &u(0,x) = 0, && s(0) = 0 \\ &u(t,0) = u_0, && u(t,s(t)) = 0 \\ &-\kappa u_x(t,s(t)) = \lambda \dot{s}(t) \end{aligned} \tag{1.0.1}$$

These equations describe the following physical configuration: initially at critical temperature $u = 0$, a slab of ice is subject to a positive temperature $u_0 > 0$ at its left end, causing it to melt. The function $s(t)$, then, represents the boundary of the region occupied by water (melting front). The last condition in this set of equations expresses the energy balance across the interface, taking into account the absorption of latent heat λ. This is what is known as the classical Stefan problem; it admits a simple similarity solution

$$u(t,x) = u_0 + A \operatorname{erf} \frac{x}{2\sqrt{\kappa t}}, \qquad s(t) = \alpha\sqrt{\kappa t}$$

where

$$A = -\frac{u_0}{\operatorname{erf}(\alpha/2)}$$

and α is determined from the transcendental equation

$$2\lambda\alpha\sqrt{\pi}e^{\alpha^2/4} \operatorname{erf}\left(\frac{\alpha}{2}\right) = u_0$$

The specific form of the conditions at the moving front depends on the problem, of course.

For example, the non-dimensional equations

$$\begin{aligned} &c_t = c_{xx} - 1, && 0 < x < s(t),\ t > 0 \\ &c(0,x) = \tfrac{1}{2}(1-x)^2, && s(0) = 1 \\ &c_x(t,0) = 0, && c(t,s(t)) = 0 \\ &c_x(t,s(t)) = 0 \end{aligned} \tag{1.0.2}$$

describe the evolution of the concentration of oxygen in an absorbing tissue, when its surface is sealed after a steady state is reached (see Section 6.2 for a more detailed discussion). The second condition at $x = s(t)$ is thus in a form of a no-flux constraint. Since no explicit expression for the dynamics of the moving boundary is given, problems of this type are often called implicit (or problems with prescribed flux), in contrast with those similar to (1.0.1), which are called Stefan problems (or Stefan-like problems, for more general settings). Note that the similarity approach can no longer give an exact solution for (1.0.2), even though a good approximation can be obtained (see p. 73 of this work).

In fact, any generalization from the simplest setting (e.g., to account for non-constant conductivity, introduction of reaction terms, time-dependent boundary condition at the fixed end, etc.) invalidates the similarity argument, and solutions should therefore be obtained by alternative means. Starting from the 1950s, a number of related models for various physical phenomena were constructed, and a number of methods for solution of general Stefan problems were proposed. With the increased availability of digital computers a focus on numerical solution of moving-boundary problems developed, and the research area centered around Stefan problems grew from a narrow confine concerned with a handful of simple mathematical models for freezing and melting to a wide field dealing with moving boundaries for general parabolic equations, with a variety of applications in many areas of science and technology. Melting and solidification of materials, crystal growth, optimal stopping of Markov processes, absorption of oxygen by biological tissue, valuation of American-style derivative securities in finance – all of these problems, taken from different branches of science, are characterized by these common features. In each case, a parabolic partial differential equation (reaction-diffusion for the physical problems and backward Kolmogorov for the stochastic ones) governs the dynamics in a time-dependent domain, whose boundary is unknown and needs to be determined as part of the solution.

The mathematical apparatus has accordingly become increasingly sophisticated over the years. To establish important theoretical results on existence, uniqueness and global behavior of solutions, the concept of weak, or generalized solutions, was introduced. As in the case of hyperbolic problems with shocks, numerical schemes converging to the weak solutions were designed. As the models became more general and complex, the bulk of practical results could only be obtained numerically. Clearly, a good numerical method able to deal accurately with problems arising from such a broad set of applications is highly desirable, especially if it is sufficiently general and flexible to accommodate the variety of possible input data, without significant change in its structure. In addition to competitive results for well-behaved problems, a good numerical method should provide direct generalizations to more challenging cases, retaining as much of its performance as possible.

Our approach, which combines a front-fixing coordinate transformation, a Chebyshev spectral method for the spatial part of parabolic operators, and a scheme for resolution of singular initial data, was designed with these concerns in mind. Firstly, due to the excellent convergence properties of spectral approximations, this method produces highly accurate numerical solutions for both the function and the interface for simple parabolic operators and smooth initial conditions. Since, as it is known, solutions of Stefan problems are smooth for positive time, the method we propose is highly competitive in terms of both speed and accuracy. Secondly, the method is flexible enough to admit straightforward generalizations to problems with piecewise smooth or otherwise singular initial conditions. The basic approach to singular problems is based on constructing certain smooth approximations of the initial data, so that the corresponding numerical solutions converge to the true solution of the singular problem as the initial approximation tends to the singular initial data. The smoothing effect of diffusion helps control the error at positive time. As we shall see, the performance of the method remains very competitive, and the accuracy is still high, even for singular problems, compared to such methods, as the integral equation approach, which were designed to overcome the effect of initial singularities. At the same time, the added complexity, with respect to the smooth cases, is reasonable. Techniques such as domain decomposition, which can be incorporated easily, lead to better resolution of more localized problems. The main importance of the approach proposed here is that, unlike all other methods available thus far, it remains purely numerical, in the sense that no knowledge of the solution is required beyond $t = 0$, i.e., no procedure (such as small-time asymptotic

solution) needs to be used to start off the computation.

We also present several alternative procedures which use the singular initial data directly and involve Padé approximations and prior integration. These techniques can often produce solutions that, while not as accurate as those obtained with our main approach, still yield very acceptable accuracies with significantly improved computing times. For example, for the oxygen diffusion problem (1.0.2), use of Padé approximation allows to carry out the computation with 5 significant digits in a quarter of the time needed to obtain 8 digits by the general method. Prior integration allows to further reduce computation time up to an additional factor of three, with at least 6 significant digits in the numerical solution. Thus, it is possible to find amongst the various methods proposed the appropriate balance of speed and accuracy for a given application.

The rest of this text is organized as follows. In Chapter 2, we provide a survey of various numerical methods which have been proposed over the years for the solution of moving boundary problems. An effort is made to point out the strengths and weaknesses of each approach; we also give a brief comparison of their performance for a classical test problem. The detailed formulation of our numerical method is given in Chapter 3. In particular, in Sections 3.1 and 3.3, we discuss front-fixing transformations and Chebyshev expansions, while in Section 3.4 we introduce the method of smooth approximations. The convergence result, which provides a bound for the maximum absolute error of the numerical solution produced by a smooth approximation and the *quadratic* convergence rate, is proved in Chapter 4 for the fixed boundary case, in anticipation of the same behavior in the moving boundary setting. In Chapter 5, we present two additional techniques, which, for certain singular problems, yield reasonably accurate solutions in short computing times. A variety of numerical examples is presented in Chapter 6, including results for simple smooth Stefan problems and for the classical oxygen diffusion problem.

Finally, Chapter 7 is devoted to the pricing of American options on a dividend-paying asset. After a review of the finance background given in Section 7.1, we present a mathematical formulation of the American option pricing as a moving boundary problem for a degenerate parabolic equation with singular initial data. In Section 7.3, we provide a simple derivation of an important symmetry result between the two kinds of American options. This result allows for reduction of the valuation problem for any American option on dividend-paying stock to one of the two canonical forms, depending on the relative magnitude of the interest

rate and the dividend yield. Both of these forms are amenable to numerical treatment by our method; results and comparisons with available small-time asymptotics are given in Sections 7.4 and 7.5. In the former, an additional singularity, due to the infinite initial velocity of the moving boundary, is fixed by a simple change of time scale, a technique which greatly facilitates numerical analysis of any similar problem. In Section 7.6, we apply our construction to some of the more complicated finance settings, describing index options and foreign currency options. Finally, concluding remarks and future research problems are presented in Chapter 8.

Chapter 2

Numerical Methods for Moving Boundary Problems

A science is any discipline in which the fool
of this generation can go beyond the point
reached by the genius of the last generation.
(Max Gluckman, 1911–1975)

Over the years, a number of methods for solving moving boundary problems were proposed, and several monographs have been published [4, 27, 39, 69, 85, 101]. The number of scientific papers devoted to this subject has been growing steadily in the past two decades, and the most comprehensive bibliography available [95] includes over 5,800 titles. A detailed comparative analysis of a material of this volume could thus warrant a study of its own. In this chapter we present merely a review of the available methods for solution of Stefan-type problems, with an attempt to explain their respective strengths and weaknesses. Throughout the discourse, we refer to the previously published surveys, notably, John Crank's book [27], from which we borrow most of the classification and terminology.

2.1 Historical remarks

The prototype parabolic moving boundary problem is the process of freezing or melting of a homogeneous medium, such as water (or ice), when subject to cooling or heating, respectively. The evolution of temperature in the medium obeys the heat equation, and the change of phase introduces a moving front, defined as the surface at which the freezing (or melting) occurs. According to [85], the earliest study in this area was conducted by Gabriel Lamé and Emile Clapeyron in 1831 [61]. They investigated the thickness of the crust forming as a result of freezing of a liquid held at crystallization temperature. The

fact that this thickness is proportional to the square root of time was established in this work, even though the constant of proportionality was not specified. The first mention of a similarity solution to a simple ice-melting problem appeared in the 1860s in the lectures given by Franz Neumann at Königsberg.

In his works on freezing of the ground [93] and melting of ice [94], published in 1889, Jozef Stefan formulated a mathematical model for a general class of phase-change phenomena. The corresponding moving boundary problems have inherited his name and are now known as one-phase and two-phase Stefan problems. In the one-phase setting, the liquid, held at a positive temperature, initially occupies the right half-space and is subject to a negative temperature front at the left end, causing crystallization. In [93] the sub-zero temperature was held constant, while in [94] it was a function of time, and the initial temperature of water was 0° C, i.e., the freezing point. In the two-phase setting, in addition to the mentioned conditions on water, the left half-space is occupied by ice held at a constant negative temperature. In both cases, freezing (or melting) is assumed to occur at a constant temperature and is accompanied by the release (or absorption) of *latent heat*. The key heat balance condition across the phase-change boundary $x = s(t)$, also due to Stefan, is

$$\lambda\rho\,\frac{ds}{dt} = -\kappa\,\frac{\partial T}{\partial x}\bigg|_{x=s(t)} \tag{2.1.1}$$

in the one-phase case and

$$\lambda\rho\,\frac{ds}{dt} = \left(\kappa_1\,\frac{\partial T_1}{\partial x} - \kappa_2\,\frac{\partial T_2}{\partial x}\right)\bigg|_{x=s(t)}$$

in the two-phase case. In the equations above, $T(t,x)$ is the temperature; λ is the specific latent heat; ρ is the density; and κ, the conductivity of the material. In the two-phase case, the index "1" corresponds to the solid and the index "2," to the liquid.

The first local existence and uniqueness result for solutions of one-dimensional Stefan problems with general initial conditions and boundary shapes was proved by Lev Rubinshtein in 1947. In his monograph [85], Rubinshtein also proved global existence in time of the classical solution to this problem, as long as the moving boundary is analytic. A more general result for two-phase problems appeared in [64]. See also references in [69].

The concept of a generalized, or weak solution of a multidimensional Stefan problem

for a possibly nonlinear parabolic partial differential equation with an arbitrary number of phases, was introduced by Svetlana Kamenomostskaja and Olga Oleinik based on the enthalpy formulation (see the discussion of the enthalpy method below). Existence and uniqueness of weak solutions of a heat conduction equation with H^1 initial data were proved in [54] by finite differences. It was also established that any classical solution, if it exists, is a generalized solution of the Stefan problem. In [81], a similar result was established for arbitrary quasi-linear parabolic equations. The same structure was later defined for problems with zero latent heat by Anna Crowley in [32]. An alternative approach to the definition of weak solutions, using variational inequalities, was pursued in the works of Georges Duvaut, David Kinderlehrer, Avner Friedman and others (see [38, 39, 44] and references therein). For example, the smoothness of the moving boundary for the one- and two-phase Stefan problems in several space dimensions was proved using variational inequalities. For a two-phase multidimesional Stefan problem, existence of the classical solution in the small was proved by Anvarbek Meirmanov, by introducing von Mises variables [69].

In practice solution of Stefan problems has relied on numerical methods ever since more complicated models than those of melting of ice slabs were formulated. Several techniques were introduced in the late 1950s, including the enthalpy method (E.L. Albasiny, 1956), front-fixing and finite differences (J. Crank, 1957), and variable grids (J. Douglas and T.M. Gallie, 1955). Since then, a variety of other numerical methods was developed, with modifications and new ideas still appearing. In general, each of the methods falls into one of the following categories: front-tracking (e.g., finite differences on fixed or variable grid, method of lines, level set method), fixed-domain (such as the enthalpy method and variational inequalities), front-fixing (via coordinate transformations or change of dependent variable), or reduction to integral equations. Each of these approaches, naturally, has its own advantages and disadvantages, making it more suitable for certain types of problems and less suitable for others. Obviously, the choice of a particular numerical method is determined by the nature of the problems studied and by the ultimate goal of the analysis (e.g., quick qualitative estimation, without much regard to accuracy; accurate resolution of the moving boundary, but not necessarily of the function; a unified framework for the most general settings; etc.). We thus proceed to analyze these approaches in more detail.

2.2 Fixed-domain methods

The idea behind this class of methods is to use the given partial differential equations on each side of the moving boundary, as well as the boundary conditions, to write down a new problem, which is valid in the whole domain. In the enthalpy method, this is done by introducing a new dependent variable, while in the variational inequality approach, the partial differential equation is used to express the solution as a minimizer of a certain nonlinear operator. The moving boundary, in a sense, disappears from the immediate formulation and is determined in such a way that the corresponding conditions are satisfied. This approach is attractive in that it is independent of the actual behavior of the moving front, which, in some cases, may not vary smoothly, have sharp peaks or even collapse. Besides, the fact that the computational domain remains fixed at all times is an additional advantage. Fixed-domain methods are very general, and their formulation does not change qualitatively in several space dimensions. The main disadvantage of these methods is the poor resolution of the moving boundary, since it is determined *a posteriori* from the numerical approximation of the unknown function. Nevertheless both the enthalpy method and the variational inequality approach are extremely popular for various moving boundary problems.

2.2.1 Enthalpy method

The enthalpy method offers a unified framework for the solution of moving boundary problems for quasi-linear parabolic partial differential equations, valid for any number of space dimensions and an arbitrary number of phases. Let us illustrate the enthalpy formulation for a two-phase Stefan problem for a generalized heat conduction equation in three dimensions, following [54]. Let $T_i(x,y,z,t)$ be the temperature; ρ_i, the density; c_i, the specific heat; and κ_i, the conductivity of phase i, $i=1,2$, where the last three quantities can, in general, depend on T. Furthermore let λ be the latent heat of phase change, and assume that the phase transition occurs at a constant temperature $T=T_0$ across the surface $\Phi(x,y,z,t)$. Then the problem can be described by the following set of equations

$$\rho_i c_i \frac{\partial T_i}{\partial t} = \nabla\cdot\big(\kappa_i \nabla T_i\big), \quad i=1,2 \tag{2.2.1}$$

$$T_1\big(\Phi(x,y,z,t)\big) = T_2\big(\Phi(x,y,z,t)\big) = T_0,$$

$$\big[\kappa_2\nabla T_2 - \kappa_1 \nabla T_1\big]\cdot\nabla\Phi + \lambda\frac{\partial\Phi}{\partial t} = 0 \tag{2.2.2}$$

The last two expressions are evaluated at the moving surface, and (2.2.2) can also be written in the form

$$\kappa_2 \frac{\partial T_2}{\partial n} - \kappa_1 \frac{\partial T_1}{\partial n} = -\lambda\, v_n$$

where n is the normal to the surface $\Phi(x, y, z, t)$, and v_n is its normal velocity. We first set

$$u(T) = \int_0^T \kappa(\xi)\, d\xi \tag{2.2.3}$$

so that $\nabla u = \kappa \nabla T$, and therefore (2.2.1) implies

$$C_i(u) \frac{\partial u_i}{\partial t} = \Delta u_i, \quad i = 1, 2$$

with $C = \rho(T)c(T)/\kappa(T)$, and (2.2.2) assumes the form

$$\big[\nabla u_2 - \nabla u_1\big] \cdot \nabla \Phi + \lambda \frac{\partial \Phi}{\partial t} = 0$$

Then we define the enthalpy function $H(u) = H(u(T))$ to satisfy the following properties [54]

- for $u < u_0 = u(T_0)$ and $u > u_0$, i.e., in each of the phases, $H(u)$ is a continuously differentiable function, satisfying $H'(u) = C(u)$;
- the right and left limits of H as $u \to u_0$ exist, and the jump (across the interface) is $H(u_0^+) - H(u_0^-) = \lambda$;
- at $u = u_0$, H may assume any value between $H(u_0^-)$ and $H(u_0^+)$.

It can be shown that $H(u)$ exists and is a monotone increasing function. Since, obviously

$$H(u(T)) = \begin{cases} \displaystyle\int_0^T \rho(\theta)c(\theta)\, d\theta, & T < T_0 \\ \displaystyle\int_0^T \rho(\theta)c(\theta)\, d\theta + \lambda, & T > T_0 \end{cases}$$

it follows that $H(u(T))$ incorporates the heat jump across the phase-change front due to the release (or absorption) of the latent heat, and therefore $H(u(T))$ is indeed the total heat,

or the enthalpy, as it is called in thermodynamics. But we now have

$$\frac{\partial H(u)}{\partial t} = \Delta u \tag{2.2.4}$$

and the boundary conditions at the interface are already incorporated in this formulation. Since $H(u)$ is monotone, we can reconstruct u from H at every time step, and determine the position of the moving boundary as the u_0 level set of $u\big(T(t,x,y,z)\big)$. Thus, as long as the boundary conditions on the fixed domain are provided, and the initial enthalpy is chosen, the Cauchy problem for (2.2.4) can be solved by any one of the known numerical methods for parabolic partial differential equations.

In [54], finite-difference discretization was used to prove existence and uniqueness of the generalized solution to the Stefan problem (2.2.1-2.2.2). A generic scheme, based on the ADI (alternating directions – implicit) method, for the discretization and numerical solution of the enthalpy formulation in several space dimensions was given in [76]. The authors represented the jump in the enthalpy as λ times the Heavyside's function, centered at the melting temperature. This introduced a δ-function into the equation for $\partial H/\partial t$, which was smoothed by a δ-like approximation. In [6], an explicit in time finite-difference scheme was used directly on the equation (2.2.4) in a one-dimensional setting. When applied to a welding problem, where phase change does not occur at a fixed temperature and a so-called "mushy region" exists, the numerical scheme [6] also produced meaningful results. The generalized enthalpy function, for the cases of zero conductivity or specific heat, was introduced in [32], where the appropriate uniqueness results of [81] were extended. In [45] the generalized enthalpy method was used to compute the solution of the oxygen diffusion problem, which we describe in Section 6.2; it corresponds to the case of zero latent heat and zero specific heat in one of the phases.

The main disadvantage of the enthalpy method is in the way it determines the position of the moving boundary. The T_0 level set of temperature can be found by inspection and bracketed between two mesh points. More accurate resolution of the moving boundary can present problems and leads to oscillatory behavior in the temperature front. This was pointed out in [98], where a method of overcoming this difficulty was proposed, based on a novel interpretation of the enthalpy, allowing to place the moving front at a particular grid point when the enthalpy function satisfies a certain relation.

Due to its simplicity and generality, the enthalpy method and its modifications (such as a hybrid with the method of lines, suggested in [90]) are one of the most popular techniques of solving phase-change problems [4].

2.2.2 Variational inequalities

Parabolic variational inequalities [38] present another way of formulating moving boundary problems on a fixed domain, with the interface conditions satisfied implicitly. This approach is especially powerful for one-phase problems with both the value and the flux prescribed at the moving end. (This corresponds to the zero latent heat in the melting and freezing formulations.) In this case, the unknown function can be continuously extended across the moving boundary, and the resulting function on the whole domain can be shown to satisfy, under certain conditions, an inequality of differential or variational nature. The original moving boundary problem is then reduced to a constrained minimization problem on a fixed domain, with a number of algorithms for solution available.

Consider the following multidimesional moving boundary problem [27, Section 6.4]

$$\begin{aligned} & u_t - \Delta u = f && \text{in } \Omega_1 \\ & u = u_n = 0 && \text{on } S(t) \\ & u = g \geq 0 && \text{on } \Gamma_1 = \partial\Omega_1 \backslash S(t) \\ & u\Big|_{t=0} = u_0 \geq 0 \end{aligned}$$

Here Ω_1 is the domain where the partial differential equation is valid; Γ_1 is the fixed part of the boundary of this domain and $S(t)$ is the moving part; and both the function and its flux ($\sim u_n$, the normal derivative) vanish at the moving end. We can then introduce the domain $\Omega = \Omega_1 \cup \Omega_0$, such that Ω_0 has a common moving boundary $S(t)$ with Ω_1, and we define $u \equiv 0$ on $\bar{\Omega}_0$ (i.e., $u = 0$ in Ω_0 and $u = 0$ on $\Gamma_0 = \partial\Omega_0 \backslash S(t)$). Then, by virtue of the conditions at $S(t)$, u is defined continuously on the whole domain Ω, which has fixed boundaries. If compatibility conditions hold for the boundary value g $\big($i.e., g, $\nabla g \to 0$ as $x \to S(t)\big)$, then $u \in C^1(\bar{\Omega})$. Define the positive definite operator

$$a(v, w) = \int_{\Omega} \nabla v \cdot \nabla w \, dx$$

as well as the usual scalar product

$$\langle v, w \rangle = \int_\Omega vw \, dx$$

Then for any test function $v \in H^1(\Omega)$, such that $v \geq 0$, $v = g$ on Γ_1 and $v = 0$ on Γ_0, we have

$$\begin{aligned}\langle u_t, v-u \rangle + a(u, v-u) &= \int_{\Omega_1} u_t(v-u)\, dx + \int_{\Omega_1} \nabla u \cdot \nabla(v-u)\, dx \\ &= \int_{\Omega_1} (u_t - \Delta u)(v-u)\, dx = \int_{\Omega_1} f(v-u)\, dx \geq \int_\Omega f(v-u)\, dx\end{aligned}$$

In the above, we used the fact that $u = 0$ in $\Omega \backslash \Omega_1$, and integrated by parts, bearing in mind that $v - u = 0$ on $\partial\Omega_1$. Thus the original moving boundary problem is equivalent to the inequality

$$\langle u_t, v-u \rangle + a(u, v-u) \geq \langle f, v-u \rangle$$

on the fixed domain Ω. Existence and uniqueness of solutions to variational inequalities of this type can be proved (cf. [39] and references therein), and numerical solutions can be obtained, e.g., using the finite element method.

It is also possible to obtain a differential inequality, or complementarity formulation, rather than a variational one. For example, the oxygen diffusion problem (1.0.2) can be written as

$$\begin{aligned} &c_t - c_{xx} + 1 \geq 0, \qquad c \geq 0 \\ &(c_t - c_{xx} + 1)c = 0 \quad \text{on } 0 \leq x \leq 1\end{aligned}$$

since $c(t, x) \geq 0$ represents the concentration of oxygen, which is 0 to the right of the moving boundary, so $c_t - c_{xx} + 1 = 1 \geq 0$ there, while one of the terms in the product vanishes at any point of the interval $(0, 1)$. The discretized version can be reduced to a quadratic programming problem, which can be solved by various methods, such as generalized successive over-relaxation (SOR) [33]. It can be shown that the finite element discretization of the corresponding variational inequality formulation leads to the same constrained minimization problem, when both are written in matrix form.

A variety of moving boundary problems with prescribed flux was treated by variational

inequalities. A number of examples can be found in [39], including a fast algorithm for solving the oxygen diffusion problem. Recently, several authors [53, 99] applied this approach to valuation of American options, the problem we consider in detail in Chapter 7. Using variational inequalities, the convergence of numerical solutions and important regularity results were established [53].

Since continuity of the solutions across the moving boundary is essential for the variational inequality approach, it is not immediately applicable to melting and freezing problems, where the nonzero latent heat causes a jump in the normal derivative. However, the following transformation

$$w(t,x) = \begin{cases} \int_{l(x)}^{t} u(\tau,x),\, d\tau, & 0 \le x \le s(t); \\ 0, & s(t) \le x \le 1 \end{cases}$$

introduced by G. Duvaut, has the effect of moving the latent heat from the boundary condition to the source term, making the new function continuous. Here $t = l(x)$ has the meaning of the time when phase change occurs at the point x.

As in any fixed domain method, the determination of the position of the moving boundary in the variational inequality setting is done by finding a particular level set of the numerical solution. In some methods, such as the projected SOR, this can be done within the main computation loop, as it is demonstrated in [99] for the American option problem, and not *a posteriori,* as in the enthalpy method.

2.2.3 Truncation method

We briefly mention the method introduced in [9] for the oxygen diffusion problem. The idea is to embed the solution of a moving boundary problem for a linear partial differential equation into a family of solutions of nonlinear equations on a fixed domain (hence the placement of this approach with fixed domain methods). In [9], the nonlinear problem was

$$\begin{aligned} &c_t = c_{xx} - g(c), && 0 < x < 1, \quad 0 < t < T \\ &\lim_{t\to 0} c(t,x) = f(x), && 0 < x < 1 \\ &c_x(t,0) = c(t,1) = 0 && \text{or } c_x(t,0) = c_x(t,1) = 0 \end{aligned}$$

Here $g(c)$ is the nonlinear source term

$$g(c) = g_\varepsilon(c) = \begin{cases} c/\varepsilon, & 0 \le c \le \varepsilon \\ 1, & \varepsilon \le c \end{cases}$$

The oxygen diffusion problem (1.0.2) corresponds to

$$g(c) = \begin{cases} 0, & c = 0 \\ 1, & c > 0 \end{cases}$$

and $f(x) = (1-x)^2/2$, with $c(t,x) \ge 0$ for all t. The last constraint forces to take prohibitively small time steps in any numerical method for the problem on a fixed domain, such as finite differences or finite elements. The truncation method overcomes this restriction by using larger time steps and enforcing $c = 0$ at all grid points, where the calculations gave $c < 0$, at each step. Thus a concentration profile is obtained, with the boundary of the region $c > 0$ tracing the shape of the moving interface, whose position is thus bracketed between two grid points. The convergence of the algorithm was established in [9]; and extensions to higher space dimensions were studied.

Summary

Fixed-domain methods thus present a good general framework for treating moving boundary problems, including multidimesional ones, without explicitly getting involved in the nonlinear boundary conditions. They are also very powerful tools for defining weak solutions and proving existence and uniqueness results for them. It is worth noting that the enthalpy method works well for problems with nonzero latent heat and is not directly applicable to the cases when it vanishes, while the exact reverse is true for the variational inequality approach. Thus these methods are good complements of each other, so that one can always find a suitable fixed-domain method for a given problem.

The main drawback of fixed-domain methods, in a sense, stems from their main advantage. Since the explicit mention of the moving front is excluded from the formulation, accurate determination of its position is prone to inaccuracies. Thus for problems, where tracking of a sharp interface is essential, these methods may not be the first choice.

2.3 Front-tracking and front-capturing methods

This group of approaches is characterized by the explicit calculation of the position of the moving interface at each time step. The name "front-capturing" is usually attributed to those techniques in which the computational grid is fixed. The earliest numerical methods for solving moving boundary problems were mostly of this type. Regular finite differences were used to update the solution away from the interface, and the formulas were appropriately modified near the moving end, to accommodate uneven spacing, since the position of the interface at every time step is, in general, not located at a grid point. In contrast, "front-tracking" methods are set up on a variable grid, which is constructed in such a way that, at each time step, the moving boundary coincides with one of the nodes. This can be achieved by modifying the spatial or temporal part of the grid, or the whole grid altogether, as in the adaptive space-time finite element technique [13, 14]. More recently, front-capturing methods for Stefan problems received a boost, when the level set method of S. Osher and J. Sethian was applied to crystal growth problems [22, 89]. In this section we also mention the method of lines, which is based on discretizing the original problem in time only and solving a sequence of boundary-value problems for ordinary differential equations at every time step. Fast algorithms proposed by G. Meyer [71] made this approach very attractive for one-dimensional moving boundary problems.

2.3.1 Fixed grids: front-capturing

Front-capturing on a fixed finite-difference grid is a simple extension of this fundamental numerical technique for partial differential equations to include problems with moving boundaries. In most of the computational domain, the conventional formulas can be used to update the solution at each time step. At every t, the moving boundary $s(t)$ is situated between two grid points, $i\Delta x$ and $(i+1)\Delta x$, say, so that $s_n = (i+p_n)\Delta x$, where $0 \leq p_n \leq 1$ and is, in general, different for each time step. Obviously, direct use of the update formulas, as well as the boundary conditions at the moving end, is not possible. However, the solution can be interpolated, using, for example, its values at the three points, $(i-1)\Delta x$, $i\Delta x$, and $(i+p_n)\Delta x$, and its first and second derivatives can be calculated and the solution advanced one more step in time. The moving boundary position, i.e., p_n, is updated using the formula for the velocity, which involves derivatives at the moving end, computable through inter-

polation as well. If p_{n+1} becomes less than 0 or larger than 1, this is simply an indication of the fact that the interface has moved away from the given computational cell to one of the neighboring ones, so the same idea can be applied over again. This approach was used in [29] to solve the oxygen diffusion problem (1.0.2). The expression for the derivative of $s(t)$, involving the third derivative of the solution at the moving end, was first derived in that paper. The same approach was employed in [63] for two- and three-dimensional Stefan problems. The drawback of this method is, mainly, the increased complication near the moving boundary, which is aggravated whenever implicit time stepping is used.

An alternative approach, used in [77], is to introduce fictitious values of the solution obtained by extrapolation and to use the standard finite-difference formulas throughout the whole computational domain. For two-phase problems, extrapolations are carried out for both the solid and the liquid region. Taylor expansions are used to compute u_x at the moving boundary, which is needed to update the position of the latter. Even though this approach appears to differ from the one described above, the actual formulas have the same form.

The idea of the level set method is to construct a function which is always zero at the moving interface. The evolution of this function is governed by a Hamilton-Jacobi-type equation, which can be solved numerically using various techniques developed in computational fluid dynamics. Once the new position of the moving boundary is established, the solution can be updated with a simple finite-difference scheme, with one-sided differences to be used in the vicinity of the interface. In [22] this approach was applied to several moving boundary problems from crystal growth. The signed distance from the interface was used to keep track of it, as it is the most trivial example of a function, whose zero level set coincides with interface. This also helped switch to the one-sided differences in the temperature calculations at the right place, as the value of this function tells how close the interface is. In [89] the level set approach was used to advance the moving boundary only, while the temperature was computed using an integral equation (see also Section 2.5 below). The level set method is well known for its generality and ability to follow singularities and topological changes in the interface. It is also one of the primary choices for higher space dimensions, since few additional complications arise. However, this method is only first order near the moving boundary, so it is usually not appropriate when accuracy is the main goal.

2.3.2 Variable grid: front-tracking

The abovementioned increased complexity and loss of accuracy near the moving boundary, exhibited by the fixed-grid methods, encouraged the advent of variable grids. The first study in this direction appeared in [37]. The idea was to modify the time step in such a way that the moving boundary would always be located at a grid point. Suppose a simple Stefan problem for the heat equation $u_t - u_{xx} = 0$ is considered, with the velocity of the moving boundary satisfying

$$\frac{ds}{dt} = -\frac{\partial u}{\partial x}$$

and with $u = 0$ on $x = s(t)$. Then the following expression for $s(t)$

$$s(t) = t - \int_0^{s(t)} u(t, x)\, dx$$

can be derived from the above equations, if appropriate boundary conditions at the fixed end hold. Discretization of this equation gives

$$\Delta t_n = \left(n + 1 + \sum_{i=1}^{n} u_{i,n}\right) \Delta x - t_n \tag{2.3.1}$$

which is the new time step size, such that the rightmost grid point coincides with the position of the moving interface at $t_{n+1} = \sum_{k=0}^{n} \Delta t_k$. If the finite difference scheme to solve the heat equation is implicit, the discretization (2.3.1) can also be made implicit (by taking $u_{i,n+1}$ instead of $u_{i,n}$), and the desired time step size can be computed iteratively. This approach was applied in [50] to the oxygen diffusion problem, except instead of integrating the expression for the velocity of the moving boundary, the authors used the finite difference form of the original boundary condition. The so-called explicit variable time step method (see [101] and references therein) is a variation of this technique, where several "virtual" substeps are taken per each time step to ensure stability of the scheme and the desired level of accuracy. This mechanism uses both storage and time step size very efficiently, reducing the computation time and allowing to start calculations from $t = 0$ even for singular problems.

An equally logical idea is to keep the time step constant, but to modify the spatial grid with time. In [77], the number of points in the interval $[0, s(t)]$ was held fixed. Thus the

solution was updated along the curvilinear grid lines $x_i(t) = i\Delta x(t)$, with

$$\frac{dx_i}{dt} = \frac{x_i}{s(t)} \frac{ds}{dt}$$

The partial differential equation on this grid had to be modified as well. This approach resembles the front-fixing technique, which we discuss in Section 2.4 below. In [30] a variable-in-space stencil was used to solve the oxygen diffusion problem. Unlike the previous method, here the whole grid moved with the speed of the interface each time step, and the values of the solution at the new grid points were computed using cubic spline or polynomial interpolation.

Space-time finite elements, in a sense, represent a combination of the previous two approaches, since the computational stencil is deformed in both variables at the same time. In [13], a space grid adapted at each time step was used to construct quadrilateral finite elements in the (t, x) space. Then the weak integral formulation of the moving boundary problem was solved in this domain. This idea was later used by the authors for two-dimensional Stefan problems, and the convergence of the method was proved. In [14] the approach was further extended to enable independent partitioning of each strip $t_n < t \leq t_{n+1}$ into biquadratic finite elements. This can be very important when singularities are present in the initial data or when the initial speed of the moving boundary is infinite. The stability and 3rd order convergence of the numerical method produced by this approach was proved in [14] as well. In [74] a finite difference time discretization was coupled with an adaptive finite-element mesh in space to solve the oxygen diffusion problem, with a possibility of extending the method to higher space dimensions.

2.3.3 Method of lines

The method of straight lines, in which a partial differential equation is replaced by a sequence of ordinary differential equations at discrete time levels, is a well-established method, both for theoretical estimates and numerical solutions of boundary-value problems, including

those with moving boundaries. Consider the following general formulation (cf. [71])

$$\begin{aligned}\frac{\partial u}{\partial t} = \frac{\partial}{\partial x}\left(\kappa(t,x)\,\frac{\partial u}{\partial x}\right) + a(t,x)\,\frac{\partial u}{\partial x} + b(t,x)u + f(t,x), \quad 0 < x < s(t)\\ u(0,x) = u_0(x), \qquad \beta_1(t)u(0,t) + \beta_2(t)u_x(0,t) = \beta(t)\\ G\big(t, u(t,s(t)), u_x(t,s(t)), u_t(t,s(t)), s(t), \dot{s}(t)\big) = 0\end{aligned}$$

where $G = (G_1, G_2)^T$ is the vector of boundary conditions at the moving end. For example, for the Stefan problem,

$$G = \begin{pmatrix} u(t,s(t)) \\ \lambda\rho\dot{s}(t) + \kappa u_x(t,s(t)) \end{pmatrix}$$

The method of lines approximation is

$$\begin{aligned}\big(\kappa(t_n,x)u_n'\big)' + a(t_n,x)u_n' + b(t_n,x)u_n - \frac{u_n - u_{n-1}}{\Delta t} + f(t_n,x) = 0 \qquad (2.3.2)\\ \beta_1(t_n)u(0) + \beta_2(t_n)u_n'(0) = \beta(t_n)\\ G\Big(t_n, u_n(s_n), u_n'(s_n), \frac{u_n(s_n) - u_{n-1}(s_n)}{\Delta t}, s_n, \frac{s_n - s_{n-1}}{\Delta t}\Big) = 0\end{aligned}$$

where $t_n = n\Delta t$, $u_n = u(t_n,x)$, $u_n' = u_x(t_n,x)$, and $s_n = s(t_n)$, $n = 1,\dots,N$. The obtained system can be solved by different means, depending on the specific form of the parabolic operator. G. Meyer proposed the invariant embedding technique, which is an efficient method for linear parabolic operators and can be extended to the nonlinear ones as well. For each n, equation (2.3.2) can be rewritten as a first-order system by letting

$$v_n = \kappa(t_n,x)u_n'$$

The solution $\{u_n(x),\, v_n(x)\}$, with the boundary conditions

$$\begin{aligned}\beta_2(t_n)v_n(0) = \big[\beta(t_n) - \beta_1(t_n)u_n(0)\big]\kappa(0,t_n)\\ G\Big(t_n, u_n(s_n), \frac{v_n(s_n)}{\kappa(t_n,s_n)}, \frac{u_n(s_n) - u_{n-1}(s_n)}{\Delta t}, s_n, \frac{s_n - s_{n-1}}{\Delta t}\Big) = 0 \qquad (2.3.3)\end{aligned}$$

is embedded into the family of solutions of the same system, but with the boundary conditions

$$\begin{aligned}\beta_2(t_n)v_n(0) = \big[\beta(t_n) - \beta_1(t_n)r\big]\kappa(0,t_n)\\ u_n(0) = r\end{aligned}$$

depending on the parameter r. The Riccati transformation

$$v_n(x,r) = R_n(x)u_n(x,r) + z_n(x)$$

is introduced, so that R_n and z_n solve two coupled initial value problems

$$R_n' = \frac{c(t_n,x)}{\Delta t} - b(t_n,x) - \frac{a(t_n,x)}{\kappa(t_n,x)}\,R_n - \frac{1}{\kappa(t_n,x)}\,R_n^2, \quad R_n(0) = -\frac{\beta_1(t_n)}{\beta_2(t_n)}\,\kappa(t_n,0)$$
$$z_n' = -\frac{R_n(x) + a(t_n,x)}{\kappa(t_n,x)}\,z_n - f(t_n,x) - \frac{u_{n-1}(x)}{\Delta t}, \quad z_n(0) = \frac{\beta(t_n)}{\beta_2(t_n)}\,\kappa(t_n,0)$$

The position of the moving boundary $s_n = s(t_n)$ is then the root of the nonlinear equation (2.3.3), and u_n can be obtained by integrating the Riccati transformation using the definition of v_n.

Convergence of this scheme to the weak solution of the moving boundary problem was proved [71]. For nonlinear equations, the Riccati transformation can be substituted by a shooting technique for solving the corresponding boundary value problem. Several attempts were made to generalize the method of lines to several space dimensions. Alternating directions was applied in [72] and an iterative SOR-type technique, based on invariant embedding in one space variable at a time, was proposed in [73]. However, both generalizations suffer when the moving boundary essentially follows one of the coordinate axes. Thus the method of lines remains a powerful approach, if only for one-dimensional problems.

Summary

Front-tracking and front-capturing methods are the most direct extensions of the conventional methods for fixed boundary value problems for partial differential equations, such as finite differences and finite elements. However, the simplest generalizations suffer from reduced accuracy near the moving boundary, and the formulas, especially in higher dimensions, become very involved. The more sophisticated techniques, like the method of lines with invariant embedding and the level set method, give better and more generally applicable recipes. The main drawback of this group of methods is their overall poor accuracy for the calculations near the moving boundary. Any singularities in the initial data can only aggravate this property, except for the special cases of the discontinuous in time finite element method [14] and the explicit variable time step method [101].

2.4 Front-fixing methods

The idea of transferring the nonlinearity from the boundary conditions to the partial differential equation by immobilizing the moving front is appealing in many circumstances. Since the computational domain becomes a rectangle, the formulas need not be adjusted near the boundaries. This is done at a price of having an additional term in the differential operator, so that the latter becomes explicitly nonlinear and often coupled with the equation for the moving boundary. Therefore any method used to numerically solve the partial differential equation has to be adjusted accordingly. Fortunately, in many practical cases this can be done in a straightforward way.

Below we discuss two major ways to fix the moving front. One is to make a change of the independent variables, in which case we get, essentially, a version of front tracking on a variable grid. However, since the transformation is made only once in the beginning, the calculations are set up as though the grid is actually the same. Another way is to take advantage of the fact that melting and freezing occur at a constant temperature, so should the temperature become one of the independent variables, the front would be fixed as well. This is a variation of the hodograph method, when evolution of the space coordinate as a function of time and the unknown function is considered, and is known as the isotherm migration method. Application of either of these approaches becomes problematic if the dynamics of the moving boundary is singular (e.g., when it is not smooth or collapses toward the fixed end).

2.4.1 Change of variables

The front-fixing change of variables in one dimension

$$\xi = \frac{x}{s(t)} \tag{2.4.1}$$

maps the interval $(0, s(t))$ to $(0, 1)$ and reduces the heat equation

$$u_t = \kappa u_{xx}$$

and the Stefan condition at the moving boundary

$$\lambda\rho\,\frac{ds}{dt} = -\kappa u_x(t, s(t))$$

respectively, to the following forms

$$s^2(t)\,u_t = u_{\xi\xi} - s(t)\,\xi\,\frac{ds}{dt}\,u_\xi$$
$$\lambda\rho\,\frac{ds}{dt} = -\frac{\kappa}{s(t)}\,u_\xi(t,1)$$

Similar expressions can be obtained for more general parabolic operators. We present this in more detail in Section 3.1 below. For two-phase problems, when the first phase occupies the region $l_1 \le x \le s(t)$, and the second phase, the region $s(t) \le x \le l_2$, the corresponding front-fixing transformations are

$$\xi_1 = \frac{x - l_1}{s(t) - l_1}$$

for the first phase and

$$\xi_2 = \frac{x - l_2}{s(t) - l_2}$$

for the second, so we get two separate equations for each of the phases, coupled through the nonlinear term and one of the boundary conditions. For Stefan problems, the moving boundary is updated according to the corresponding ordinary differential equation (the Stefan condition) and is then used to update the solution at the next time step. For implicit moving boundary conditions, one can either find the root of the appropriate nonlinear equation, or derive the differential equation for the moving front, as we do below in Section 3.2.

The front-fixing transformation was first proposed in [62] for the heat equation. In [45] it was described for a general linear parabolic operator and two phases. Finite differences were used to solve the partial differential equation. An alternative way, which is taken in the current work, is to use spectral methods instead of finite differences. In [34], the authors introduced a Fourier cosine expansion of the solution to the oxygen diffusion problem and obtained very good results for larger times. However, due to the incompatible initial and boundary conditions and the non-periodic structure of the problem, the numerical procedure was only be applied for $t \ge 0.01$, when the solution becomes sufficiently smooth, while the analytical approximation of [29] was used for smaller times. In [92], the Chebyshev collo-

cation method was applied to the equation resulting from a boundary-fixing transformation of a two-phase Stefan problem for the heat equation, and the results compared favorably to those obtained by finite differences. In this case as well, the problem had a singularity at $t = 0$, and the exact solution was used to start off the computations. In [58], a Lagrangian-interpolation based numerical scheme was proposed for the solution of nonlinear diffusion problems. The Chebyshev collocation points were taken as the interpolation nodes in space. The construction was applied to the oxygen diffusion problem after a front-fixing change of variables. Here again, as in [34], accurate interpolation was not possible from $t = 0$, so the problem was treated as one with fixed boundaries for $t \leq 0.04$. Numerical results still compared well to those obtained by other methods, especially for larger times.

There has been considerable effort devoted to the generalization of the front-fixing coordinate transformation to several space dimensions. In general, if the new variables ξ and η are introduced, then the Laplace's operator in two dimensions becomes

$$\Delta_{\xi,\eta} = A\,\frac{\partial^2}{\partial\xi^2} + B\,\frac{\partial^2}{\partial\xi\partial\eta} + C\,\frac{\partial^2}{\partial\eta^2} + D\,\frac{\partial}{\partial\xi} + E\,\frac{\partial}{\partial\eta}$$

where

$$\begin{aligned} A = \xi_x^2 + \xi_y^2 = \frac{x_\eta^2 + y_\eta^2}{J^2}, \quad C = \eta_x^2 + \eta_y^2 = \frac{x_\xi^2 + y_\xi^2}{J^2} \\ B = 2(\xi_x\eta_x + \eta_y\xi_y) = -2\,\frac{x_\xi x_\eta + y_\xi y_\eta}{J^2} \\ D = \xi_{xx} + \xi_{yy}, \qquad E = \eta_{xx} + \eta_{yy} \end{aligned}$$

with the Jacobian

$$J = x_\xi y_\eta - x_\eta y_\xi \neq 0$$

Similar expressions can be obtained for more general second-order elliptic operators in any number of space dimensions. Normal and time derivatives are also transformed, as follows

$$\begin{aligned} \frac{\partial}{\partial n} = \frac{1}{\sqrt{1 + {F_x}^2}}\left(F_x\,\frac{\partial}{\partial x} - \frac{\partial}{\partial y}\right) = \frac{1}{J\sqrt{1 + {F_x}^2}}\left[(F_x y_\eta + x_\eta)\,\frac{\partial}{\partial\xi} - (F_x y_\xi + x_\xi)\,\frac{\partial}{\partial\eta}\right] \\ \left.\frac{\partial}{\partial t}\right|_{x,y\,\mathrm{const}} = \left.\frac{\partial}{\partial t}\right|_{\xi,\eta\,\mathrm{const}} - \frac{x_t}{J}\left(y_\eta\,\frac{\partial}{\partial\xi} - y_\xi\,\frac{\partial}{\partial\eta}\right) - \frac{y_t}{J}\left(x_\xi\,\frac{\partial}{\partial\eta} - x_\eta\,\frac{\partial}{\partial\xi}\right) \end{aligned}$$

In the above, $y = F(x,t)$ is the moving surface with the outward normal n, and x_t, y_t denote

the time derivatives of the original coordinates in the frame associated with ξ and η. Thus the whole moving boundary problem can be transformed and solved numerically in the new variables.

There is significant freedom in choosing a particular change of variables for a given problem. One approach is to solve a sequence of boundary value problems at each time step and introduce a new coordinate system every time. In this case, it is important to be able to do this in a fast and simple way within the code. A review of numerical grid generation techniques can be found in [59]. In earlier paper the authors suggested choosing ξ and η in such a way that they solve linear elliptic problems at each step. More recently, in [96] a computer code was presented to fully automate the generation of boundary-fitting coordinate systems for free and moving boundary problems.

As an alternative, in [87] two- and three-dimensional moving boundary problems were written in polar (or, respectively, spherical) coordinates and the boundary was fixed in the radial variable. This approach works especially well for the so-called "star-shaped" domains in two or three dimensions, when the angular variables can be conveniently separated, e.g., by Fourier expansions. For example, the following freezing problem in an annular sector was considered in [87]

$$\begin{aligned}
&\frac{\partial T}{\partial t} = \kappa\,\Delta T, \qquad 0 \le \theta \le \theta_0, \quad B(\theta) \le r \le F(t,\theta) \\
&\quad \frac{\partial T}{\partial \theta}(t,r,0) = \frac{\partial T}{\partial \theta}(t,r,1) = 0 \\
&\quad T(t,B(\theta),\theta) = T_w(t,\theta) \\
&\quad T = 0, \quad \rho L V_n = \lambda \frac{\partial T}{\partial n} \qquad\qquad \text{on } r = F(t,\theta)
\end{aligned}$$

Here $r = F(t,\theta)$ is the freezing surface with normal n, so that

$$V_n = \left(\frac{\partial F}{\partial t}\right) \Bigg/ \left[1 + \left(\frac{1}{F}\,\frac{\partial F}{\partial \theta}\right)^2\right] \frac{\partial T}{\partial r}$$

The new variable

$$\eta = \frac{r - F(t,\theta)}{B(\theta) - F(t,\theta)}$$

was introduced, mapping the curvilinear region to the sector $[0,1] \times [0,\theta_0]$, and the resulting nonlinear partial differential equation was solved using finite differences. In three space

dimensions, where the freezing surface can be written as $r = F(t, \theta, \phi)$, the corresponding change of variables is

$$\eta = \frac{r - F(t, \theta, \phi)}{B(\theta, \phi) - F(t, \theta, \phi)}$$

which gives a method to solve moving boundary problems in spherical and near-spherical geometry.

2.4.2 Isotherm migration method

Let us consider once again the simple one-phase Stefan problem

$$\begin{aligned} &u_t = u_{xx}, && 0 < x < s(t) \\ &u(0, x) = 0; && u(t, 0) = 1 \\ &u(t, s(t)) = 0, && \dot{s}(t) = -\lambda u_x(t, s(t)) \end{aligned}$$

Note that since the temperature u is 0 along the moving boundary $s(t)$, this curve is an isotherm. Moreover the temperature is also fixed at the other end, so all the dynamics happens between two isotherms, $u = 1$ and $u = 0$, corresponding to $x = 0$ and $x = s(t)$. Thus it is tempting to consider $x = x(t, u)$ as the new dependent variable, since the domain will then be a finite box. Using the chain rule we get

$$\begin{aligned} \frac{\partial x}{\partial t} = \Big(\frac{\partial x}{\partial u}\Big)^{-2} \frac{\partial^2 x}{\partial u^2}, \qquad & 0 < u < 1 \\ \frac{ds}{dt} = -\lambda \Big(\frac{\partial x}{\partial u}\Big)^{-1} & \end{aligned}$$

which is then solved for $x(t, u)$ using finite differences. Derivative boundary conditions at the fixed end can also be handled — for example, by approximating u with a parabola and finding the value of u at $x = 0$ at each time level.

The idea was first mentioned in [24], where explicit differential equations for isotherms were written down for general heat conduction problems with phase transitions. The approach can be generalized to several space dimensions [31] by expressing one of the spatial coordinates as the function of u and the remaining ones [27, §5.4.2]. However, this particular idea fails for problems where the motion of the interface does not allow for a consistent representation of this sort for all times (e.g., $\partial x/\partial u$ vanishes for some $t > 0$). In [28] the same approach was used to track the movement of isotherms along orthogonal flow lines by

solving locally one-dimensional problems in the radial variable, representing $r = r(t, u, \theta)$.

Summary

Fixing the moving front and shifting the nonlinearity from the boundary conditions to the differential operator is an attractive way of avoiding the complications which would otherwise emerge on a variable domain. Since in the new variables, the computations are carried out on a fixed box, the accuracy is uniform and depends only on that of the method of integration used for the resulting differential equations. As we intend to show further in this work, even in the most general cases, highly accurate numerical solutions can be obtained with such approaches. Viable extensions of the front-fixing technique exist in two and three dimensions, thus contributing even more to the generality of this approach. There are some numerical difficulties with it, however. Firstly, the nonlinear differential equations obtained after the boundary-fixing transformation are often very stiff, so care must be taken in what integration method to choose at the next stage. Explicit methods tend to have harsh stability constraints, while the implicit ones can be complicated and slow, due to the nonlinear equations to be solved at each time step. One way to overcome this is to use semi-implicit methods (see [16]) or explicit ones with extended stability region, such as the Runge-Kutta-Chebyshev [2, 91] or Chebyshev-Euler [3] methods.

2.5 Integral equations

All the methods described so far deal with a given moving boundary problem directly, through its differential equation formulation. However, frequently in the general theory of boundary value problems of mathematical physics, differential operators are converted to integral operators. While the former are not bounded, the latter usually are. This makes the integral formulation a powerful tool both in theory (e.g., convergence proofs and various norm estimates) and practice (due to the many iterative solution algorithms available). In most cases, the dimensionality of the problem is decreased by one, since the integrals are usually taken along the boundary of the original domain. It is true, however, that conventional integral formulations apply to linear problems, while moving boundary problems do not fall into this category. Nevertheless, for certain linear differential operators, the integral equation approach can still be used, with slight modifications.

2.5.1 Green's functions

The integral method most widely used is based on the fundamental solution of parabolic differential operators. The framework for moving boundary problems consists of the following stages. First, the appropriate Green's function, satisfying the time causality property and the boundary conditions on the fixed end, is found. The formal solution can then be written down in the usual manner, by integrating the Green's function or its normal derivative, times the initial and boundary values and, possibly, the source term. However, unlike in the linear case, the corresponding expression cannot be immediately resolved, since the domain of integration and, possibly, the integrands depend on the moving boundary, which is unknown. Nevertheless letting x approach the interface $s(t)$ and using the additional condition at the moving front, an integral equation for $s(t)$ can be derived. Once this is solved, the moving boundary is substituted into the formal expression for the unknown function on the whole domain, and the solution is obtained. In some cases, the kernels may depend on the velocity of the moving boundary, so the equation for $s(t)$ is integro-differential. However, this can often be avoided by deriving another integral equation for the flux at the moving front, since in many boundary conditions, it is related to the speed of the front's propagation. This is the approach taken in [43]. It is important that the resulting integral equations are of Volterra type of the second kind, and thus amenable to numerical solution using iterative algorithms.

As an illustration, consider the integral equation approach, applied in [51] to the oxygen diffusion problem (1.0.2). The Green's function satisfies

$G_t + G_{xx} = \delta(x - x')\delta(t - t')$		fundamental solution of the adjoint operator
$G(x, x', t, t') = 0$	for $t > t'$	causality
$G_x(0, x', t, t') = 0$		boundary condition at the fixed end

Now, the integral

$$\int_0^{t'} \int_0^{s(t)} \big[(c_{xx} - c_t)G - (G_t + G_{xx})c\big]\, dx\, dt$$

can be evaluated in two ways. First, from the differential equations satisfied by c and G,

the integral equals

$$\int_0^{t'} \int_0^{s(t)} G\, dx\, dt + c(t', x')$$

On the other hand, integration by parts gives another expression for the same integral

$$\int_0^{t'} \Big[Gc_x - cG_x \Big]_{x=0}^{x=s(t)} dt - \int_0^1 \big[Gc \big]_{t=0}^{t=s^{-1}(x)} dx$$

Boundary conditions require that the first of the last two integrals, as well as the contribution from $t = s^{-1}(x)$ in the second one, vanish, and therefore

$$c(t', x') = -\int_0^{t'} \int_0^{s(t)} G(x, x', t, t') dx\, dt + \frac{1}{2} \int_0^1 G(x, x', 0, t')(1 - x)^2 dx \tag{2.5.1}$$

In the last integral, initial conditions for c and s were used. This is the form of the above-mentioned expression for $c(t, x)$. For this particular problem, the Green's function has the familiar form

$$G(x, x', t, t') = G(x, x', t' - t) = \frac{1}{2\sqrt{\pi(t' - t)}} \left\{ \exp\Big[-\frac{(x - x')^2}{4(t' - t)} \Big] + \exp\Big[-\frac{(x + x')^2}{4(t' - t)} \Big] \right\}$$

Therefore it is possible to simplify (2.5.1), and in [51] this is done as follows. The partial differential equation for G is integrated in time and causality used to write

$$G(x, x', 0, t') = G(x, x', t') = \int_0^{\infty} \big[\delta(x - x')\delta(t - t') + G_{xx}(x, x', t' - t) \big]\, dt$$

This is substituted into the second integral in (2.5.1), and the G_{xx} term is integrated by parts twice with respect to x, taking into account the boundary conditions. Thus (2.5.1) becomes

$$c(t', x') = \frac{1}{2}(1 - x')^2 - \int_0^{t'} G(0, x', t' - t)\, dt + \int_0^{t'} \int_{s(t)}^1 G(x, x', t' - t)\, dx\, dt$$

Now the exact form of G can be used to evaluate the integrals explicitly, so that

$$c(t',x') = \frac{1}{2}(1-x')^2 - 2\sqrt{\frac{t'}{\pi}}\exp\Big(-\frac{x'^2}{4t'}\Big) + x'\,\mathrm{erfc}\Big(-\frac{x'}{2\sqrt{t'}}\Big) + R(t',x') \tag{2.5.2}$$

where

$$R(t',x') = \frac{1}{2}\int_0^{t'}\Big\{\mathrm{erfc}\Big[\frac{s(t)-x'}{2\sqrt{t'-t}}\Big] - \mathrm{erfc}\Big[\frac{1-x'}{2\sqrt{t'-t}}\Big] + \mathrm{erfc}\Big[\frac{s(t)+x'}{2\sqrt{t'-t}}\Big] - \mathrm{erfc}\Big[\frac{1+x'}{2\sqrt{t'-t}}\Big]\Big\}dt$$

From (2.5.2), an integral equation for $s(t)$ can be obtained by letting $x' \to s(t')$ and using one of the conditions $c(t,s(t)) = c_x(t,s(t)) = 0$ (in the latter case, of course, (2.5.2) needs to be differentiated in x' first). In [51], the second approach was taken; the resulting integral equation was solved using a simple iterative technique, and $c(t',x')$ then found from (2.5.2).

In [17], a similar approach was taken to model thermal solidification with undercooling. If the solid-liquid interface moves in the direction of the z-axis, then a simple one-dimensional heat equation governs the temperature distribution on both sides of the moving front. If temperatures adjust to an undercooled value T_∞ far from the interface, then the following integral equation describes the motion of the front

$$\begin{aligned}\Delta = \frac{T_M - T_\infty}{\kappa\lambda} = \frac{1}{2\sqrt{\pi\kappa}}\int_0^t \exp\Big[-\frac{(s(t)-s(t'))^2}{4\kappa(t-t')}\Big]\frac{ds(t')}{dt'}\,\frac{dt'}{\sqrt{t-t'}} \\ + \frac{1}{2\sqrt{\pi\kappa t}}\int_{-\infty}^{\infty}\exp\Big[-\frac{(s(t)-z')^2}{4\kappa t}\Big]T_0(z')\,dz'\end{aligned} \tag{2.5.3}$$

Here Δ is the scaled undercooling parameter, T_M is the melting temperature, κ is the diffusivity, λ is the latent heat, and $T_0(z)$ is the initial temperature distribution. Numerical evaluation of the time integral in (2.5.3) (called the memory integral, since it includes the whole history of motion) can be cumbersome, since the number of operations and storage increase with the number of time steps. In [17], an efficient computational technique was proposed, making the number of required operations fixed at each time step. The idea is to separate the smooth part of the integral (i.e., $t' < t-\epsilon$, $0 < \epsilon \ll 1$), which has derivatives of any order and can be calculated using any suitable method for the heat equation. The remaining part has an integrable singularity due to the presence of the moving boundary,

and Gaussian quadrature can be used to evaluate it accurately. Time is discretized, so that $t - \epsilon = n\Delta t$ at each level. At each new time step, the integral equation for $s(t)$ is solved using Newton's method; then the smooth temperature field is advanced according to the heat equation discretization; and finally, the added contribution of the memory integral to the smooth field is computed, by evaluating the integral

$$\frac{1}{2\sqrt{\pi\kappa}} \int_{t-n\Delta t}^{t-(n-1)\Delta t} \exp\Big[-\frac{(s(t)-s(t'))^2}{4\kappa(t-t'+\Delta t)}\Big] \frac{ds(t')}{dt'} \frac{dt'}{\sqrt{t-t'+\Delta t}}$$

for all z (fortunately, this contribution decays rapidly away from the interface). Implementation details are given in [17], where it is demonstrated that computation can be carried out to any given accuracy; generalizations to nonsymmetric problems (i.e., when $\kappa_{\text{liquid}} \neq \kappa_{\text{solid}}$) are also provided.

In [89], an integral equation formulation was coupled with the level set method to solve a problem of dendritic solidification in two dimensions. For the problems of this class, the conditions at the moving boundary $\Gamma(t)$ are different from those in the Stefan problem. Instead of the constant temperature on the interface, the so-called Gibbs-Thompson relation

$$u(t,x) = -\varepsilon_C(n)C - \varepsilon_V(n)V \quad \text{for } x \in \Gamma(t) \tag{2.5.4}$$

holds. Here C is the curvature and V, the normal velocity of the moving interface $\Gamma(t)$ with outward normal n, and the anisotropy coefficients

$$\varepsilon_C(n) = \varepsilon_C\big(1 - A\cos(k_A\theta + \theta_0)\big)$$
$$\varepsilon_V(n) = \varepsilon_V\big(1 - A\cos(k_A\theta + \theta_0)\big)$$

model surface tension (ε_C) and molecular kinetic (ε_V) effects. The energy balance condition

$$\left[\frac{\partial u}{\partial n}\right] = -\lambda V \quad \text{for } x \in \Gamma(t)$$

still holds as the second moving boundary condition for this model as well. The integral expression for $u(t,x)$ in terms of $\Gamma(t)$ was derived in [89] using the heat kernel, just as it was done above. Since the interface in this setting is usually a closed curve in two dimensions, which can develop spikes and cusps, the integral equation for $\Gamma(t)$ was not considered; rather,

the interface was updated using the level set construction, by evolving an auxiliary function $\phi(t,x)$, whose zero level set is $\Gamma(t)$ (see also the discussion above in Section 2.3.1). Thus the algorithm of [89] consisted of four main stages: determine and extend off the interface the normal velocity (the extension was done smoothly by means of the integral expression for u); advance the level set function ϕ; update the temperature field by solving the heat equation; and determine the new position of the interface as the level set $\phi = 0$. The numerical results demonstrated the ability of this approach to successively track singularities and topological changes in the interface.

The integral equation approach was used extensively for the American option valuation problem, which appears in Chapter 7 of this work. Various forms were proposed [56, 60, 65] for the integral equation to determine the moving boundary, which in this problem corresponds to the critical stock price, beyond which the option should be optimally exercised (see details in Chapter 7). In [56], the integral formulation was discretized in time, but without the use of a sophisticated numerical technique, such as the one in [17]. In [60], asymptotic behavior of the moving boundary was derived for small times, which can be used to start off numerical procedures.

It should be noted that the fundamental solution approach has also been heavily used for theoretical purposes. Existence and uniqueness results for Stefan problems with analytic moving boundaries were established in [85] by first converting the differential formulation into an integral one. Convergence results for the finite-element methods [14] were proved using integral equations as well. In this work, we also use Green's functions for general linear parabolic operators to prove the convergence of our numerical method (see Chapter 4 below).

2.5.2 Other integral methods

The formulation involving the integral of the Green's function along the boundary is the most popular one. However, other techniques based on integration have also been applied to Stefan problems. For the most part, the resulting integral expressions are very close, or even identical to those obtained with Green's functions, and we present a short review of other approaches.

In [40], the moving boundary $x = s(t)$ for the classical Stefan problem was written as $t = f(x)$, using its monotonicity property. The temperature function was then extended

continuously (i.e., as $u = 0$) below $t = f(x)$, and the Laplace transform was applied. Solution of the boundary value problem for the resulting ordinary differential equation, followed by the inverse Laplace transform, gave an integral equation for the moving boundary. Further developments of the integral transform methods appear in [80, p. 138], where, in particular, the Laplace transform approach to the oxygen diffusion problem produces the same equations as those obtained in [51] via Green's functions (see above).

The embedding technique was introduced in [12] for an ice-melting problem, with the water removed instantaneously on formation. The idea is to "embed" the solution, which is valid in $s(t) < x < l$, in a larger domain $0 < x < l$ of constant size and shape. The "fictitious," extended values of the solution in $0 < x < s(t)$, as well as the boundary conditions at $x = 0$, are chosen so that the given conditions are satisfied at $x = s(t)$. In [12], Duhamel's principle was used to write the integral solution for the temperature field in $[0, l]$, and this expression was used to write a system of integro-differential equations for $s(t)$ and the fictitious boundary condition. A short time solution, using series expansion, was obtained.

Finally, we briefly mention the heat-balance integral method of T. Goodman [47], which uses the integrated form of the Stefan condition to obtain an integral expression for the energy balance. The dependence of temperature on the space variable is assumed to be polynomial and consistent with the boundary conditions. This dependence is then integrated in space up till the moving boundary, and using the interface conditions and the flow equations, a heat balance integral is written. Then the moving boundary has to satisfy a certain integral equation, which is solved and the solution is substituted into the assumed expression for the temperature. This approach worked extremely well for the simpler Stefan problems, but it becomes much less viable for more general problems. Also, since the assumed polynomial dependence of temperature on the space variable is not satisfied exactly, this method is more suitable for qualitative estimates, than for calculations. For several extensions of the heat-balance integral method, see [27, § 3.5.4-3.5.6].

Summary

Reformulation of moving boundary problems as integral equations along the moving front not only reduces the dimensionality, but in most cases also provides regularization and several choices of numerical methods. When valid, this approach is capable of producing highly

accurate numerical solutions to problems with a variety of interface conditions, including Stefan problems, crystal growth problems and problems with prescribed flux, without any modification. Complicated interface dynamics can also be incorporated, if a combination with effective front-capturers, such as the level set method, is employed. The main drawback of this approach arises from the fact that it relies on the explicit calculation of the corresponding Green's function, which restricts the application of this method to linear parabolic operators with either constant-coefficient or well-studied special spatial parts. Direct use of this method for problems in higher space dimensions is not usually very practical.

2.6 Numerical results: a comparison

We are now in a position to compare the performance of the methods described in this chapter. Numerical results are presented for the oxygen diffusion problem (1.0.2). Our presentation is based on the original published work, as well as on the reviews citing the results, notably [27] and [45].

Before we go on to describe each particular implementation, we wish to caution the readers in their interpretation of the results appearing on page 39. One should be aware of the fact that the comparative performance of any two numerical techniques is heavily dependent on the particular problem, with respect to which they are evaluated. It is quite possible that, should we have considered a different test problem, the relative "rankings" (in terms of accuracy) of the numerical methods would have changed dramatically. Our choice of the oxygen diffusion problem was driven mainly by the fact that our own interest lies in the field of one-dimensional, one-phase moving boundary problems with singularities in the initial data, of which this is an excellent example. It is also worth noting that this problem is, perhaps, second only to the classical Stefan problem of ice melting in the interest developed towards it since its advent in 1972 by J. Crank and R. Gupta [29]. Thus we ran into no difficulty in finding studies of this problem by various methods. However, it is not our intention to even attempt to develop an absolute ranking among the existing numerical methods. As we have numerously pointed out in the previous sections, each approach has its own advantages and disadvantages and usually works better for some problems and worse for others.

The following is the description of the numerical methods mentioned in Tables 2.1

and 2.2.

- **FGL:** fixed-grid front-capturing with Lagrangian interpolation near moving boundary; reported from [29]. Parameters: $\Delta x = 0.05$, $\Delta t = 0.001$.

- **VGX:** variable grid (in space), with moving boundary always at grid point [77]; reported from [27, § 4.3.2]. Parameters: $\Delta x = 0.01$, $\Delta t = 0.001$.

- **VTS:** variable time step front-tracking, with moving boundary always at grid point; reported from [50]. Parameters: $\Delta x = 0.01$.

- **EVT:** explicit variable time step method [102]; reported from [101]. Parameters: $\Delta x = 0.02$.

- **MGT:** grid moving (in time) at the speed of the front, with polynomial interpolation used for values at old grid points; reported from [30]. Parameters: $\Delta x = 0.05$, $\Delta t = 0.001$.

- **FEM:** finite differences in time, finite elements in space method, with moving boundary position computed via extrapolation; reported from [74]. Parameters: linear basis, $\Delta x = 0.05$, Crank-Nicolson time stepping, $\Delta t = 0.002$.

- **LIM:** method of lines with invariant imbedding [71]; reported from [45]. Parameters: $\Delta x = 0.005$, Crank-Nicolson time stepping, $\Delta t = 0.001$.

- **FFD:** front fixing, with finite difference solution of the resulting partial differential equation and a *regula falsi* estimation of moving boundary position from the no-flux condition; reported from [27], based on [42]. Parameters: $\Delta x = 0.025$, $\Delta t = 0.0005$.

- **FFL:** front fixing with solution of the resulting partial differential equation by the method of lines; reported from [45]. Parameters: $\Delta x = 0.025$, fully-implicit time stepping (stiff ODE solver).

- **FFC:** front fixing with Lagrangian interpolation based on Chebyshev collocation points; reported from [58]. Parameters: $N = 9$ nodes, Crank-Nicolson time stepping, $\Delta t = 0.005$.

- **FFS:** front fixing with spectral (Fourier) solution of the resulting partial differential equation; reported from [34]. Parameters: $N \approx 20$ modes, fully implicit time stepping (stiff ODE solver).

- **ENT:** generalized enthalpy method [32]; reported from [45]. Parameters: $\Delta x = 0.025$, Crank-Nicolson time stepping, $\Delta t = 0.005$.

- **VEM:** variational inequality — complementarity formulation with finite element discretization; reported from [39] and [27, §6.4.1]. Parameters: linear elements, $\Delta x = 0.01$, $\Delta t = 0.001$.

- **IEM:** integral equation; reported from [51]. Parameters: Simpson integration formula, $\Delta t = 0.0005$, tolerance $\varepsilon = 10^{-9}$ or $K = 40$ iterations.

All calculations, except IEM, VTS, and FFD, start from a positive time (usually 0.0025 or 0.025), because of the initial singularity at $x = 0$; asymptotic approximation [29, 51] is used for start-off. For all methods, just the first four significant digits are reported for uniformity. Further resolution is available for several methods (FGL, IEM, FFS, VTS, FFC), and some of these numbers will be shown in Section 6.2, when we compare them with the results produced by our method.

Generally, there is less discrepancy across methods in the computed values of the concentration at the fixed surface, than in those of the moving boundary. This is natural, given the fact that most of the dynamics happens at the other end, while the same approximate values were used to start off the majority of the computations. It is widely accepted that among all numerical methods previous to this work, the integral equation technique (bottom entry in the tables on page 39) gives the most reliable results for all times. We see that these are replicated well by the front-fixing-spectral and variational inequality calculations; however, both of the latter were performed for $t \geq t_0 > 0$ ($t_0 \approx 0.01$ and $t_0 = 0.025$, respectively). This confirms the predicted success of the variational inequality approach for the problems with prescribed flux, if somewhat smeared by its inability to handle singularities at $t = 0$. Fixed- and variable-grid techniques produce results which are similar to one another; the explicit variable time step method is less accurate, but it requires less storage and CPU time, while enjoying the additional advantage of starting at $t = 0$. The method of lines clearly works better in conjunction with front-fixing. In [45], this property is attributed to

the way the moving boundary is estimated. The enthalpy method does not work as well in this particular setting, which is not unexpected, given the degeneracy (i.e., zero latent heat) and also the initial singularity of the problem.

Method	Time t						
	$t = 0.04$	$t = 0.06$	$t = 0.10$	$t = 0.12$	$t = 0.14$	$t = 0.16$	$t = 0.18$
FGL	0.2745	0.2237	0.1433	0.1092	0.0779	0.0489	0.0218
VGX	0.2745	0.2238	0.1434	0.1093	0.0780	0.0489	0.0218
VTS	-	-	0.1423	0.1093	0.0780	0.0489	0.0218
EVT	-	-	0.1433	-	-	-	0.0218
MGT	0.2742	0.2234	0.1429	0.1089	0.0776	0.0486	0.0216
FEM	-	-	0.1432	-	-	-	-
LIM	0.2746	-	0.1436	-	-	-	0.0222
FFD	-	-	0.1438	0.1097	0.0783	0.0493	0.0222
FFL	0.2745	-	0.1433	-	-	-	0.0219
FFC	0.2744	0.2236	0.1431	0.1091	0.0778	0.0488	0.0218
FFS	0.2743	-	0.1432	0.1091	0.0779	0.0488	0.0218
ENT	0.2766	-	0.1439	-	-	-	0.0221
VEM	0.2743	0.2236	0.1432	0.1091	0.0779	0.0488	0.0218
IEM	-	0.2236	0.1432	0.1091	0.0779	0.0488	0.0218

Table 2.1: Oxygen concentration at fixed sealed surface, $c(t, 0)$, calculated with different methods.

Method	Time t						
	$t = 0.04$	$t = 0.06$	$t = 0.10$	$t = 0.12$	$t = 0.14$	$t = 0.16$	$t = 0.18$
FGL	0.9992	0.9922	0.9352	0.8789	0.7976	0.6813	0.4961
VGX	0.9988	0.9904	0.9309	0.8740	0.7930	0.6776	0.4974
VTS	0.9950	0.9899	0.9249	0.8703	0.7916	0.6825	0.4767
EVT	-	0.9811	0.9256	0.8701	0.7901	0.6748	0.4928
MGT	0.9992	0.9918	0.9344	0.8780	0.7968	0.6798	0.4948
FEM	0.9993	0.9920	0.9356	0.8796	0.7992	0.6832	0.4985
LIM	0.9993	-	0.9361	-	-	-	0.5065
FFD	-	-	0.9354	0.8800	-	0.6850	0.5046
FFL	0.9992	-	0.9358	-	-	-	0.5028
FFC	1.0000	0.9916	0.9350	0.8792	0.7991	0.6837	0.5021
FFS	0.9992	-	0.9350	0.8792	0.7989	0.6834	0.5013
ENT	1.0000	-	1.0000	-	-	-	0.4750
VEM	0.9991	0.9916	0.9343	0.8792	0.7987	0.6833	0.5018
IEM	0.9992	0.9918	0.9350	0.8792	0.7989	0.6834	0.5011

Table 2.2: Position of the moving boundary (zero-concentration front), calculated with different methods.

Chapter 3

General Formulation

The justification of such a mathematical construct is solely and precisely that it is expected to work.
(John von Neumann, 1903–1957)

In this work we consider general one-dimensional one-phase moving boundary problems for linear parabolic equations, which can be written in the following form

$$u_t = L_x[u] + f(t,x), \quad t > 0,\ x \in I_s, \tag{3.0.1}$$

$$u(x,0) = \phi(x), \quad s(0) = s_0 \tag{3.0.2}$$

$$B[u] = \psi(t), \quad u(t,s(t)) = \theta(t), \tag{3.0.3}$$

Here L_x is a linear (possibly, time-dependent) elliptic differential operator

$$L_x = \alpha_2(t,x)\,\frac{\partial^2}{\partial x^2} + \alpha_1(t,x)\,\frac{\partial}{\partial x} + \alpha_0(t,x) \tag{3.0.4}$$

(for parabolicity we need $\alpha_2(t,x)$ to be nonnegative); I_s is one of the intervals, $[0,\, s(t)]$ or $[s(t),\, \infty)$; and $B[u]$ is the boundary condition at the fixed end (0 or ∞, respectively), e.g., $B[u] = b_1 u + b_2 u_x$. We call the problem "finite" when $I_s = [0,\, s(t)]$ and "semi-infinite" in the other case.

Since the position of the moving front $s(t)$ is unknown, we need an additional condition to complete the statement of the problem. This is usually provided in a form of a relation involving the flux across the moving boundary. The Stefan condition (2.1.1) is characteristic of phase change problems, as it expresses the energy balance across the moving front when the latent heat is released or absorbed. In several other moving boundary problems, e.g., those arising in statistics and optimal stopping of Markov processes, $u(t,x)$ has to be

continuously differentiable across the interface, and hence the additional condition explicitly prescribes the first derivative (i.e., flux) at $s(t)$. Since (see Section 3.5.1 below) we recast the problem so that all boundary conditions are homogeneous, the value $u_x(t, s(t)) = 0$ is consistent with the continuity condition. Indeed, this relation frequently appears in moving boundary problems with prescribed flux (see, e.g., [86, 88, 97]). In [27], these problems are also called "implicit moving boundary problems," since the evolution of the interface is not explicitly specified. Thus, following this terminology, we consider below two main settings, corresponding to the following interface conditions

$$u_x(t, s(t)) = -\lambda \frac{ds}{dt} \quad \text{(Stefan problems)} \tag{3.0.5}$$

$$u_x(t, s(t)) = 0 \quad \text{(implicit problems)} \tag{3.0.6}$$

Note that for other physical models, other interface conditions may arise. For example, in crystal growth, the Stefan condition is complemented by the so-called Gibbs-Thompson relation (2.5.4), describing molecular kinetics and surface tension effects (see Section 2.5). We do not address these problems in this work, so no details are given here, even though our approach can be applied to them equally well.

3.1 Front-fixing transformation

The first stage of our method is the front-fixing coordinate transformation. We set $\xi = x/s(t)$ for the finite problem and $\xi = x - s(t)$, for the semi-infinite one. The former maps I_s to $[0, 1]$, while the latter maps it to $[0, \infty]$. This results in changing the differential operator to

$$\tilde{L}_{t,\xi} = \frac{\tilde{\alpha}_2(t, \xi)}{s^2(t)} \frac{\partial^2}{\partial \xi^2} + \left(\frac{\tilde{\alpha}_1(t, \xi)}{s(t)} + \frac{\xi}{s(t)} \frac{ds}{dt} \right) \frac{\partial}{\partial \xi} + \tilde{\alpha}_0(t, \xi) + \tilde{f}(t, \xi)$$

in the finite case and

$$\tilde{L}_{t,\xi} = \tilde{\alpha}_2(t, \xi) \frac{\partial^2}{\partial \xi^2} + \left(\tilde{\alpha}_1(t, \xi) + \frac{ds}{dt} \right) \frac{\partial}{\partial \xi} + \tilde{\alpha}_0(t, \xi) + \tilde{f}(t, \xi)$$

in the semi-infinite case. In both of the above equations, $\tilde{\alpha}_i(t, \xi) = \alpha_i(t, x(\xi, s(t)))$, $i = 0, 1, 2$, and analogous relations hold for $\tilde{f}(t, \xi)$. The new initial conditions are obviously

$u(0,\xi) = \phi(s_0\xi)$, and the boundary conditions become

$$\begin{aligned} &B[u](t,0) = \psi(t), \quad u(t,1) = \theta(t), && \text{finite case;} \\ &u(t,0) = \theta(t), \qquad B[u](t,\infty) = \psi(t), && \text{semi-infinite case} \end{aligned} \tag{3.1.1}$$

Below, we shall solve the equation $u_t = \tilde{L}_{t,\xi}[u] + \tilde{f}$ by Chebyshev expansions. Since Chebyshev polynomials form a complete orthogonal system on the interval $[-1, 1]$, we need to map the ξ domain to this interval. This presents no ambiguity for the finite problem, where we set

$$y = 2\xi - 1 = \frac{2x}{s(t)} - 1,$$

which results in multiplication by 2 wherever differentiation with respect to the new variable y takes place in the operator $\tilde{L}$ and the boundary conditions. For the semi-infinite problem, a number of mappings was proposed in the literature ([20, section 2.5.3] or the rational Chebyshev functions TL_n in [16]). In this work, we prefer to use

$$y = \frac{4}{\pi}\,\arctan(\xi) - 1 = \frac{4}{\pi}\,\arctan(x - s(t)) - 1.$$

This brings about a more complicated adjustment to the corresponding operator $\tilde{L}$, namely,

$$\tilde{L}_{t,y} = A_1^2(y)\,\tilde{\alpha}_2(t,y)\,\frac{\partial^2}{\partial y^2} + A_2(y)\,\left(A_1(y) + \tilde{\alpha}_1(t,y) + \frac{ds}{dt}\right)\,\frac{\partial}{\partial y} + \tilde{\alpha}_0(t,y) + \tilde{f}(t,y)$$

where

$$A_1(y) = \frac{2}{\pi}\,\left(1 - \sin\Big(\frac{\pi}{2}y\Big)\right), \quad A_2(y) = -\cos\Big(\frac{\pi}{2}y\Big) \tag{3.1.2}$$

Note that we have, effectively, transformed the nonlinearity of the problem from the boundary conditions to the differential operator: $\tilde{L}_{t,y}$ is nonlinear, because both $s(t)$ and ds/dt are unknown. However, the modified problem is now amenable to accurate numerical treatment by spectral methods, and we outline the framework in Section 3.3. Before we do that, however, we need to specify the way the position of the moving front is determined at each time step.

3.2 Velocity of the moving boundary

To determine the moving boundary $s(t)$ as part of the solution, we seek a differential equation that it satisfies. We also note that ds/dt appears in the nonlinear operator $\tilde{L}_{t,y}$, so an expression for this quantity is necessary. In the case of Stefan-type problems, such differential equation is already given by (3.0.5). For implicit moving boundary problems, we need to differentiate the boundary conditions at the moving front to obtain the desired equation, as described in what follows.

Differentiating the second relation in (3.0.3) with respect to t yields

$$\frac{d\theta}{dt} = \frac{d}{dt}\, u(t, s(t)) = u_t(t, s(t)) + \frac{ds}{dt}\, u_x(t, s(t)),$$

and since $u_x(t, s(t)) = 0$ (3.0.6), we have

$$u_t(t, s(t)) = L_x(u)(t, s(t)) = \dot{\theta}(t)$$

From here, provided $\alpha_2(t, s(t)) \neq 0$, we can find $u_{xx}(t, s(t))$ in terms of u, u_x and f, all evaluated at $x = s(t)$. Now, after differentiating equation (3.0.6) with respect to time, just as we did with the first boundary condition, we obtain

$$0 = \frac{d}{dt}\, u_x(t, s(t)) = u_{tx}(t, s(t)) + \frac{ds}{dt}\, u_{xx}(t, s(t)) = \big(L_x(u)\big)_x + \frac{ds}{dt}\, u_{xx}(t, s(t)),$$

and therefore

$$\frac{ds}{dt} = -\frac{\big(L_x(u)\big)_x}{u_{xx}}\bigg|_{(t,s(t))} = -\frac{s(t)\,\big(\tilde{L}_{t,\xi}(u)\big)_\xi}{u_{\xi\xi}}\bigg|_{(t,b)},\ b = 0 \text{ or } 1 \tag{3.2.1}$$

which is a valid differential equation if only $u_{xx}(t, s(t)) \neq 0$. This idea originates from [29, Section 4.3], where

$$L_x = \frac{\partial^2}{\partial x^2} - 1, \quad \theta(t) \equiv 0,$$

and the resulting equation for $s(t)$ is

$$\frac{ds}{dt} = -u_{xxx}(t, s(t)), \tag{3.2.2}$$

leading to

$$\frac{ds}{dt} = -\frac{u_{\xi\xi\xi}(t,1)}{s^3(t)} = -\frac{8}{s^3(t)} u_{yyy}(t,1)$$

in our method, as we shall see later in Section 6.2.

Note that since L is a second-order differential operator in the space variable, the form of (3.2.1) suggests that the velocity $\dot{s}(t)$ of the moving boundary is typically expressed as some combination of up to third-order spatial derivatives of the solution, evaluated at $t = 1$. It is easy to express these as simple linear combinations of the Chebyshev coefficients of u, since the third y-derivative, evaluated at 1, equals [49, Appendix]

$$u_{yyy}(t,1) = \sum_n \frac{n^2(n^2-1)(n^2-4)}{15} a_n(t). \tag{3.2.3}$$

An alternative approach to finding an explicit expression for the velocity of the moving boundary is based on the equivalence, under some general conditions, of problems with prescribed flux to Stefan problems for a derivative of the function sought [88]. As it was shown in [88], if $u(t,x)$ solves an implicit moving boundary problem, then either $v(t,x) = u_t$ or $w(t,x) = u_x$ solves a related Stefan problem with the same moving boundary $s(t)$. Since the expression for $\dot{s}(t)$ is incorporated into the Stefan formulation, as we have established above, this transformation can provide a useful reduction of the original problem. We use it in our approach to the American option problem in Chapter 7.

3.3 Chebyshev expansion

The front-fixing transformation allowed us to reduce a linear parabolic equation on a variable domain to a nonlinear equation on $[-1,1]$. A number of methods have been used to solve the resulting partial differential equation (see Section 2.4 and references therein). The most accurate results were obtained by a Fourier cosine expansion, so the use of spectral methods appears as a good choice. However, since boundary conditions in the problems we study are usually not periodic, we choose Chebyshev polynomials as our basis functions. Among different spectral constructions, we choose Chebyshev tau (in the terminology of [49]), which seems to be best suited for our approach. The tau method differs from the perhaps better known Galerkin method in that the basis functions are not required to satisfy the boundary conditions individually. Instead, the two highest-order coefficients in the truncated sum are

chosen (at every time step), so that the boundary conditions are satisfied by the whole sum. This boils down to a relation, or a constraint, imposed on the Chebyshev coefficients at each step. For example, for a truncated Chebyshev expansion of the solution

$$u(t,x) = \sum_{n=0}^{N-1} a_n(t) T_n(x) \tag{3.3.1}$$

satisfying $u = 0$ (Dirichlet) at $x = -1$ and $u_x = 0$ (Neumann) at $x = 1$, we have

$$\sum_{n=0}^{N-1} (-1)^n \, a_n = 0$$

$$\sum_{n=0}^{N-1} n^2 \, a_n = 0$$

In the tau method, then, the coefficients a_{N-1} and a_{N-2} are chosen so that these relations (or their analogs for other boundary conditions) are satisfied exactly. If the Chebyshev coefficients of $u(t,x)$ decay fast enough and $u(t,x)$ is consistent with the boundary conditions imposed, then the values of these two coefficients computed in this way are sufficiently close to their true values.

When the expansion (3.3.1) is assumed, we can also get similar expansions for all spatial derivatives of $u(t,x)$. Any space-dependent coefficients in $\tilde{L}$, as well as the source term, are also expanded in Chebyshev series; then, using the multiplication rule (see, for example, [20])

$$(uv)_k = \frac{1}{2} \sum_{p+q=k} u_p v_q + \sum_{|p-q|=k} u_p v_q$$

we can write the whole right-hand side as a function of a_n's. Thus we get a coupled system of $N+1$ nonlinear ordinary differential equations (N Chebyshev coefficients and the moving boundary), which can be integrated by any of the standard algorithms.

If at $t = 0$, $u(0,x) = \phi(x)$ is a sufficiently smooth function, then we can expand it in a rapidly convergent Chebyshev series and use the corresponding coefficients, together with $s(0) = s_0$, as the initial values for the abovementioned system of ordinary differential equations. However, if $\phi(x)$ has singularities, its Chebyshev series will converge slowly, and even though the solution at larger, positive t may be quite smooth, we shall be forced, in general, to take a very large number of Chebyshev coefficients to accurately resolve it

initially and for small times. Therefore direct application of this method to problems with only piecewise smooth initial data may not be very practical. This restriction is highly undesirable, since many moving boundary problems of practical interest have some sort of singularity in the initial conditions. One remedy is to use small-time asymptotics (as in [34]) to start off the solution up till some time $t_0 > 0$ and perform the actual computations for $t \geq t_0 > 0$. Such an approach, though justified, lacks the universality of a purely numerical method, which needs only the initial data as input. We choose to pursue a different avenue and propose to take advantage of the fact that diffusion tends to smooth out singularities very fast, and therefore solutions corresponding to appropriate approximations of the initial conditions should be close to the true solution of a singular problem.

3.4 Approximation of singular initial data

Let us assume that the given singular initial data belong to a certain functional space $\mathcal{F}$. We then construct a sequence of smooth functions, which converges to the given initial data in the space $\mathcal{F}'$, where $\mathcal{F}' \supseteq \mathcal{F}$. If we choose the functional spaces appropriately, then the sequence of solutions produced by the elements of the smooth sequence will converge to the true solution of the problem in a chosen norm (e.g., in the supremum norm, if we wish to bound the maximum error). This gives us a convergent method for solving arbitrary singular problems, as long as we can find a sequence of smooth functions, converging in the appropriate functional space.

For example, if the initial conditions involve a δ-function, (e.g., in (7.3.5) below), we can use

$$\phi(x) = \begin{cases} \frac{1}{N_k}\,(1-x^2)^k, & |x| \leq 1 \\ 0, & \text{otherwise} \end{cases} \tag{3.4.1}$$

where

$$N_k = \int_{-1}^{1} (1-x^2)^k\,dx = \frac{\sqrt{\pi}\,\Gamma(k+1)}{\Gamma(k+3/2)}$$

is chosen so that $\int \phi(x)\,dx = 1$. This is a C_0^k approximation of the δ-function (a so-called delta-like sequence) [103]. Thus if we take

$$\phi_\epsilon = \frac{1}{\epsilon}\,\phi\Big(\frac{x}{\epsilon}\Big) \tag{3.4.2}$$

then $\phi_\epsilon(x)$ converges to $\delta(x)$ as $\epsilon \to 0$ in the sense of distributions, with ϕ_ϵ piecewise polynomial with compact support on (-1,1). In Chapter 4, we discuss the convergence of solutions as $\epsilon \to 0$. In the practical calculations below, we used the value of $k = 6$.

3.5 Remarks on implementation

3.5.1 Nonhomogeneous boundary conditions

It is well known in the theory of partial differential equations that it suffices to construct a method for homogeneous boundary conditions and an arbitrary nonzero source term. Thus, if either or both of $\psi(t)$ and $\theta(t)$ in (3.1.1) are nonzero, we use the following standard technique: define a modified function, which differs from the original one by a polynomial with given values at the boundaries, so that the new function satisfies the modified equation with homogeneous boundary conditions. For example, in the case of a finite problem with Dirichlet boundary conditions (i.e., $B[u] = u$), we choose

$$v(t,\xi) = u(t,\xi) - \xi\theta(t) + (\xi - 1)\psi(t) \tag{3.5.1}$$

It can be shown that v satisfies

$$v_t = \tilde{L}_{t,\xi}[v] + F(t,\xi),$$

$$F(t,\xi) = \tilde{f}(t,\xi) - \xi\dot{\theta}(t) + (\xi - 1)\dot{\psi}(t)$$
$$+ \left(\frac{\tilde{\alpha}_1(t,\xi)}{s(t)} + \frac{\xi}{s(t)}\frac{ds}{dt}\right)\big(\theta(t) - \psi(t)\big) + \tilde{\alpha}_0(t,\xi)\big(\xi\theta(t) - (\xi - 1)\psi(t)\big)$$

and $v = 0$ at $\xi = 0$, 1. Similar manipulations can be performed for other types of boundary conditions as well. Thus without loss of generality we further assume all boundary conditions homogeneous.

3.5.2 Domain decomposition

Often the accuracy of computations can be improved by decomposing $[-1,1]$ into several subdomains. To do this we set

$$-1 = \beta_0 < \beta_1 < \ldots < \beta_{K-1} < \beta_K = 1$$

and we write the equations on each interval $\Delta_j = [\beta_j, \beta_{j+1}]$, $j = 0, \ldots, K-1$, with boundary conditions that reflect the continuity of u and u_y at each node β_j. The transformation

$$z_j = \frac{2}{\beta_{j+1} - \beta_j}(y - \beta_j) - 1 = \frac{2y - (\beta_j + \beta_{j+1})}{\beta_{j+1} - \beta_j}, \quad j = 0, \ldots, K-1$$

maps each of the subintervals to $[-1,1]$, and we can thus solve each of the K "small" problems with the same technique as the original "large" one, but with the new boundary conditions

$$\begin{aligned}
B_1\big[u^{(0)}\big] &= 0 \\
u^{(j)}(t,1) &= u^{(j+1)}(t,-1), && j = 0, \ldots, K-2 \\
\frac{2}{\beta_{j+1} - \beta_j} u_z^{(j)}(t,1) &= \frac{2}{\beta_{j+2} - \beta_{j+1}} u_z^{(j+1)}(t,-1), && j = 0, \ldots, K-2 \\
B_2\big[u^{(K-1)}\big] &= 0
\end{aligned}$$

Here, B_1 and B_2 are the originally prescribed boundary conditions at ± 1, and $u^{(j)}$ is the function u restricted to the interval Δ_j, i.e., $u^{(j)} = u(t, y(z_j))$.

This is not an uncommon technique in spectral methods [16, Chapter 22]. A whole class of numerical methods — the so-called spectral elements — is devoted to the development of this idea, especially in more than one space dimension. In our setting, it serves two purposes. Firstly, any isolated singularities in the initial data are localized in the smaller interval and interact with the solution at other points in the domain only through matching at the boundaries of adjacent segments. Secondly, if enough subintervals are taken, each of the $u^{(j)}$'s is "flatter" than the original u, so we can use fewer Chebyshev polynomials per interval to represent it at the same level of accuracy. This can benefit higher derivative calculations, like (3.2.3), since any errors in higher-order modes there are multiplied by large numbers ($O(n^6)$ for the third derivative), which has the potential of deteriorating the

accuracy of the computation; so it is important to use a reduced number of polynomials if possible.

There is, obviously, a great deal of freedom in choosing the position of the nodes β_j. It is not the purpose of this work to present a general method of doing so, since we only use domain decomposition as an auxiliary tool. We have found, for instance, that even simple partitioning of the domain in subintervals of equal length can decrease the error significantly at the cost of a reasonable increase in complexity. If the dynamics of the problem is more localized, the β_j's can be distributed more densely around the more significant parts of the large interval. As the solution gets smoother for larger times, the number of subintervals may decrease and their lengths may become more uniform. In certain cases (see Section 7.5), such adaptivity in the domain decomposition substantially reduces the number of subintervals required to resolve the solution accurately, and the savings in computation time over uniform decomposition are considerable.

3.6 Reduced form

In view of the previous considerations, the original moving boundary problem in the form,

$$u_t = L_{t,\,y;\,s(t)}(u) + f(t,y;s(t)), \quad t>0,\ -1\le y\le 1, \tag{3.6.1}$$

$$u(0,y)=\phi(y), \quad s(0)=s_0, \tag{3.6.2}$$

$$B_1[u](t,-1)=0,\ B_2[u](t,1)=0, \tag{3.6.3}$$

$$\frac{ds}{dt} = \begin{cases} -\dfrac{2}{\lambda\, s(t)}\, u_y(t,1) & \text{Stefan} \\ -\dfrac{s(t)\,\left[L_{t,\,y;\,s(t)}(u)\right]_y(t,1)}{2\,u_{yy}(t,1)} & \text{implicit} \end{cases} \tag{3.6.4}$$

can be reduced to a system of $N+1$ differential equations of the form

$$\frac{da_n}{dt} = \sum_{m=0}^{N-1} A_{nm}(s,\dot{s})\, a_m + f_n, \qquad 0\le n\le N-3, \tag{3.6.5}$$

$$a_n(0)=\phi_n, \quad s(0)=s_0, \tag{3.6.6}$$

$$\sum_{n=0}^{N-1} q_1(n)\, a_n = \sum_{n=0}^{N-1} q_2(n)\, a_n = 0, \tag{3.6.7}$$

$$\frac{ds}{st} = G(t,s,a_0,\ldots,a_{N-1}), \tag{3.6.8}$$

where $a_n(t)$, $f_n(t)$ and ϕ_n are the Chebyshev coefficients of the solution, source term and the initial data, respectively; and the exact forms of A_{nm}, $q_i(n)$ and G depend on the specific form of the spatial operator L and boundary conditions. For example, the Chebyshev coefficients of the first and second derivatives have the form

$$a_n^{(1)} = \frac{2}{c_n} \sum_{\substack{m=n+1 \\ m+n \text{ odd}}}^{\infty} m a_m,$$

$$a_n^{(2)} = \frac{1}{c_n} \sum_{\substack{m=n+2 \\ m+n \text{ even}}}^{\infty} m(m^2 - n^2) a_m,$$

with

$$c_0 = 2, \quad c_n = 1, \ n > 0.$$

For similar expressions for other derivatives and combinations, see [49].

Thus, for example, the classical Stefan problem for the melting of an ice slab,

$$\begin{aligned} &u_t = u_{xx}, && 0 < x < s(t), \\ &u(0,x) = 0, && s(0) = s_0, \\ &u(t,0) = 1 \\ &u(t,s(t)) = 0, \quad u_x(t,s(t)) = -\lambda \frac{ds}{dt} \end{aligned}$$

after the transformations is reduced to the following system,

$$\begin{aligned} \frac{da_n}{dt} = \frac{1}{c_n} \frac{4}{s^2(t)} \sum_{\substack{m=n+2 \\ m+n \text{ even}}}^{N-1} m(m^2 - n^2) a_m + \frac{2}{c_n} \frac{\dot{s}(t)}{s(t)} \left(\sum_{m=n+1}^{N-1} m a_m + \frac{n a_n}{2} \right) \\ - \frac{u_0}{2} \frac{\dot{s}(t)}{s(t)} \Big(\delta_{n,1} + \delta_{n,0} \Big), \qquad 0 \le n \le N-3, \\ a_n(0) = \frac{u_0}{2} \Big(\delta_{n,1} - \delta_{n,0} \Big), \quad s(0) = s_0, \\ \sum_{n=0}^{N-1} (-1)^n a_n = \sum_{n=0}^{N-1} a_n = 0, \\ \frac{ds}{dt} = -\frac{2}{\lambda s(t)} \left(\sum_{n=0}^{N-1} n^2 a_n - \frac{u_0}{2} \right) \end{aligned}$$

(Here, $\delta_{n,k}$ is Cronecker's delta symbol.)

Chapter 4

Convergence

A mathematician's reputation rests
on the number of bad proofs he has given.
(A. S. Besicovich, 1891–1970)

In the previous Chapter we introduced convergent approximations of singular initial data with sequences of smooth functions. From the general theory of Stefan problems [81, 85], we know that the solution produced by each element of the approximating sequence is classical, i.e., at least $C^2(I_s) \times C^1[0,t]$ for all t, so it can be computed accurately by spectral methods. To determine the way these smooth solutions relate to the true solution of the singular problem, we investigate their convergence, as the initial approximation gets sharper, and study the corresponding convergence rates. For simplicity we restrict our analysis to the linear (i.e., fixed boundary) setting. This provides a rationalization for the convergence rates observed in the examples presented in Chapters 6 and 7.

4.1 Main result

The general moving boundary problem was formulated in Chapter 3 for the parabolic equation

$$u_t = L_x[u] + f(t,x) = \alpha_2(t,x)\, u_{xx} + \alpha_1(t,x)\, u_x + \alpha_0(t,x)\, u + f(t,x)$$

with $x \in I_s$, where $I_s = [0, s(t)]$ (finite case) or $I_s = [s(t), \infty)$ (semi-infinite case). For $s(0) = s_0$, we define I_0 similarly. Restricting ourselves to the following singular initial-boundary value problem with $s(t) \equiv s_0$

$$\begin{aligned} &u_t = L_x[u] + f(t,x), \quad x \in I_0,\ t > 0 \\ &u(0,x) = u_0(x), \qquad\quad B[u] = 0 \end{aligned} \tag{4.1.1}$$

we prove a general convergence result.

Since we shall be working with initial data that are distributions, we briefly review the basic concepts and notation, following [75, Chapter 4]. The space $\mathcal{D}(\mathbb{R})$ contains all infinitely differentiable functions on the real line with compact support and is equipped with topology of uniform convergence on compact subsets of $\mathbb{R}$. Distributions are the elements of the space $\mathcal{D}'(\mathbb{R})$ of continuous linear functionals on $\mathcal{D}(\mathbb{R})$. The spaces $\mathcal{E}(\mathbb{R})$ and $\mathcal{E}'(\mathbb{R})$ are defined similarly for C^∞ functions with no restriction on support. For example, Dirac's δ-function is an element of both $\mathcal{D}'(\mathbb{R})$ and $\mathcal{E}'(\mathbb{R})$. We say that $T \in \mathcal{D}'(\mathbb{R})$ (or $\mathcal{E}'(\mathbb{R})$) is a *zero distribution* on an open set $\Omega \subset \mathbb{R}$, if $T[\psi] = 0$ for every $\psi \in \mathcal{D}(\mathbb{R})$ (respectively, $\psi \in \mathcal{E}(\mathbb{R})$), such that the support of ψ is contained inside Ω. Then the *support of a distribution* T, denoted $\operatorname{supp}(T)$, is defined as the complement in $\mathbb{R}$ of the largest open subset of $\mathbb{R}$ where T is a zero distribution. For any set $S \subset \mathbb{R}$, we say that $T \in \mathcal{E}'(S)$ if $T \in \mathcal{E}'(\mathbb{R})$ and $\operatorname{supp}(T) \subset S$. Finally, a sequence of distributions $T_n \in \mathcal{E}'$ is said to *converge weakly* to a distribution $T \in \mathcal{E}'$ as $n \to \infty$ if $\forall\, \psi \in \mathcal{E}$, the numerical sequence $\{T_n[\psi]\}$ converges to $T[\psi]$:

$$T_n \rightharpoonup T \quad \text{as } n \to \infty \quad \text{in } \mathcal{E}' \qquad \text{if} \qquad T_n[\psi] \to T[\psi] \quad \text{in } \mathbb{R}$$

We now formulate the convergence result for the problem (4.1.1).

Theorem 1. *Assume that $\alpha_i \in C^2_x \times C^1_t$, $i = 0, 1, 2$, and the source term $f(t,x)$ is continuous in both variables. Consider an initial-boundary value problem with $u(0,x) = \varphi(x) \in \mathcal{E}'(I_0)$ and a family of problems with $u_n(0,x) = \phi_n(x) \in C^k(I_0)$ for some some $k > 0$, so that $\operatorname{supp}\phi_n \subset I_0$. Suppose $\phi_n \rightharpoonup \varphi$ in $\mathcal{E}'$; and denote $u_n(t,x)$ the solutions of each problem with $u_n(0,x) = \phi_n(x)$ and $u(t,x)$ the solution of (4.1.1) with $u(0,x) = \varphi(x)$. If for any $\psi \in \mathcal{E}(I_0)$,*

$$\big|\phi_n[\psi] - \varphi[\psi]\big| \le M_\psi \varepsilon_n \tag{4.1.2}$$

for some sequence $\varepsilon_n \to 0$ and a constant M_ψ depending on ψ, then on any finite interval $(0,T]$ we have

$$\sup_{x \in I_0} |u_n(t,x) - u(t,x)| \le K(t)\, \varepsilon_n \tag{4.1.3}$$

where $K(t)$ is bounded on any segment $[t_0, T]$, $t_0 > 0$, and $K(t) \to \infty$ as $t \to 0$. In particular, $u_n(t,x)$ converges to $u(t,x)$ uniformly in I_0 as $n \to \infty$ for all finite positive t, and $u(t,x)$ is continuous.

Remark. The dependence of K in (4.1.3) on t reflects the fact that convergence is faster for larger t, as the initial singularities smooth out, while at $t = 0$ the estimate is not valid, since the limiting initial value $\varphi \in \mathcal{E}'(I_0)$ is, in general, not bounded.

Proof. We present the proof for Dirichlet boundary conditions, i.e.,

$$\begin{aligned} &u(t,0) = u(t,s_0) = 0 \quad I_0 = [0,s_0] \quad \text{(finite problem)} \\ &u(t,s_0) = u(t,\infty) = 0 \quad I_0 = [s_0,\infty) \quad \text{(semi-infinite problem)} \end{aligned} \tag{4.1.4}$$

Other types of boundary conditions can be treated in the same way.

Recall that the adjoint operator to L_x (3.0.4) is [43]

$$L_x^* = \alpha_2(t,x)\,\frac{\partial^2}{\partial x^2} + (2\alpha_{2,x}(t,x) - \alpha_1(t,x))\,\frac{\partial}{\partial x} + \alpha_0(t,x) - \alpha_{1,x}(t,x) + \alpha_{2,xx}(t,x). \tag{4.1.5}$$

In view of the assumed regularity of the coefficients, we can construct a fundamental solution $G(x,t;\xi,\tau)$ of the operator L_x^*, which is in class C^2 in x and C^1 in t for $(x,t) \neq (\xi,\tau)$ [43]. For a finite problem, we choose the fundamental solution vanishing at $x = 0$; the corresponding condition in the semi-infinite case (i.e., $G \to 0$ as $x \to \infty$) is verified automatically. Integrating Green's identity [43, p. 27]

$$\begin{aligned} &\int_0^{t_\varepsilon}\int_{I_0} \left\{(G_t + L_x^*[G])u + (u_t - L_x[u])G\right\} d\xi\, d\tau \\ &= \int_0^{t_\varepsilon}\int_{I_0} \left\{ \frac{\partial}{\partial\xi}\left[\alpha_2 G u_\xi - \alpha_2 u G_\xi + (\alpha_1 - \alpha_{2,\xi})uG\right] - (uG)_\tau \right\} d\xi\, d\tau \end{aligned}$$

by parts using the initial and boundary conditions, and letting $t_\varepsilon \to t$ from below, we obtain the following integral equation for $u(t,x)$ (cf. [43])

$$\begin{aligned} u(t,x) = -\int_0^t\int_{I_0} G(x,t;\xi,\tau)\, f(\tau,\xi)\, d\xi\, d\tau + \int_{I_0} G(x,t;\xi,0)\, u_0(\xi)\, d\xi \\ + \int_0^t \alpha_2(\tau,s_0)\, G(x,t;s_0,\tau) u_\xi(\tau,s_0)\, d\tau. \end{aligned} \tag{4.1.6}$$

Note that $u_0(x)$ is supported on I_0, and therefore the second term on the right-hand side is well-defined. The last term appears due to the fact that G does not satisfy the boundary

condition at $x = s_0$. Taking $u_0(x) = \phi_n(x)$ produces the solution $u_n(t,x)$, while $u_0(x) = \varphi(x)$ produces $u(t,x)$. Since for each n, $\phi_n \in C^k(I_0)$ with $k > 0$, it follows that the corresponding solutions of the parabolic equation satisfy $u_n \in C_x^2 \times C_t^1$ for $t > 0$ for any n. We take two such solutions u_m and u_n and subtract the corresponding versions of equation (4.1.6) from each other. Estimating the absolute value of the difference yields

$$|u_n(t,x) - u_m(t,x)| \le \left| \int_{I_0} G(x,t;\xi,0)(\phi_n(\xi) - \phi_m(\xi))\, d\xi \right| \tag{4.1.7}$$
$$+ \left| \int_0^t \alpha_2(\tau,s_0)\, G(x,t;s_0,\tau)\big[u_{n,\xi}(\tau,s_0) - u_{m,\xi}(\tau,s_0)\big]\, d\tau \right| = J_1 + J_2$$

For the first term we write

$$J_1 = \left| \int_{I_0} G(x,t;\xi,0)(\phi_n(\xi) - \phi_m(\xi))\, d\xi \right|$$
$$\le \left| \int_{I_0} G(x,t;\xi,0)(\phi_n(\xi) - \phi(\xi))\, d\xi \right| + \left| \int_{I_0} G(x,t;\xi,0)(\phi(\xi) - \phi_m(\xi))\, d\xi \right|$$

According to the estimates in [43, p. 134, formula (1.4)], the fundamental solution $G(x,t;\xi,\tau)$ satisfies

$$\big|\, G(x,t;\xi,\tau)\big| \le \frac{\text{const}}{(t-\tau)^\mu} \frac{1}{|x-\xi|^{1-2\mu}} \tag{4.1.8}$$

for $\mu \in (0,1)$. Therefore $G(x,t;\xi,0) = t^{-\mu}\tilde{G}(x,t;\xi,0)$, where $\tilde{G}(x,t;\xi,0) \in \mathcal{E}$ in the variable ξ for all x and t. It follows that if (4.1.2) holds, then we have

$$J_1 \le \frac{M_G}{t^\mu}\,(\varepsilon_n + \varepsilon_m) \tag{4.1.9}$$

where the M_G is a constant. For the second term in (4.1.7) we simply write

$$J_2 \le \int_0^t \big|\, \alpha_2(\tau,s_0)\, G(x,t;s_0,\tau)\big|\, \big|u_{n,\xi}(\tau,s_0) - u_{m,\xi}(\tau,s_0)\big|\, d\tau \tag{4.1.10}$$

Thus (4.1.7) implies that, as long as (4.1.2) holds for the initial data, we have

$$|u_n(t,x) - u_m(t,x)| \le \frac{M_G}{t^\mu}\,(\varepsilon_n + \varepsilon_m) + J_2 \tag{4.1.11}$$

The conclusion is now based on the following

Lemma 1 . *Let $u_m(t,x)$ and $u_n(t,x)$ be the solutions defined above. Then for any $t > t_0$, the fluxes across the line $x = s_0$ satisfy the inequality:*

$$\left|u_{n,x}(t,s_0) - u_{m,x}(t,s_0)\right| \leq \left(\frac{2\tilde{M}_G}{t^\gamma} + K_1(t)\right)(\varepsilon_n + \varepsilon_m) \tag{4.1.12}$$

for any t, if only (4.1.2) holds, where $\frac{1}{2} < \gamma < 1$, $\tilde{M}_G$ is a constant, depending on G, and K_1 is bounded on $[0,T]$ and independent of m and n.

Once we establish this result, the theorem is proved as follows. Combining (4.1.10) and (4.1.11), we conclude that

$$J_2 \leq (\varepsilon_n + \varepsilon_m) \int_0^t \left|\, \alpha_2(\tau, s_0)\, G(x,t;s_0,\tau)\right| \left(\frac{\tilde{M}_G}{\tau^\gamma} + K_1(\tau)\right) d\tau$$

Due to the estimate (4.1.8), J_2 can further be bounded by

$$J_2 \leq \tilde{M}_G\,(\varepsilon_n + \varepsilon_m)\, F(x;s_0) \int_0^t \frac{v(\tau)\, d\tau}{\tau^\gamma (t-\tau)^\mu}$$

where $F(x,s_0)$ carries the spatial dependence of G_x and α_2, and $v(\tau)$ is bounded. Since both γ and μ are strictly less than 1, the singularities at 0 and t are integrable, and we conclude that

$$J_2 \leq \tilde{M}_G K_2(t)\, F(x;s_0)\,(\varepsilon_n + \varepsilon_m)$$

where $K_2(t)$ and $F(x;s_0)$ are bounded for all x, t. Combining this inequality with (4.1.11), we obtain

$$|u_n(t,x) - u_m(t,x)| \leq \left(\frac{M_G}{t^\mu} + \tilde{M}_G K_2(t)\, F(x;s_0)\right)(\varepsilon_n + \varepsilon_m)$$

for any $t > 0$ and $x \in I_0$, which implies

$$\sup_{x \in I_0} |u_n(t,x) - u_m(t,x)| \leq K(t)\,(\varepsilon_n + \varepsilon_m) \tag{4.1.13}$$

where

$$K(t) = \frac{M_G}{t^\mu} + \tilde{M}_G K_2(t) \max_{x \in I_0} |F(x;s_0)| \to \infty \quad \text{as } t \to 0$$

However, $K(t)$ is bounded on any segment $[t_0, T]$ for any $t_0 > 0$, so taking the limit as $m, n \to \infty$ yields

$$\sup_{x \in I_0} |u_n(t,x) - u_m(t,x)| \to 0 \quad \text{as } m, n \to \infty$$

and by Cauchy's criterion, the sequence u_n converges uniformly in $C^0(I_0)$ for any $t \in [t_0, T]$. Hence the limit is a continuous function as well, which, by linearity, satisfies the integral equation (4.1.6) with $u(0,x) = \varphi(x)$, i.e., is a solution of the given problem with the singular initial data. By uniqueness of solutions of parabolic initial-boundary value problems, $u(t,x)$ has to be the sought solution of the singular problem. Since $t_0 > 0$ and T were chosen arbitrarily, it follows that the convergence result holds for any finite positive t.

Proof of Lemma 1. Since $\alpha_2(t,x)$ is smooth on the closed domain $I_0 \times [t_0, T] \subset \mathbb{R}^2$, it is also bounded on it. We assume, without loss of generality, that

$$\sup_{x,\,t} |\alpha_2(t,x)| \le 1 \tag{4.1.14}$$

(If $h \equiv \sup |\alpha_2| > 1$, we stretch the t variable according to $t \to t/h$. This results in dividing the spatial part of the original differential equation by h, and in particular, makes the maximum of the new α_2 no larger than 1.)

For any $t > 0$ and any $x \neq s_0$, differentiating (4.1.6) yields

$$u_x(t,x) = -\int_0^t \int_{I_0} G_x(x,t;\xi,\tau)\, f(\tau,\xi)\, d\xi\, d\tau + \int_{I_0} G_x(x,t;\xi,0)\, u_0(\xi)\, d\xi + \int_0^t \alpha_2(\tau,s_0)\, G_x(x,t;s_0,\tau)\, u_\xi(\tau,s_0)\, d\tau. \tag{4.1.15}$$

By virtue of the estimates of [43, p. 134, formulas (1.3), (1.5) and (1.6)], we have

$$\left| G_x(x,t;\xi,\tau) \right| \le \frac{\text{const}}{(t-\tau)^{\mu_1}} \frac{1}{|x-\xi|^{2-2\mu_1}} + \frac{\text{const}}{(t-\tau)^{\mu_2}} \frac{1}{|x-\xi|^{2-2\mu_2-\nu}} \tag{4.1.16}$$

where $\nu > 0$, $\frac{1}{2} < \mu_1 < 1$ and $1 - \frac{\nu}{2} < \mu_2 < 1$. Thus all integrals in (4.1.15) are uniformly convergent and differentiation under the integral sign is justified. Letting $x \to s_0^-$ creates no problems for the first two integrals, while the last one has a jump, like that of the derivative of a single-layer potential [43]. We thus have the following equation for the flux across

$x = s_0$

$$u_x(t,s_0) = -\int_0^t \int_{I_0} G_x(s_0,t;\xi,\tau)\, f(\tau,\xi)\, d\xi\, d\tau + \int_{I_0} G_x(s_0,t;\xi,0)\, u_0(\xi)\, d\xi$$
$$+ \int_0^t \alpha_2(\tau,s_0)\, G_x(s_0,t;s_0,\tau)\, u_\xi(\tau,s_0)\, d\tau + \frac{1}{2}\,\alpha_2(t,s_0)\, u_x(t,s_0).$$

Writing two copies of the above equations for $u_{n,x}$ and $u_{m,x}$, with initial conditions ϕ_n and ϕ_m, respectively, and subtracting one from the other, we obtain

$$|u_{n,x}(t,s_0) - u_{m,x}(t,s_0)| \le \left| \int_{I_0} G_x(s_0,t;\xi,0)\,\big(\phi_n(\xi) - \phi_m(\xi)\big)\, d\xi \right| \tag{4.1.17}$$
$$+ \int_0^t \big|\alpha_2(\tau,s_0)\, G_x(s_0,t;s_0,\tau)\big|\big|u_{n,\xi}(\tau,s_0) - u_{m,\xi}(\tau,s_0)\big|\, d\tau$$
$$+ \frac{1}{2}\,|\alpha_2(t,s_0)|\,\big|u_{n,x}(t,s_0) - u_{m,x}(t,s_0)\big|.$$

The first term in (4.1.17) can be estimated in the same manner as J_1 in (4.1.7). In the estimates (4.1.16), let $\gamma = \max\{\mu_1,\mu_2\}$. Then $G_x(s_0,t;\xi,0) = t^{-\gamma}\tilde{F}(s_0,t;\xi,0)$, where $\tilde{F} \in \mathcal{E}'(I_0)$ in the variable ξ for all t. Thus, if (4.1.2) holds, we have $\big($cf. (4.1.9)$\big)$

$$\left| \int_{I_0} G_x(s_0,t;\xi,0)\,\big(\phi_n(\xi) - \phi_m(\xi)\big)\, d\xi \right| \le \frac{\tilde{M}_G}{t^\gamma}\,(\varepsilon_n + \varepsilon_m). \tag{4.1.18}$$

where $\tilde{M}_G$ depends on $G_x(s_0,t;\xi 0)$, and therefore on G. According to the estimate [43, p. 137], the derivative of the fundamental solution at the boundary satisfies

$$|G_x(s_0,t;\xi,\tau)| \le \frac{\text{const}}{(t-\tau)^\mu}\,\frac{1}{|s_0-\xi|^{2-2\mu-\beta}} \tag{4.1.19}$$

for any $1 - \beta/2 < \mu < 1$, i.e., $\mu + \beta/2 > 1$, so $G_x(s_0,t;\xi,\tau)$ is finite as $\xi \to s_0$ for a fixed τ, and the singularity as $\tau \to t$ is integrable. Thus the $\alpha_2\, G_x$ in the second term of (4.1.17) has a finite integral.

Finally, in view of the relation (4.1.14), the last term in (4.1.17) is bounded by

$\frac{1}{2}\left|u_{n,x}(t,s_0)-u_{m,x}(t,s_0)\right|$, and we can move it to the left-hand side to obtain

$$|u_{n,x}(t,s_0)-u_{m,x}(t,s_0)| \le \frac{2\tilde{M}_G}{t^\gamma}\,(\varepsilon_n+\varepsilon_m) + 2\int_0^t \left|\alpha_2(\tau,s_0)\,G_x(s_0,t;s_0,\tau)\right|\left|u_{n,\xi}(\tau,s_0)-u_{m,\xi}(\tau,s_0)\right|\,d\tau \tag{4.1.20}$$

We can now apply the following version of Gronwall's inequality (see, e.g., [25]), which we prove below:

Lemma 2. *Suppose for continuous function $w(t)\ge 0$, and absolutely integrable functions $g(t),\psi(t)>0$*

$$w(t)\le \psi(t)+\int_0^t g(\tau)w(\tau)\,d\tau \tag{4.1.21}$$

Then

$$w(t)\le \psi(t)+\int_0^t g(\tau)\,\psi(\tau)\exp\left(\int_\tau^t g(y)\,dy\right)\,d\tau \tag{4.1.22}$$

In (4.1.20), we let $w(\tau)=|u_{n,x}(\tau,s_0)-u_{m,x}(\tau,s_0)|$, $g(\tau)=2|\alpha_2(\tau,s_0)\,G_x(s_0,t;s_0,\tau)|$, and $\psi(t)=2\tilde{M}_G t^{-\gamma}(\varepsilon_n+\varepsilon_m)$. Then by (4.1.22) we have

$$|u_{n,x}(t,s_0)-u_{m,x}(t,s_0)| \le \frac{2\tilde{M}_G}{t^\gamma}\,(\varepsilon_n+\varepsilon_m) + 4\,(\varepsilon_n+\varepsilon_m)\int_0^t |\alpha_2(\tau,s_0)\,G_x(s_0,t;s_0,\tau)|\,\exp\left(2\int_\tau^t \left|\alpha_2(y,s_0)\,G_x(s_0,t;s_0,y)\right|\,dy\right)\,\frac{d\tau}{\tau^\gamma}$$

We use the estimates (4.1.19) once again to observe that the integrand in the second term is $\le \text{const}\,(t-\tau)^{-\gamma}t^{-\gamma}$, so the singularities at 0 and t are integrable, and we indeed have

$$|u_{n,x}(t,s_0)-u_{m,x}(t,s_0)| = \left(\frac{2\tilde{M}_G}{t^\gamma}+K_1(t)\right)(\varepsilon_n+\varepsilon_m)$$

with K_1 bounded and depends only on α_2, G and s_0, so Lemma 1 is proved.

Proof of Lemma 2. Denote

$$q(t)=\int_0^t g(\tau)\,w(\tau)\,d\tau \tag{4.1.23}$$

Then, after multiplying both sides of (4.1.21) by $g(t) > 0$, we obtain

$$q'(t) \leq \psi(t)\, g(t) + g(t)\, q(t)$$

Moving the last term to the left-hand side produces

$$q'(t) - g(t)\, q(t) = e^{\int_0^t g(y)\, dy} \frac{d}{dt} \left(q(t)\, e^{-\int_0^t g(y)\, dy} \right) \leq \psi(t)\, g(t)$$

Multiplying through by $\exp\left(-\int_0^t g(y)\, dy\right)$ and integrating from 0 to t yields

$$q(t)\, e^{-\int_0^t g(\tau)\, d\tau} - q(0) \leq \int_0^t \psi(\tau)\, g(\tau)\, \exp\left(-\int_0^\tau g(y)\, dy\right) d\tau$$

implying, since $q(0) = 0$ (4.1.23), that

$$q(t) \leq \int_0^t \psi(\tau)\, g(\tau)\, \exp\left(-\int_\tau^t g(y)\, dy\right) d\tau$$

Using the definition of $q(t)$ (4.1.23) and the given inequality (4.1.21), we conclude that

$$w(t) \leq \psi(t) + \int_0^t g(\tau)\, \psi(\tau) \exp\left(\int_\tau^t g(y)\, dy\right)\, d\tau$$

as required.

Theorem 1 is thus proved completely.

4.2 Rate of convergence for δ-like sequences

Clearly, for practical purposes, it is important to have an estimate on the rate of convergence of the approximate solutions to the exact solution. We present the result for a class of distributional initial data, valid for most of the singular problems considered below.

We see from the formulas (4.1.2) and (4.1.3) that the rate of convergence of u_n to u in the supremum norm is driven by the rate of the weak convergence of ϕ_n to φ in $\mathcal{E}'$. Therefore for those problems whose initial data are distributions, the following statement is

important.

Proposition 1 . *Recall the C^k approximation of the δ-function introduced in Section 3.4*

$$\phi(x) = \begin{cases} \frac{1}{N_k}\,(1-x^2)^k, & |x| \le 1 \\ 0, & \text{otherwise} \end{cases} \tag{4.2.1}$$

where

$$N_k = \int_{-1}^{1} (1-x^2)^k\,dx = \frac{\sqrt{\pi}\,\Gamma(k+1)}{\Gamma(k+3/2)}$$

is chosen so that $\int \phi(x)\,dx = 1$, and the corresponding family

$$\phi_\epsilon = \frac{1}{\epsilon}\,\phi\Big(\frac{x}{\epsilon}\Big) \tag{4.2.2}$$

Then $\phi_\epsilon \rightharpoonup \delta_0$, Dirac's functional, in $\mathcal{E}'(\mathbb{R})$ as $\epsilon \to 0$ quadratically, i.e., for any $\psi \in \mathcal{E}(\mathbb{R})$

$$|\phi_\epsilon[\psi] - \delta_0[\psi]| = O(\epsilon^2). \tag{4.2.3}$$

Proof. For any $\psi \in \mathcal{E}$ we have

$$\big|\phi_\epsilon[\psi] - \delta_0[\psi]\big| \le \left| \int_{-\infty}^{+\infty} \phi_\epsilon(x)\psi(x)\,dx - \psi(0) \right|$$

Since ϕ_ϵ were constructed in such a way that their integral over the real line is equal to unity, we can write

$$\psi(0) = \int_{-\infty}^{+\infty} \phi_\epsilon(x)\psi(0)\,dx$$

Furthermore, ϕ_ϵ is supported on the segment $[-\epsilon, \epsilon]$, so the integral is only evaluated in these limits. Finally, we make the change of variables $x \to x/\epsilon$ and use (3.4.2) so that

$$\big|\phi_\epsilon[\psi] - \delta[\psi]\big| \le \left| \int_{-1}^{1} \phi(x)\big(\psi(\epsilon x) - \psi(0)\big)\,dx \right| \tag{4.2.4}$$

Using Taylor series, we find

$$\psi(\epsilon x) - \psi(0) = \epsilon x \psi'(0) + \frac{\epsilon^2 x^2}{2}\,\psi''(0) + O(\epsilon^3)$$

Substituting this back into (4.2.4), we find

$$\left|\phi_\epsilon[\psi] - \delta[\psi]\right| \le \left| \int_{-1}^{1} \phi(x)\big(\epsilon x \psi'(0) + \frac{\epsilon^2 x^2}{2}\,\psi''(0) + O(\epsilon^3)\big)\,dx \right|$$

Since the interval of integration is symmetric about 0, and the function $\phi(x)$ is even by construction (4.2.1), the integral of $x\,\phi(x)$ vanishes, and we have

$$\left|\phi_\epsilon[\psi] - \delta[\psi]\right| \le |\psi''(0)|\,\frac{\epsilon^2}{2}\,\left(\int_{-1}^{1} x^2\phi(x)\,dx\right) + o\,(\epsilon^2)$$

But $|\psi''(0)| \le M < \infty$, since ψ is smooth, and the integral of $x^2\phi(x)$ is obviously finite. Thus we have $\left|\phi_\epsilon[\psi] - \delta[\psi]\right| \le \tilde{M}\,\epsilon^2 + o\,(\epsilon^2)$, and Proposition 1 is thus proved.

We can now use the definition of weak derivatives to prove that if (4.2.3) holds, then the subsequent primitives of ϕ_ϵ converge in $\mathcal{E}'$, respectively, to Heavyside's function, $H(x)$, the function $\max(0, x)$, and so forth. Note also that Proposition 1 remains valid in $\mathcal{E}'(a, b)$, for any real interval (a, b), as long as it contains 0 as its interior point. The same result will hold if the peak of the δ-function is at any point x_0, such that $a < x_0 < b$.

Now we can prove the corresponding statement about the rate of convergence of solutions with approximated initial data, to the true solution.

Theorem 2. *In the problem (4.1.1), let x_0 be a point inside I_0. Suppose the initial condition is a distribution of the following general form,*

$$u(0, x) = u_0 = c_0(x)\delta(x - x_0) + c_1(x)H(x - x_0) + c_2(x)\max(0, x - x_0) + \ldots \qquad (4.2.5)$$

i.e., involves the δ-function and its primitives of any order. Let $u_{0,\phi,\epsilon}(x)$ be based on the approximation of $\delta(x - x_0)$ by $\phi_\epsilon(x - x_0)$ of (4.2.2). Then $u_{\phi,\epsilon}(t, x)$, the solution of (4.1.1) using $u_{0,\phi,\epsilon}(x)$ as the initial data, converges to $u(t, x)$, the true solution of this problem as $\epsilon \to 0$, uniformly in I_0, and the convergence is quadratic in ϵ.

Proof. By definition, $\phi_\epsilon \in C^k(I_0)$ for sufficiently small ϵ. By Proposition 1, $\phi_\epsilon \rightharpoonup \delta$ in $\mathcal{E}'(I_0)$, and the convergence rate is quadratic in the following sense: for any $\psi \in \mathcal{E}'(I_0)$, the sequence $\phi_\epsilon[\psi]$ converges quadratically to $\delta[\psi]$ as $\epsilon \to 0$. Thus if we pick any sequence $\epsilon_n \to 0$ as $n \to \infty$ and denote $\phi_n = \phi_{\epsilon_n}$, we have, due to (4.2.3) and the extension of Proposition 1,

$$\big|u_{0,\phi_n,\epsilon_n}[\psi] - u_0[\psi]\big| \le \text{const}\,\epsilon_n^2$$

which is an estimate of type (4.1.2). The δ-function and its primitives, restricted to I_0, all lie in $\mathcal{E}'(I_0)$. Therefore we can use Theorem 1 to conclude that $u_{\phi,\epsilon} \rightrightarrows u$ (uniformly) in I_0 for all finite positive t, and the convergence rate is also quadratic in ϵ, due to the estimate (4.1.3).

Remark 1. In general, the rate of convergence may no longer be quadratic in the case when $u(0,x)$ of (4.2.5) is supported on the boundary of I_0, unless the Green's function in (4.1.6) is of special form. However, if the singularity is weaker, the quadratic convergence rate may still be attained. For example, let $I_0 = [0, s_0]$ and

$$u(0,x) = \max(0,x) + \ldots$$

where $< \ldots >$ indicate smoother terms. We define $F(x)$ so that $F''(x) = \phi(x)$ of (4.2.1), and F_ϵ similarly with respect to ϕ_ϵ, so that $F_\epsilon(x) = \epsilon\, F(x/\epsilon)$ $\big($cf. (4.2.2)$\big)$. We have

$$\begin{aligned}\big|F_\epsilon[\psi] - \max(0,x)[\psi]\big| &= \left|\int_0^{s_0} \big[F_\epsilon(x) - \max(0,x)\big]\,\psi(x)\,dx\right| \\ &= \left|\int_0^{\epsilon} \Big[\epsilon\, F\big(\frac{x}{\epsilon}\big) - \max(0,x)\Big]\,\psi(x)\,dx\right|\end{aligned}$$

Making a change of variables $y = x/\epsilon$, we obtain

$$\big|F_\epsilon[\psi] - \max(0,x)[\psi]\big| = \epsilon\left|\int_0^{1} \big[\epsilon\, F(y) - \max(0,\epsilon y)\big]\,\psi(\epsilon y)\,dy\right|$$

But $\max(0, \lambda x) = \lambda \max(0, x)$, so we conclude that

$$\left|F_\epsilon[\psi] - \max(0,x)[\psi]\right| = \epsilon^2 \left| \int_0^1 \left[F(y) - \max(0,y)\right] \psi(\epsilon y)\, dy \right| = O(\epsilon^2) \tag{4.2.6}$$

This estimate will be useful in the discussion of the oxygen diffusion problem in Section 6.2.

Remark 2. We have proved convergence of our approximation construction to the true solution in a linear setting, since in the proof above, we assumed $s(t) \equiv s_0$ throughout. The estimate of convergence rates provided clearly suggests similar error bounds in the moving boundary setting. These are substantiated by various numerical experiments presented in Chapters 6 and 7. A complete generalization of these results to moving boundary problems is not direct, however. This is due to the fact that we have to account for the difference in the moving boundary values produced by different initial data, and the corresponding estimates have non-integrable kernels. For example, the formula (4.1.7) in the moving boundary setting becomes

$$\begin{aligned} |u_n(t,x) - u_m(t,x)| \le & \left| \int_0^t \left(\int_{s_m(\tau)}^{s_n(\tau)} G(x,t;\xi,\tau) f(\tau,\xi)\, d\xi \right) d\tau \right| \\ & + \left| \int_0^{s_0} G(x,t;\xi,0)(\phi_n(\xi) - \phi_m(\xi))\, d\xi \right| \\ & + \Bigg| \int_0^t \big[\alpha_2(\tau, s_n(\tau))\, G(x,t;s_n(\tau),\tau) u_{n,\xi}(\tau, s_n(\tau)) \\ & - \alpha_2(\tau, s_m(\tau))\, G(x,t;s_m(\tau),\tau) u_{m,\xi}(\tau, s_m(\tau))\big]\, d\tau \Bigg| \end{aligned}$$

and the difference of the fluxes (4.1.17) will contain expressions like

$$\int_0^t \left[\alpha(\tau, s_m(\tau))\, G_x(\tau, s_m(\tau); t, s_m(t)) - \alpha(\tau, s_n(\tau))\, G_x(\tau, s_n(\tau); t, s_n(t))\right] u_{n,\xi}(\tau, s_n(\tau))\, d\tau$$

If we proceed along the same lines as above to obtain bounds for these expressions, those will involve integrals of G_{xx}, whose singularity as $s_n(\tau) \to s_m(\tau)$ and $\tau \to t$ is no longer integrable [43]. Therefore we fall short of a rigorous proof of convergence for the full moving boundary case. We do want to point out that, in fact, even existence of generalized solutions

to Stefan problems has only been proved for initial data in class $H^1(I_0)$ [54], and there is no general result for problems whose initial conditions are distributions.

Chapter 5

Generalizations and Enhancements

Everything should be made as simple as possible,
but not simpler.
(Albert Einstein, 1879–1955)

The framework presented in Chapter 3, enforced by the convergence mechanism established in Chapter 4, gives a general numerical method for solving singular moving boundary problems. As we shall illustrate below (Chapters 6 and 7), this numerical method is capable of producing quantitative results of high quality for a wide range of problems. In certain practical cases, however, the goal is not to consistently produce progressively more accurate calculations, but to obtain a quick estimate of what the solution looks like, with reasonable, but not necessarily highest accuracy. Below we present two techniques which allow us to do just that. The applicability of these techniques can be limited, and convergence has not been established rigorously; therefore, these methods should be used with caution. Nevertheless in many cases these techniques act as very good extensions of our method and are capable of providing only slightly less accurate results for singular problems with a noticeable time economy (up to a factor of 10 for certain problems). The first procedure uses the ideas of analytic continuation to numerically evaluate certain expressions, while the second one uses prior integration in time to gain a degree of smoothness to the solution.

5.1 Padé approximations

In some of the problems we encounter, the initial data has only one singularity, which lies within the interval $(-1, 1)$. The resulting slow decay of Chebyshev coefficients deteriorates the accuracy of the spectral approximation at any point in $[-1, 1]$. This is the well-known "globalization" effect of spectral methods. This can be even more problematic in some of

the cases we investigate, as becomes evident from the following example.

Suppose we were solving an implicit moving boundary problem with initial data having a corner singularity inside the interval $(-1, 1)$. The Chebyshev coefficients decay initially like $O(1/n^2)$. As we have seen (e.g., (3.2.2)), the derivative of the moving boundary is proportional to the third derivative of the solution there, so that numerical evaluation of the velocity involves summing series like (3.2.3). But for $a_n = O(1/n^2)$ this series does not even converge, despite the fact that the third derivative itself is a well-defined function at that point.

For a related problem, recall the classical example of the geometric series

$$S(z) = \sum_{n=0}^{\infty} z^n = 1 + z + z^2 + \ldots + z^n + \ldots$$

which converges in for $|z| < 1$ and diverges for $|z| > 1$. At the same time, we know that this is a power series representation of the rational function

$$R(z) = \frac{1}{1 - z}$$

so identifying the power series with $R(z)$ for $|z| > 1$ is a way to continue $S(z)$ analytically beyond the circle of convergence. This is the idea behind Padé approximations of power series with rational functions.

We use this idea to resolve the difficulty stated above. We look at the series (3.2.3) as the definition of an analytic function. Thus computing u_{xxx} at $x = 1$ is equivalent to evaluating this analytic function outside of its circle of convergence, and Padé approximation can help. We can keep using the approximation for several time steps, until the coefficients start to decay fast enough for $x = 1$ to be inside the circle of convergence. We found this technique to be very helpful in starting off solutions from singular initial data.

5.2 Prior integration

The simplest case of a singularity in the initial data occurs when the initial value of the solution does not satisfy the boundary conditions. In their study of Chebyshev series solutions of linear parabolic equations, D. Knibb and R.E. Scraton [57] proposed to write a new problem for the time integral of the unknown function. The equation and boundary

conditions are modified slightly (or not at all, as in the case of homogeneous unforced problems), while the new initial condition satisfies a second-order differential equation and thus has two free constants, which can be chosen in a way to satisfy the boundary conditions. The new problem is therefore smooth, and it can be solved by the regular Chebyshev tau method. The solution of the original problem is obtained from the auxiliary solution by differentiation in time.

In [57], the following boundary value problem for the heat equation was considered

$$\begin{aligned} \frac{\partial^2 u}{\partial x^2} = P(x)\frac{\partial u}{\partial t}, \quad |x| < 1 \\ u(0,x) = K(x) \\ u(t,-1) = u(t,1) = 0 \end{aligned} \tag{5.2.1}$$

with $K(\pm 1) \neq 0$. The authors choose the new initial condition $K^*(x)$, so that

$$\frac{d^2 K^*(x)}{dx} = P(x)K(x)$$

which is consistent with (5.2.1), and take the solution that satisfies $K^*(\pm 1) = 0$. This can be done, since it is equivalent to solving a simple boundary value problem for a second-order ordinary differential equation. Consequently they find the solution $u^*(t,x)$ to (5.2.1) with the initial condition $u^*(0,x) = K^*(x)$ and the same boundary conditions as u. Once u^* is found, it is easy to show that

$$u(t,x) = \frac{\partial u^*}{\partial t} = \frac{1}{P(x)}\frac{\partial^2 u^*}{\partial x^2}$$

solves the original problem. We refer the reader to the original paper [57] for the details.

As shown in what follows, this ingenious method admits a direct generalization to moving boundary problems. To illustrate this fact we consider the following autonomous Stefan

problem,

$$u_t = L_x[u] + f(x), \quad 0 < x < s(t),\ t > 0 \tag{5.2.2}$$
$$u(0,x) = \phi(x), \quad s(0) = s_0$$
$$\beta_0 u(t,0) + \beta_1 u_x(t,0) = 0$$
$$u(t,s(t)) = 0, \quad u_x(t,s(t)) = -\lambda \frac{ds}{dt}$$

where the second-order differential operator $L_x[\,\cdot\,]$ does not depend on time. It is easy to see that if the pair $\{u^*(t,x),\ s(t)\}$ solves

$$u_t^* = L_x[u^*] + (t+1)f(x), \quad 0 < x < s(t),\ t > 0 \tag{5.2.3}$$
$$u^*(0,x) = \varphi(x) \text{ with } L_x[\varphi] + f(x) = \phi(x) \tag{5.2.4}$$
$$\beta_0 u^*(t,0) + \beta_1 u_x^*(t,0) = 0, \qquad L_x[u^*]\big(t,s(t)\big) + f\big(s(t)\big) = 0$$
$$\frac{ds}{dt} = -\frac{1}{\lambda}\frac{\partial}{\partial x}\Big(L_x[u^*](t,x) + (t+1)f(x)\Big)\Big|_{x=s(t)}, \quad s(0) = s_0$$

then the pair $\{u_t^*(t,x),\ s(t)\}$ solves (5.2.2). Note that, just as in the fixed-boundary case above, (5.2.4) is a second-order differential equation, which can be solved for $u^*(0,x) = \varphi(x)$, satisfying the boundary conditions at both ends. Also, the boundary condition at the moving end involves higher-order spatial derivatives of u^*, but these can all be expressed in terms of the Chebyshev coefficients of u^* just as well. If the solution of the original problem is unique, then this is what this condition will determine. The problem (5.2.3) is indeed smooth, so solving it with the Chebyshev tau method gives accurate solutions. We can also use the spectral representation of $L_x + (t+1)f$ to find the value of $u_t^* = u$ without accumulating any significant error from numerical differentiation. Thus we find the extended Knibb-Scraton approach to be a good way of enhancing accuracy.

Note that the same procedure applies to implicit moving boundary problems as well. The differential equation for the moving boundary will typically contain not the third, but the fifth spatial derivative of $u^*(t,x)$. If this series is divergent, we can use Padé approximations to sum it, as described in the preceding section.

The main difficulty with this approach becomes apparent for complicated spatial operators L_x. In these cases the representation of boundary conditions for the auxiliary function in terms of its Chebyshev coefficients may become very involved. As it is, the method is

not suitable for time-dependent right-hand sides, since in this case, the partial differential equation for u^* is essentially different from that for u and can be technically hard to derive.

Chapter 6

Numerical Results

Whenever you can, count.
(Sir Francis Galton, 1822–1911)

It is unworthy of excellent men to lose hours,
like slaves, on the labors of calculation.
(Gottfried Leibnitz, 1646–1716)

In this chapter we present results of the numerical experiments we used to test the performance of our methods. In Section 6.1, we apply the Chebyshev tau method directly to two Stefan-type problems with smooth initial data, for which the analytical solutions are known. We are able to confirm the spectral accuracy in this setting In Section 6.2, we give the results for the oxygen diffusion problem, which has a singularity at $t = 0$, as the initial data is not compatible with the condition prescribed at the fixed boundary. The exact solution is not available for this problem, but there is a vast amount of literature with numerical results available (see also Section 2.6 of the current work). We solve these problems by means of the smooth approximations of initial conditions introduced in Section 3.4. In particular, these experiments give the convergence rate predicted by Theorem 2; arbitrarily high accuracies can be achieved provided sufficiently sharp initial approximations are used. We also demonstrate the performance of the techniques of Chapter 5 above, and show that introduction of Padé approximations allows to perform the calculations four times faster, albeit with a certain loss of accuracy, while prior integration can increase the time savings by an additional factor of three with even smaller accuracy reduction.

		$t = 0.1$	$t = 0.5$	$t = 1$
u	exact	1.1618342427282831	1.4190675485932571	1.8221188003905089
	$\Delta t = 5 \cdot 10^{-6}$	1.1618342427282831	1.4190675485932571	1.8221188003903754
	$\Delta t = 0.001$	1.1618342427270414	1.4190675485848743	1.8221188003575279
$s(t)$	exact	0.3	0.7	1.2
	$\Delta t = 5 \cdot 10^{-6}$	0.3000000000000000	0.7000000000000001	1.2000000000001261
	$\Delta t = 0.001$	0.2999999999992889	0.6999999999940465	1.1999999999803832
error	$\Delta t = 5 \cdot 10^{-6}$	$2 \cdot 10^{-16}$	$2 \cdot 10^{-15}$	$9.7 \cdot 10^{-13}$
	$\Delta t = 0.001$	$1.3 \cdot 10^{-12}$	$8.5 \cdot 10^{-12}$	$3.3 \cdot 10^{-11}$

Table 6.1: Values of the function at $x = s(t)/2$ and the position of the moving boundary at different times for problem (6.1.1 - 6.1.2), $V = \lambda = 1,\ \alpha = 0.2$, calculated using RK4 ($\Delta t = 5 \cdot 10^{-6}$) and G3 ($\Delta t = 0.001$), both with $N = 11$ Chebyshev polynomials.

6.1 Stefan problems

Consider the following Stefan-like problems, one of which has the fixed boundary at zero and the other, at infinity.

$$\frac{\partial u}{\partial t} = \frac{V}{\lambda}\frac{\partial^2 u}{\partial x^2}, \quad 0 < x < s(t),\ t > 0; \tag{6.1.1}$$

$$u(0,x) = e^{-\lambda(x-\alpha)}, \qquad s(0) = \alpha;$$

$$u(t,0) = e^{\lambda(Vt+\alpha)}, \quad u(t,s(t)) = 1,$$

$$\frac{\partial u}{\partial x}(t,s(t)) = -\frac{\lambda}{V}\frac{ds}{dt}. \tag{6.1.2}$$

and

$$\frac{\partial u}{\partial t} = \frac{V}{\lambda}\frac{\partial^2 u}{\partial x^2},, \quad x > s(t),\ t > 0; \tag{6.1.3}$$

$$u(0,x) = e^{-\lambda(x-\alpha)}, \qquad s(0) = \alpha;$$

$$u(t,s(t)) = 1, \quad u(t,+\infty) = 0,$$

$$\frac{\partial u}{\partial x}(t,s(t)) = -\frac{\lambda}{V}\frac{ds}{dt}. \tag{6.1.4}$$

These two problems admit the same exact solution: $u(t,x) = \exp\big(-\lambda(x - Vt - \alpha)\big)$, $s(t) = Vt + \alpha$, which was used to test the performance of the numerical schemes.

In accordance with the method described in Chapter 3, the moving boundary in problem (6.1.1 - 6.1.2) was fixed at $y = 1$ by the change of variables $y = 2x/s(t) - 1$. Since the boundary conditions are not homogeneous, we invoked the technique described in Sec-

		$t = 0.1$	$t = 0.5$	$t = 1$
u	exact	0.1495686192226351	0.2231301601484298	0.3678794411714426
	$\Delta t = 1 \cdot 10^{-8}$	0.1495686192226232	-	-
	$\Delta t = 0.001$	0.1495686192226325	0.2231301601484236	0.3678794411714293
$s(t)$	exact	0.1	0.5	1.
	$\Delta t = 1 \cdot 10^{-8}$	0.0999999999880300	-	-
	$\Delta t = 0.001$	0.0999999999999920	0.5000000000000112	1.0000000000000671
error	$\Delta t = 1 \cdot 10^{-8}$	$9.0 \cdot 10^{-14}$	-	-
	$\Delta t = 0.001$	$2.3 \cdot 10^{-14}$	$3.5 \cdot 10^{-14}$	$3.8 \cdot 10^{-14}$

Table 6.2: Values of the function at $x = 2$ and the position of the moving boundary at different times for problem (6.1.3 - 6.1.4), $V = \lambda = 1$, $\alpha = 0$, calculated using RK4 ($\Delta t = 1 \cdot 10^{-8}$) and G3 ($\Delta t = 0.001$), both with $N = 115$ Chebyshev polynomials.

tion 3.5.1, to introduce the new dependent variable $v(t, y)$ (see (3.5.1)).

Similarly, in the problem (6.1.3 - 6.1.4), the moving boundary was fixed at $y = -1$ by the transformation $y = \frac{4}{\pi} \arctan(x - s(t)) - 1$; the adjusted function $v(t, y)$ was introduced; and the appropriate system of equations for its Chebyshev coefficients was generated. As it was noted above, in this problem, the resulting partial differential equation for v has space-dependent coefficients (see (3.1.2)) which were also expanded in Chebyshev series. This required the use of more polynomials to represent the solution at each time step, but did not add any complication to the algorithm.

Numerical results are summarized in Tables 6.1 and 6.2. The systems of nonlinear ordinary differential equations for the moving boundary and the Chebyshev coefficients of the solution were solved using both explicit (fourth-order Runge-Kutta scheme — "RK4" in the tables) and implicit (third-order Gear backward differentiation scheme — "G3" in the tables) methods. We quote the values of the solution at a point inside the computational region, as well as the maximum absolute error in $u(t, x)$ with respect to the exact solution, for several values of t. Note, however, that because of the stability restriction on the time step size, due to the large number of polynomials used in problem (6.1.3 - 6.1.4), no explicit time marching calculation was carried out for $t > 0.1$ in this problem. The overall results were selected to balance accuracy and speed: it is clearly possible to push the error level to machine accuracy by making the time step smaller thus also increasing computation time.

6.2 Oxygen diffusion problem

In 1972, J. Crank and R. Gupta [29] introduced the following moving boundary problem, which models diffusion of oxygen in an absorbing tissue:

$$\frac{\partial c}{\partial t} = \frac{\partial^2 c}{\partial x^2} - 1, \quad 0 \le x \le s(t),\ t \ge 0, \tag{6.2.1}$$

$$c(0,x) = \frac{1}{2}(1-x)^2, \quad 0 < x < 1, \qquad s(0) = 1,$$

$$\frac{\partial c}{\partial x}(t,0) = 0,$$

$$c(t,s(t)) = \frac{\partial c}{\partial x}(t,s(t)) = 0 \tag{6.2.2}$$

Here $c(t,x)$ represents the non-dimensionalized concentration of oxygen in the tissue. At the initial stage, the oxygen is supplied to the medium at a constant rate, until a steady state is reached, in which the oxygen does not penetrate any further into the medium. Then, the inflow is cut off and the surface is sealed. The oxygen continues to be absorbed by the tissue, and the point of zero concentration consequently recedes towards $x = 0$. The moving front $s(t)$, then, represents the boundary of the oxygen-saturated portion of the medium, and the boundary conditions express the fact that the surface is sealed, so that no more oxygen can flow in or out. In [29], the following short-time asymptotic solution was derived, based on a fixed-boundary approximation and Laplace transform

$$c(t,x) = \frac{1}{2}(1-x)^2 + 2\sqrt{\frac{t}{\pi}}\sum_{n=0}^{\infty}(-1)^n\left[\exp\left\{-\left(\frac{2n+2-x}{2\sqrt{t}}\right)^2\right\} - \exp\left\{-\left(\frac{2n+x}{2\sqrt{t}}\right)^2\right\}\right]$$
$$-\sum_{n=0}^{\infty}(-1)^n\left\{(2n+2-x)\operatorname{erfc}\left(\frac{2n+2-x}{2\sqrt{t}}\right) - (2n+x)\operatorname{erfc}\left(\frac{2n+x}{2\sqrt{t}}\right)\right\}$$

The series are rapidly convergent, and according to [29], just the $n = 0$ terms from the first and fourth series

$$c(t,x) = \frac{1}{2}(1-x)^2 - 2\sqrt{\frac{t}{\pi}}\exp\left\{-\left(\frac{x}{2\sqrt{t}}\right)^2\right\} + x\operatorname{erfc}\left(\frac{x}{2\sqrt{t}}\right) \tag{6.2.3}$$

represent the solution for $t \le 0.02$ with an accuracy of about 10^{-5}. This expression was rederived in [51] as the first term in the asymptotic solution of an integral equation, and was later used extensively in the literature to start off various numerical methods, not capable

		$t = 0.01$	$t = 0.04$	$t = 0.1$	$t = 0.18$	$t = 0.19$
$c(t,0)$	**CH**	**0.38716208**	**0.27432417**	**0.14317671**	**0.02178097**	**0.00902092**
	IE	0.387162	0.2743	0.143177	0.021781	0.009021
	FS	0.387162	0.274324	0.143177	0.021781	0.009021
	FC	-	0.27438	0.14314	0.02175	0.00900
	FE	-	-	0.14315	-	0.00893
	FG	0.387497	-	0.143287	0.021824	0.009039
	VT	-	-	0.14326	0.02175	0.00899
$s(t)$	**CH**	**1.00000000**	**0.99918230**	**0.93502290**	**0.50135419**	**0.34602560**
	IE	1.00000	0.99918	0.93501	0.50109	0.34537
	FS	1.000000	0.999180	0.935018	0.501329	0.346000
	FC	-	1.000000	0.93502	0.50205	0.34617
	FE	1.000000	0.99927	0.93559	0.49849	0.33971
	FG	1.00000	-	0.93518	0.49607	0.33873
	VT	-	-	0.92564	0.49276	0.33763

Table 6.3: Oxygen concentration at $x = 0$ and moving boundary position for problem (6.2.1-6.2.2): CH - this work, 7 polynomials, adaptive domain decomposition, $\epsilon = 2^{-13}$; IE - integral equations [51], FS - Fourier series [34], FC - Lagrange collocation [58], FE - finite elements [74], FG - fixed grid [29], VT - variable time step [102].

of resolving the initial singularity.

This is an example of an implicit moving boundary problem, since $s(t)$ must be backed out by solving an implicit equation. We have reviewed a number of techniques for its solution in Chapter 2; additional surveys can be found in [27, 101].

We apply the method of Chapter 3 to the oxygen diffusion problem. After front fixing and differentiation of the two conditions at the moving end, (6.2.1 - 6.2.2) is transformed to the following

$$c_t = \frac{4}{s^2(t)} c_{yy} + (y+1)\frac{\dot{s}(t)}{s(t)} c_y - 1, \quad |y| < 1,\ t > 0 \tag{6.2.4}$$

$$c(0,y) = \frac{1}{8}(1-y)^2, \qquad s(0) = 1$$

$$c_y(t,-1) = c(t,1) = 0$$

$$\frac{ds}{dt} = -\frac{8}{s^3(t)}\, c_{yyy}(t,1) \tag{6.2.5}$$

Note that the initial and boundary conditions do not match at $y = -1$, corresponding to the original $x = 0$:

$$0 = c_x(t,0)\Big|_{t=0} \neq \frac{d}{dx}\, c(0,x)\Big|_{x=0} = -1$$

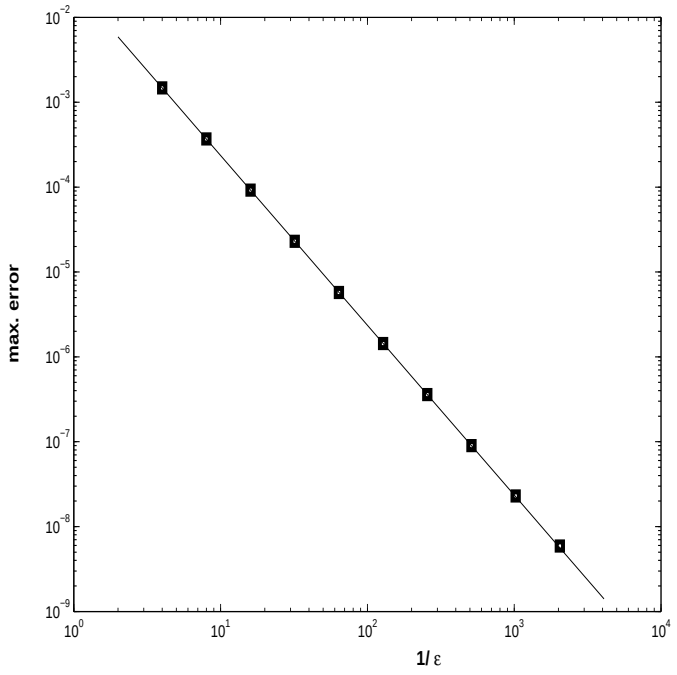

Figure 6.1: Convergence of the numerical solution $c(t, y)$ at $t = 0.01$ as $\epsilon \to 0$; solid line represents quadratic convergence, plotted for reference.

or, in the variable y,

$$0 = c_y(t, 0)\Big|_{t=0} \neq \frac{d}{dy}\, c(0, y)\Big|_{y=-1} = -\frac{1}{2}$$

so that $c(t, y)$ has a corner singularity at $t = 0, y = -1$. We rewrite the initial condition in the form

$$c(0, y) = \frac{1}{2} - \max\left(0, \frac{y+1}{2}\right) + \frac{1}{2}\max\left(0, \left(\frac{y+1}{2}\right)^2\right)$$

to reflect this fact. Next, we construct a smooth approximation of the initial data, based on (3.4.1), using the fact that

$$\frac{d^2}{dx^2}\, \max(0, x) = \frac{d^3}{dx^3}\, \frac{1}{2} \max(0, x^2) = \delta(x)$$

so we are within the same setting as in Theorem 2 of Chapter 4. We solve the approximate problem with Chebyshev tau, choosing ϵ sufficiently small, so that the initial approximation is sharp enough to produce the solution at the desired accuracy level. For example, $\epsilon = 4$ gives two correct digits at $t = 0.01$, while $\epsilon = 2^{-12}$, gives eight digits. The convergence rate is illustrated in Figure 6.1, where it is can be seen clearly that as $\epsilon \to 0$, the maximum ab-

solute error goes down quadratically, as anticipated by the results of Chapter 4 (see (4.2.6) and the Remark after Theorem 2). For the purposes of this calculation, the "exact" solution was the one calculated with $\epsilon = 2^{-13}$. To resolve the solution accurately at small times, we use domain decomposition, with nodes initially clustered around the singularity (i.e., $y = -1$) and gradually spreading out more evenly over the whole interval $(-1, 1)$. Numerical results for the value of oxygen concentration at the fixed end and the position of the moving boundary are reported in Table 6.3, compared with those obtained by several methods mentioned in Chapter 2 (see Section 2.6 for explanations of particular methods). As we have pointed out previously, the integral equation solution [51] is considered to be the most accurate, and the Fourier series method [34] is consistent with it, but uses the approximation (6.2.3) to start off computations for smaller times. We see that our results agree perfectly with these two for the concentration of oxygen, and are more accurate for the moving boundary position at later times. The comparison is based on the published results, which may not reflect the best performance capabilities of the corresponding methods. However, if we believe that these results represent the optimal accuracy levels, given the computing time constraints, then our *general* method will have produced solutions which are better than all of those previously reported, even those given by integral equations, for which this problem is ideally suited.

For the oxygen diffusion problem, we also tested the performance of the computational techniques presented in Chapter 5. We compare the results given by these methods with our earlier results for a wide selection of time levels in Table 6.4. The first row of each entry gives the most accurate calculation by the general method. We can see that we are usually able to obtain 5 to 6 correct digits using Padé approximation to evaluate the third derivative in (6.2.5), using the original (singular) initial data (2nd row in each entry). The gain in computation speed, on the other hand, is considerable. For example, to obtain 8 significant digits at $t = 0.01$ with the general method, approximately 3.5 minutes of computation on a 700 MHz PC is required. The calculation involving Padé approximants, thus, loses 2 to 3 digits of accuracy, but it takes only 45 seconds on the same architecture. Prior integration by the modified method of Knibb and Scraton (3rd row in each entry) smoothes the problem and normally gains an extra digit of accuracy over the previous calculation (i.e., 6 to 7 correct digits), even if larger time steps are taken with an implicit scheme (such as Gear's backward differentiation). At the same time, taking larger steps can

further reduce computing time: the same calculation (i.e., up to $t = 0.01$) with $\Delta t = 0.0001$ and implicit time stepping took only 17 seconds. This substantial speed-up is due to the fact that neither approximations nor domain decomposition is used in these two calculations. Finally, we observe that even uniform partitioning of the computational domain into several subintervals of equal length can reduce the influence of the singularity: the results the 4th row of each entry in Table 6.4 were obtained without any approximation of the initial data. However, their practical significance should not be overstated, as these simulations take only slightly less time to run than the general approximation-based method (1.5 minutes versus 3.5 minutes), but do not produce convergent numerical solutions.

t	$c(t,0)$	$s(t)$	t	$c(t,0)$	$s(t)$
0.01	0.38716208	1.00000000	0.12	0.10912923	0.87917869
	0.38716491	0.99999635		0.10913004	0.87916937
	0.38716214	0.99999781		0.10912925	0.87916884
	0.38716294	1.00000000		0.10912948	0.87917146
0.02	0.34042309	0.99999895	0.14	0.07785023	0.79895619
	0.34042518	0.99999520		0.07785096	0.79894423
	0.34042313	0.99999666		0.07785023	0.79894267
	0.34042369	0.99999885		0.07785045	0.79894507
0.04	0.27432417	0.99918230	0.15	0.06307754	0.74674379
	0.27432558	0.99917688		0.06307898	0.74673299
	0.27432420	0.99917767		0.06307754	0.74672783
	0.27432459	0.99917996		0.06307764	0.74672945
0.05	0.24768675	0.99679638	0.16	0.04882276	0.68346775
	0.24768801	0.99678939		0.04882344	0.68345214
	0.24768678	0.99619067		0.04882275	0.68344906
	0.24768713	0.99679306		0.04882296	0.68345124
0.06	0.22360468	0.99180625	0.18	0.02178097	0.50135419
	0.22360583	0.99179884		0.02178159	0.50133627
	0.22360471	0.99179964		0.02178094	0.50133027
	0.22360503	0.99180246		0.02178115	0.50133268
0.08	0.18084626	0.97155469	0.19	0.00902092	0.34602560
	0.18084726	0.97154715		0.00902150	0.34601185
	0.18084630	0.97154788		0.00902088	0.34600149
	0.18084656	0.97155054		0.00902109	0.34600520
0.1	0.14317671	0.93502289	0.195	0.00288362	0.20847525
	0.14317760	0.93501497		0.00288418	0.20847436
	0.14317673	0.93501516		0.00288345	0.20859419
	0.14317698	0.93501787		0.00288378	0.20846149

Table 6.4: Miscellaneous Chebyshev spectral methods for problem (6.2.1-6.2.2): 7 polynomials, adaptive domain decomposition, $\epsilon = 2^{-13}$ ("exact") (1st line); 31 polynomials, whole domain, with Padé approximation (2nd line); 31 polynomials, whole domain, with prior integration and Padé approximation (3rd line); 7 polynomials, 50 subintervals, $\epsilon = 1$ (4th line).

Chapter 7

Valuation of American Options

The economic world is a misty region. The first explorers
used unaided vision. Mathematics is the lantern by which
what before was dimly visible now looms up in firm, bold outlines.
The old phantasmagoria disappear. We see better. We also see further.
(Irving Fisher, 1867–1947)

An important application of our analysis can be found in mathematical finance, namely, in the valuation of American options. An approach to this problem, based on probability theory, has established itself as a growing branch of stochastic calculus and martingale theory, with many significant contributions over the last two decades (see [55, 78]). More recently, applied mathematicians and numerical analysts have started to address these problems as well, and there have been several texts that study financial derivative products and in particular, options from the point of view of partial differential equations [7, 99, 100]. Since these problems have been considered in the mathematical community in the last few years, we feel an outline of the finance background is appropriate. Such an outline is presented in the next Section; the mathematical formulation and a simple derivation of a symmetry result [21] are given in Sections 7.2 and 7.3. In Sections 7.4 and 7.5, we present the numerical analysis of our method in this context, preceded, as necessary (Section 7.4) by a convenient change of time scale to remove a singularity in the velocity of the moving boundary. Several advanced examples of American options are given in Section 7.6.

7.1 Options: key concepts

The main products traded in financial markets are securities. These include basic securities, such as stocks and bonds, as well as more complicated instruments — futures, options, convertibles, mortgage-backed securities, swaps, etc. Most of mathematical finance deals

with a class of securities called *derivatives.* According to the classical finance text [52, p. 1], "a derivative security is a financial instrument whose value depends on the values of other, more basic underlying variables." One of the best studied examples of a derivative product is an option — a contract that gives its owner the right to purchase (*call* option) or sell (*put* option) another security (underlying asset, or simply, *underlying*) at a pre-specified price (*strike* price) on or, perhaps, before a specified date (*expiration,* or *expiry*). Since an option gives a right and not an obligation, entering the contract involves paying a premium, which is the price of the option. Choosing to purchase or sell the underlying on the conditions specified by the contract is termed *exercising* the option. Depending on the permissible exercise patterns, options are separated into several groups. The so-called European options may only be exercised at a certain date, i.e., at expiration of the contract. American options admit an *early exercise* feature: it is allowed to exercise them at any time before expiration. There are numerous other possibilities (e.g., when exercising the option is allowed at a finite set of dates before expiry, etc.), but we do not focus on them here.

The payoff of an option at the time of exercise is known in advance, but the price of the option at any given time is unknown and depends, in general, on the price of the underlying, among other factors. The underlying can be either a simple asset, like a stock or a bond, or a more complicated structure, like a stock index or foreign currency. We first focus on options written on a single stock and address the more complicated structures later.

In the classical setting, the price of the option is assumed to depend only on the price of the underlying stock and time. Thus choosing a model of stock price movement is critical in determining the value of the option. The unpredictable behavior of stock price suggests a probabilistic approach, in favor of a deterministic one, and this was, in fact, the avenue pursued by most theorists. The most basic stochastic model postulates that the relative change in the stock price over a small time interval Δt is distributed normally with both mean and variance proportional to Δt, i.e.,

$$\frac{\Delta S}{S} \sim \mathcal{N}\big(\mu\Delta t, \sigma\sqrt{\Delta t}\,\big)$$

Here S is the stock price and μ is the expected return on the stock. In the limit as $\Delta t \to 0$, we get a continuous stochastic process for the stock price, which can be written in the

stochastic differential notation as

$$dS = \mu S\, dt + \sigma S\, dW \tag{7.1.1}$$

and is called *geometric Brownian motion.* Here dW is an elementary Wiener process, i.e., $dW \sim \mathcal{N}(0, \sqrt{dt})$. The parameter σ, which characterizes the random part of the stock's behavior, is called the volatility of the stock.

Note that the geometric Brownian motion model (7.1.1) for stock price movements is one of the simplest possible, since it assumes a continuous symmetric distribution for price increments and disregards the possibility of large jumps. It goes back to Louis Bachelier who was the first to apply stochastic methods to the processes in financial markets.[1] It turns out that this model is a good starting point, which works remarkably well, given its simplicity. The theory of option pricing based on this model of stock price movements, although not faultless, describes real-life processes adequately in most cases.

In the final part of our introduction, we give a derivation of the partial differential equation satisfied by the price of an option. This equation, known as the Black-Scholes PDE, is a key point in any of the modern texts on derivatives, e.g., [52, 79, 99]. The derivation we present is closest in spirit to the one in [79], since it takes into account an important concept of self-financing portfolios, which most of other texts tend to neglect.

Denoting the price of the option $F(t, S)$, where S follows the process (7.1.1), the stochastic differential equation describing the dynamics of F is obtained in stochastic calculus by Itô's lemma (see, e.g., [82]) for a fairly general class of stochastic processes followed by S. A corollary of this result for (7.1.1) gives

$$dF = \Big(\frac{\partial F}{\partial t} + \mu S\, \frac{\partial F}{\partial S} + \frac{1}{2}\, \sigma^2 S^2 \frac{\partial^2 F}{\partial S^2}\Big) dt + \mu S\, \frac{\partial F}{\partial S}\, dW \tag{7.1.2}$$

It is crucial that the random part is driven by the same Wiener process dW, that appears in (7.1.1). This enables one to construct a riskless portfolio with just the option and the underlying.

[1] In fact, Bachelier was the one who truly introduced into mathematics the continuous-time stochastic processes, notably the process currently known as Brownian motion, long before the works of N. Wiener, P. Lévy, A. Einstein, and others. Unfortunately his work was not very popular with his colleagues and remained virtually unknown for decades. It was not until the development of mathematical finance that Bachelier and his contribution to science was recognized [26].

Indeed, consider a portfolio Π consisting of n shares and m options. The value of this portfolio at any time t is

$$\Pi = mF + nS$$

To specify the weights m and n, we need two constraints on the structure of the portfolio. Hence we require that Π be *self-financing* and *riskless.* The first of these statements simply means that by dynamically changing the weights, we keep the portfolio feasible without additional cash inflows or outflows over the infinitesimal interval dt. Mathematically, this can be written as

$$(S + dS)\, dn + (F + dF)\, dm = 0$$

i.e., the changes in the values of components offset each other. This equality implies

$$d\Pi = mdF + ndS$$

The second condition (absence of risk) means that m and n must be chosen, at time t, in such a way that the stochastic (i.e., risky) component in $d\Pi$ vanishes identically. Looking at (7.1.1) and (7.1.2), we deduce that we must have

$$n = -m\,\frac{\partial F}{\partial S} \tag{7.1.3}$$

Then the dynamics of Π is described by

$$d\Pi = \Big(m\frac{\partial F}{\partial t} + m\mu S\,\frac{\partial F}{\partial S} + m\frac{1}{2}\,\sigma^2 S^2\frac{\partial^2 F}{\partial S^2} + n\mu S\Big)\,dt = m\Big(\frac{\partial F}{\partial t} + \frac{1}{2}\,\sigma^2 S^2\frac{\partial^2 F}{\partial S^2}\Big)\,dt \tag{7.1.4}$$

since the μ and dW terms cancel because of (7.1.3). We see that the portfolio Π is indeed locally risk-free. Therefore its return over the infinitesimal interval dt must be equal to the risk-free rate r. This argument is a particular case of the fundamental principle of financial mathematics, *absence of arbitrage opportunities.* In its essence, it means that no positive profits can be made without a positive investment. For a more detailed discussion of this concept, see, e.g., [79, Chapter 2]. The risk-free rate r is considered constant and is another parameter of the model. Thus the following identity must hold

$$d\Pi = r\Pi dt = r(mF + nS)dt = mr\Big(F - \frac{\partial F}{\partial S}\,S\Big)dt$$

Comparing this to (7.1.4), we conclude that

$$m\Big(\frac{\partial F}{\partial t}+\frac{1}{2}\,\sigma^2 S^2\frac{\partial^2 F}{\partial S^2}-rF+r\,\frac{\partial F}{\partial S}\,S\Big)dt=0$$

and therefore $F(t,S)$ has to satisfy

$$\frac{\partial F}{\partial t}+\frac{1}{2}\,\sigma^2 S^2\frac{\partial^2 F}{\partial S^2}+rS\,\frac{\partial F}{\partial S}=rF \tag{7.1.5}$$

This is the celebrated Black-Scholes partial differential equation [11, 70]. It admits several generalizations, including the cases when the underlying is not a traded asset (e.g., bets on the risk-free rate) or when there are multiple underlyings. However, the form of (7.1.5) is quite general, and prices of a variety of derivative securities satisfy similar equations, with the nature of any particular one determined by the initial and boundary conditions. (Note that since the equation (7.1.5) is backward parabolic, the initial data must be prescribed at a final time and the solution worked out backwards; otherwise, the problem is ill-posed. Fortunately, this requirement is in line with the practical situation: the value of an option is indeed known only at expiration, but not at the time the contract is written.) Exact solutions have been found [11, 70] in several cases, mostly for European options.

Traditionally, most of the practical work in the valuation of American options was done via the probability approach to this problem, using such techniques as integration along sample paths of S and Monte-Carlo simulations. This is a separate field, which is beyond the scope of this work. The basic concepts are explained, e.g., in [55]. We refer an interested reader to the available surveys, such as [83], and more recent work, such as [66], and references therein. At the same time, since the equivalence of the American option problem to a moving boundary problem was established in [68], there have been certain developments of the differential equation approach. In [97], a related optimal stopping problem was studied, and certain key results regarding the moving boundary were proved. Apparently the first numerical scheme for the valuation of American options, based on finite differences, was proposed in [18]. The convergence of this algorithm was proved later in [53], where the variational inequality framework was applied to pricing of American options. This is also the approach taken in [99]. Various integral equation formulations are available [48, 56, 65], which often allow to explicitly represent the value of an American

option as the sum of the value of its European counterpart and a nonnegative term, called *the early exercise premium.* Exact solutions for several special cases were given in [70]; in particular, it was established that an American call on a stock which does not pay any dividends, has no early exercise value, and therefore should always be held till expiration. A general analytical approximation for the American put was given in [46]. Short-time asymptotics were studied in [23, 36, 41, 60]. For other cases and examples, see the review [19], where a good comparison of different numerical methods for American options is also given.

Finally we mention one simple extension of the above model. Suppose the stock pays a dividend, which can be represented as a constant yield q to the investor in the form of a percentage of the stock price. This changes the process (7.1.1) to

$$dS = (\mu - q)S\,dt + \sigma S\,dW$$

The derivation of the Black-Scholes equation can be carried through with only minor changes (cf. [52, Appendix 12A]), and in the end we obtain the following, slightly modified form of (7.1.5) for derivatives on dividend-paying stock

$$\frac{\partial F}{\partial t} + \frac{1}{2}\,\sigma^2 S^2 \frac{\partial^2 F}{\partial S^2} + (r - q)S\,\frac{\partial F}{\partial S} = rF \tag{7.1.6}$$

We thus have a model describing the evolution of the price of an option by a differential equation. We proceed to give a comprehensive mathematical formulation for the American option valuation problem from this point of view.

7.2 Mathematical formulation

Recall that American options can be exercised at any date before expiration. Intuitively, then, one may expect that these option must be significantly harder to price than their European counterparts, since determining *when* to exercise the option in an optimal way becomes part of the problem. It can be proved that the point of optimal exercise can be found by monitoring the price of the underlying stock: when the stock price crosses a certain critical value, the option should be exercised. Naturally, the value of a call option (i.e., an option to buy stock) goes up with the stock price, so this option is exercised when the stock price rises above the critical value, while for a put option (i.e., an option to sell stock),

the stock price has to drop below the critical value for exercise to be optimal. The Black-Scholes equation governs the behavior of an American call (put) only below (respectively, above) the critical price, which has to be determined as part of the solution. This is a very familiar setting indeed, and therefore the equivalence of American option pricing to a moving boundary problem, first established in [68], is not surprising. We proceed with the formulation of this problem for the case of an American call on a dividend-paying stock.

Let $C(t, S)$ denote the value of the call at time t when the price of the underlying stock is S. Let K be the strike price of the call; r be the interest rate; q, the dividend yield; and σ, the volatility of the stock. Then, at any time before expiration T and for any stock price below the optimal exercise value $B(t)$, $C(t, S)$ satisfies the Black-Scholes equation (7.1.5)

$$\frac{1}{2}\sigma^2 S^2 C_{SS} + (r - q)SC_S + C_t - rC = \mathcal{L}_{BS}[C] = 0$$

At expiration, the option will be exercised only if the stock price is larger than the strike price. (Since, otherwise, it is preferable for the investor to buy the stock on the market for S dollars, rather than buy it for $K > S$ dollars from the writer of the option.[2]) Therefore the value of the call at expiration is

$$C(T, S) = \max(0, S - K)$$

It can be proved that zero is an absorbing barrier for the geometric Brownian motion process; therefore, if the stock price ever hits 0, it stays at 0. But the call is worthless in this case, so we have

$$C(t, 0) = 0$$

By definition of the optimal exercise price, when the stock price hits $B(t)$, the call is exercised, and its value is

$$C(t, B(t)) = B(t) - K$$

Combining these equations, we obtain the differential equations and boundary conditions

[2]The call option is called *in the money* at a given time, if the stock price satisfies $S > K$ at this time; if $S = K$ or $S < K$, the corresponding terms are *at-the-money* and *out-of-the-money* calls, respectively. For put options, the terminology is the same, but the inequalities have to be reversed.

for call-option problem:

$$\frac{1}{2}\sigma^2 S^2 C_{SS} + (r-q)SC_S + C_t = rC, \quad t < T,\ 0 < S < B(t)$$
$$C(T,S) = \max(0, S-K),$$
$$C(t,0) = 0, \qquad C(t,B(t)) = B(t) - K$$

As we know from our experience with moving boundary problems, the above formulation is not complete: we need an additional condition on the moving front to be able to solve for $B(t)$. A finance argument, relying on absence of arbitrage opportunities, was used to find this condition in [70]. In [7, Section 5-A.1], integration over a small neighborhood of $B(t)$ was used to derive the corresponding condition for an American put. P. Bossaerts [15] suggested an alternative approach, based on the fact that the optimal exercise boundary is chosen in such a way as to maximize the value of the call option at any instant of time. Our derivation, based on these ideas, is presented below.

Mathematically speaking, the above argument implies that

$$B(t) = \arg\max_{f(t)} C\big(t, S;\ f(t)\big)$$

The maximum is taken over a suitable class of admissible functions $f(t)$. For example, we can consider all continuous functions $f(t)$ with $f(T) = B(T)$. In the neighborhood of $B(t)$

$$f(t) = B(t) + \epsilon g(t)$$

with $g(t)$ continuous and $g(T) = 0$. Denote $C_\epsilon = C\big(t, S;\ f(t)\big) = C\big(t, S;\ B(t) + \epsilon g(t)\big)$. The necessary condition for C_ϵ to be maximized by $B(t)$ is

$$\left.\frac{\partial C_\epsilon}{\partial \epsilon}\right|_{\epsilon=0} = 0 \tag{7.2.1}$$

Let $U = \partial C_\epsilon / \partial \epsilon$. By differentiating the partial differential equation, obtain

$$\frac{1}{2}\sigma^2 S^2 U_{SS} + (r-q)SU_S + U_t - rU = \mathcal{L}_{BS}\Big[\frac{\partial C_\epsilon}{\partial \epsilon}\Big] = 0, \quad t < T,\ 0 < S < B(t) + \epsilon g(t)$$

Also,

$$\frac{\partial C_\epsilon}{\partial \epsilon}(t,S) = 0 = \frac{\partial C_\epsilon}{\partial \epsilon}(t,0)$$

since the right-hand sides do not depend on ϵ. Now find the boundary value of $\partial C/\partial \epsilon$. By the chain rule,

$$\frac{dC_\epsilon}{d\epsilon}\big(t, B(t)+\epsilon g(t)\big) = C_S\big(t, B(t)+\epsilon g(t)\big)\, g(t) + \frac{\partial C_\epsilon}{\partial \epsilon}$$

On the other hand, direct differentiation of the boundary condition for C_ϵ gives

$$\frac{dC_\epsilon}{d\epsilon}\big(t, B(t)+\epsilon g(t)\big) = \frac{d}{d\epsilon}\big(B(t)+\epsilon g(t) - K\big) = g(t)$$

so we have

$$\big[C_S\big(t, B(t)+\epsilon g(t)\big) - 1\big]\, g(t) = \frac{\partial C_\epsilon}{\partial \epsilon}$$

Thus for

$$C'_{0,\epsilon} \equiv \frac{\partial C_\epsilon}{\partial \epsilon}\Big|_{\epsilon=0}$$

we have

$$\begin{aligned}
\frac{1}{2}\sigma^2 S^2 \big[C'_{0,\epsilon}\big]_{SS} + (r-q)S\big[C'_{0,\epsilon}\big]_S + \big[C'_{0,\epsilon}\big]_t - r\big[C'_{0,\epsilon}\big] = 0, \quad t<T,\ 0<S<B(t) \\
\big[C'_{0,\epsilon}\big](T,S) = 0 \\
\big[C'_{0,\epsilon}\big](t,0) = 0 \\
\big[C'_{0,\epsilon}\big](t,B(t)) = \big[1 - C_S\big(t,B(t)\big)\big]\, g(t)
\end{aligned}$$

For (7.2.1) (i.e., $C_\epsilon \equiv 0$) to be the solution of this problem, we need the last condition to be homogeneous, so we must have

$$\big[1 - C_S\big(t, B(t)\big)\big]\, g(t) = 0$$

for *any* admissible function $g(t)$. This immediately implies that the desired second condition on the moving front

$$C_S(t, B(t)) = 1 \tag{7.2.2}$$

holds. This expression is known as the "smooth pasting," or high-contact condition for

American options. If we perform the same analysis for an American put $P(t,S)$ (see below), we get this condition in the form

$$P_S(t,B(t)) = -1 \tag{7.2.3}$$

Thus for the call option, we have the following formulation

$$\frac{1}{2}\sigma^2 S^2 C_{SS} + (r-q)SC_S + C_t = rC, \quad t < T,\ 0 < S < B(t) \tag{7.2.4}$$

$$C(T,S) = \max(0, S-K), \tag{7.2.5}$$

$$C(t,0) = 0,$$

$$C(t,B(t)) = B(t) - K, \quad C_S(t,B(t)) = 1,$$

$$B(T^-) = K\max\Big(1, \frac{r}{q}\Big) \tag{7.2.6}$$

The expression (7.2.6) for the optimal exercise price just before expiration was derived in [56]. For the put option, we have

$$\frac{1}{2}\sigma^2 S^2 P_{SS} + (r-q)SP_S + P_t = rP, \quad t < T,\ S > B(t) \tag{7.2.7}$$

$$P(T,S) = \max(0, K-S), \tag{7.2.8}$$

$$P(t,+\infty) = 0,$$

$$P(t,B(t)) = K - B(t), \quad P_S(t,B(t)) = -1,$$

$$B(T^-) = K\min\Big(1, \frac{r}{q}\Big) \tag{7.2.9}$$

The description is analogous to the case of the American call. Note the difference between (7.2.5) and (7.2.8) and the resulting differences in the boundary conditions at the moving end. We also recognize the two option problems, in the notation of Chapter 3, as a finite one for the call and a semi-infinite one for the put. An important symmetry result between these two problems greatly facilitates further analysis.

7.3 Put-call parity for American options

As derivative instruments which are, in a sense, dual, a call and a put written on the same underlying asset are related to each other, and their prices cannot be independent. An

elegant argument gives the following identity for European options [52, Section 12.1]

$$C(t,S) - P(t,S) = Se^{-q(T-t)} - Ke^{-r(T-t)} \tag{7.3.1}$$

This result is called the *put-call parity*. For verification, consider the following two portfolios (we repeat the presentation in [52, Section 12.1])

A: one European call and $Ke^{-r(T-t)}$ dollars in the bank;

B: one European put and $e^{-q(T-t)}$ shares, with all dividends to be reinvested in the stock.

At expiration T, the call is worth $\max(0, S-K)$ and the money in the bank earns $e^{r(T-t)}$ in interest, so that the total amount of cash at time T is K dollars. Thus portfolio A pays $\max(0, S-K) + K = \max(S, K)$ at expiration. At the same time T, the put is worth $\max(0, K-S)$, while the continuously reinvested dividend brings up the effective number of shares from $e^{-q(T-t)}$ at t to exactly one at T, which will be worth S dollars. Thus portfolio B pays $\max(0, K-S) + S = \max(S, K)$ dollars, i.e., the same amount, at expiration. If the prices of these two portfolios at time t were different, a smart investor would have bought the cheaper of the two and sold the more expensive one, collecting the difference and making a profit with no risk (since his or her assets would have exactly offset the liabilities at time T). This would have constituted what is called an arbitrage opportunity (i.e., a possibility of a positive riskless profit), which is impossible by the no-arbitrage postulate. Hence the values of both portfolios at time t should be equal, which implies (7.3.1).

This argument works very well for European options, but is bound to fail for the American options, since the possibility of early exercise (i.e., exercise before T) at an *a priori* unknown time does not permit to work out the final payoffs as cleanly. The most that a similar procedure for American options can give us is an estimate in the form of an inequality [52, Section 12.1].

However, the symmetry between C and P is still striking, even for American options. The duality of the two problems becomes obvious mathematically when we introduce the following new variables

$$\tau = \frac{1}{2}\sigma^2(T-t), \quad s = \frac{S}{K}; \quad c(\tau, s) = \frac{C(t,S) - S}{K}, \quad b(\tau) = \frac{B(t)}{K},$$

for the call and

$$\tau = \frac{1}{2}\sigma^2(T-t), \quad s = \frac{K}{S}; \quad p(\tau, s) = \frac{P(t,S)-K}{S}, \quad b(\tau) = \frac{K}{B(t)},$$

for the put. The problems (7.2.4) - (7.2.6) and (7.2.7) - (7.2.9) then become

$$\begin{aligned} &c_\tau = s^2 c_{ss} + (\rho - \kappa) s c_s - \rho c - \kappa s, && \tau > 0,\ 0 < s < b(\tau) \\ &c(0,s) = \max(0, s-1) - s, \quad b(0^+) = \max(1, \rho/\kappa) \\ &c(\tau, 0) = 0 \\ &c(\tau, b(\tau)) = -1,\ c_s(\tau, b(\tau)) = 0 \end{aligned} \tag{7.3.2}$$

and

$$\begin{aligned} &p_\tau = s^2 p_{ss} - (\rho - \kappa) s p_s - \kappa p - \rho s, && \tau > 0,\ 0 < s < b(\tau) \\ &p(0,s) = \max(0, s-1) - s, \quad b(0^+) = 1/\min(1, \rho/\kappa) = \max(1, \kappa/\rho) \\ &p(\tau, 0) = 0 \\ &p(\tau, b(\tau)) = -1,\ p_s(\tau, b(\tau)) = 0 \end{aligned} \tag{7.3.3}$$

respectively. Here $\rho = r \cdot \left(\sigma^2/2\right)^{-1}$ and $\kappa = q \cdot \left(\sigma^2/2\right)^{-1}$ are the two crucial dimensionless quantities, which describe the relation between interest rate, dividend yield and volatility.

The problems (7.3.2) and (7.3.3) are almost identical, and it is now evident that if the pair $\{c(\tau, s),\ b(\tau)\}$ solves (7.3.2) for some specified values of ρ and κ, then it also solves (7.3.3) for the values of ρ and κ interchanged. Going back to the original formulations (7.2.4) and (7.2.7), we conclude that if $C(t, S;\ r, q)$ is the price of an American call option and $B^c(t)$ is the corresponding optimal exercise boundary, found for interest rate r and dividend yield q, and $P(t, S;\ r, q)$ and $B^p(t)$ are the corresponding quantities for an American put option, then

$$\frac{C(t,S;\ r,q) - S}{K} = \frac{P(t,S;\ q,r) - K}{S} \quad \text{and} \quad \frac{B^c(t)}{K} = \frac{K}{B^p(t)} \tag{7.3.4}$$

This expression gives the put-call parity for American option and is a particular case of the result established in [21], built on the ideas of [10, 67]. Although not as general as the formula in [21], our result is derived in a more direct fashion, straight from the partial differential equation in the original variables.

For the analysis we present below, the parity formula gives the advantage of having to solve only one of the problems (7.2.4), (7.2.7), with the solution of the other one following immediately by (7.3.4). Thus for the remainder of this section, we shall concentrate on equation (7.3.2).

Note that the first of the formulas (7.3.4) does not reflect the fact that the independent variable S lies in different domains for the call and put options (see the original formulations, (7.2.4) and (7.2.7)). However, one is mapped to the other by the coordinate transformation $S \to K^2/S$. Thus for practical calculations, we should incorporate this change of variables into the parity formula and write

$$P(t, S;\, q, r) = \frac{S}{K}\, C\Big(t, \frac{K^2}{S};\, r, q\Big);$$
$$P\Big(t, \frac{K^2}{S};\, q, r\Big) = \frac{K}{S}\, C(t, S;\, r, q)$$

To solve the problem (7.3.2), we make another transformation of the dependent variable. It is easy to see that the setting satisfies all the conditions in [88], so we can write a Stefan problem for $u(\tau, s) \equiv c_\tau(\tau, s)$ (see Chapter 3). Up to a numerical factor, u is what is called the *theta* of an option: the sensitivity of its price with respect to time. $u(\tau, s)$ solves the following

$$u_\tau = s^2 u_{ss} + (\rho - \kappa) s u_s - \rho u, \qquad 0 < s < b(\tau),\ \tau > 0$$
$$u(0, s) = s^2 \delta(s-1) + (\rho - \kappa) s H(s-1) - \rho \max(0, s-1) \tag{7.3.5}$$
$$u(\tau, 0) = u(\tau, b(\tau)) = 0 \tag{7.3.6}$$
$$\frac{db}{d\tau} = \frac{b^2(\tau)\, u_s(\tau, b(\tau))}{\kappa b(\tau) - \rho}, \tag{7.3.7}$$
$$b(0^+) = \max(1, \rho/\kappa)$$

The initial condition is obtained from that of (7.3.2) by substituting for c_τ the sum of spatial derivatives, i.e., the right-hand side of the partial differential equation in (7.3.2). $\delta(\cdot)$, the Dirac δ-function, and $H(\cdot)$, the Heavyside step function, emerge as a result of differentiating the function $\max(0, s-1)$, which is only C^0, but not even C^1 in the intervals $\big(0, b(0^+)\big)$. The boundary conditions at the moving end, i.e., the second one of (7.3.6), and the expression for the derivative of $b(\tau)$ are obtained from the corresponding conditions for $c(\tau, s)$ using

the differential equation (7.3.2). Clearly, two distinct cases emerge:

(i) $r > q$, implying $\rho/\kappa > 1$; and

(ii) $r \leq q$, so that $\rho/\kappa \leq 1$

7.4 The case $r > q$

Since $\rho > \kappa$, it follows that $b(0^+) > 1$, and the initial data are singular at $s = 1$, inside the interval $\big(0, b(0^+)\big)$. Moreover, the denominator of (7.3.7) vanishes as $\tau \to 0^+$, so

$$\frac{db}{d\tau} \to \infty \qquad \text{as} \quad \tau \downarrow 0$$

However, as noted in the introduction to this Chapter, scaling time according to the formula $\tau_* = \sqrt{\tau}$ yields

$$\frac{\partial}{\partial \tau} = 2\tau_* \frac{\partial}{\partial \tau_*}$$

and in particular,

$$\frac{db}{d\tau_*} = -\frac{2\tau_* t b^2(\tau_*)\, u_s(\tau_*, b(\tau_*))}{\kappa b(\tau_*) - \rho}$$

which is finite initially, as long as $u_s(\tau_*, b(\tau_*))$ remains bounded as $\tau_* \downarrow 0$. Thus we have removed the initial singularity in $db/d\tau$ with a simple change of variables. This technique appears quite general and very useful for certain ordinary differential equations with singular right-hand sides.

The precise value of the initial velocity of the moving boundary can be determined from local analysis of $u(\tau_*, x)$ near $x = b(0^+)$ for small τ_*. Asymptotic formula from [99] gives $\dot{b}(0^+) = (\rho/\kappa)\,\xi_0$, where ξ_0 is the solution of the transcendental equation

$$\xi_0^3 e^{\xi_0^2/4} \int_{-\infty}^{\xi_0} e^{-y^2/4} dy = 2(2 - \xi_0^2)$$

with a numerical value of $\xi_0 = 0.90344659788\ldots$. We wish to emphasize that the asymptotic solution is used here exclusively to determine the initial speed of the moving boundary and not to approximate or start off the solution for any positive value of τ_*.

We see that the initial conditions (7.3.5) are a particular case of those mentioned in Theorem 2, Chapter 4. (Since $\rho > \kappa$, $b(0^+) > 1$, the singularity lies in the interior of

$(0, b(0^+).)$ $\Omega = [0, \rho/\kappa].)$ Moreover, $u(0, x)$ is a distribution supported on $(0, b(0^+)$, which is the same class of functions, as considered in Theorem 1 of Chapter 4. Existence of a solution follows from the fact that u is the derivative of c ($u = c_\tau$), and the solution $c(\tau, s)$ exists and is differentiable by the general theory (since the initial data for c are continuous). To calculate u numerically, we use an approximation for δ, H and max, which is based on (3.4.1), just as in Section 6.2 above, expecting to obtain numerical solutions that converge to the true solution with singular initial data quadratically as $\epsilon \to 0$, as in the construction presented in Chapter 4. Figure 7.5 (bottom curve) confirms these expectations perfectly and demonstrates quadratic convergence rate. For the purposes of this analysis, the "exact" solution is the one computed using $\epsilon = 1/32$. Note that in this calculation, we set less ambitious accuracy goals than in the oxygen diffusion problem. In this setting, more biased towards the practical side, speed is a greater priority, while relative error of about 0.1% is quite acceptable. The more complicated form of the Black-Scholes differential operator, relative to the simple diffusion one in (6.2.1), demands smaller values of ϵ and lengthier computations. For example, three correct digits in the option price can be obtained by a 10-minute calculation on a 700 MHz PC, with $\epsilon = 1/4$. Thus we have once again chosen the parameters of our method in an optimal way for the given problem.

Figure 7.1 shows the optimal exercise price, calculated for various values of ϵ, the "concentration" parameter of the δ approximation. We take $\sigma = 30\%, r = 10\%, q = 8\%$, and $K = \$100$. We compare (Figure 7.1(a)) our calculations to the small-time asymptotics of [99] and observe improved agreement as $\epsilon \to 0$ near expiry. In Figure 7.2 we plot the calculated price of the option described above, expiring in 1 year for crude ($\epsilon = 1$) and sharp ($\epsilon = 1/32$) initial approximations. The optimal exercise price at this time is \$172.13. For reference, we also show the price of the European call option (i.e., the one with no early exercise feature, and therefore no moving boundary) with the same values of K, r, q and σ. An early exercise premium, which makes the prices of the two options different, is also plotted. As expected, the difference is always nonnegative, since an American option provides an additional feature and hence must be worth at least as much as its European counterpart. The difference in prices is, essentially, zero for low stock prices (deep out-of-the-money calls) and grows steadily as the stock price approaches the strike price and increases past it. For this particular problem, however, the early exercise premium is fairly small, not more than 5% of the option value.

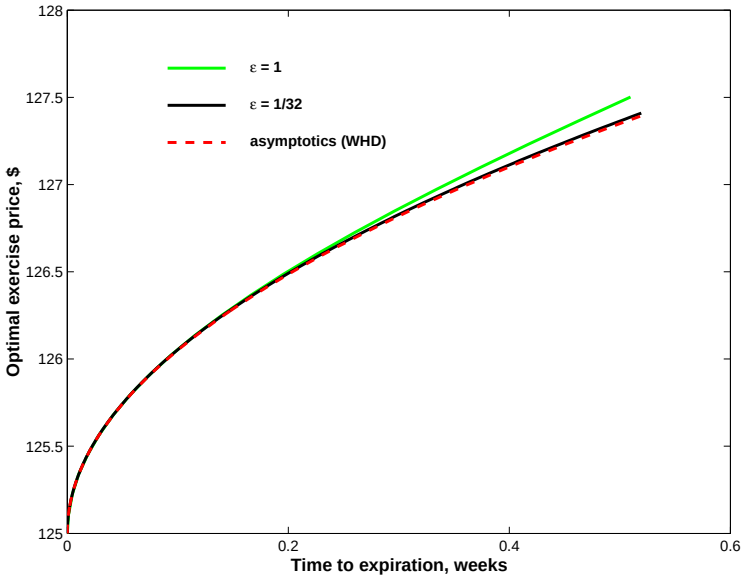

(a) Near expiration, vs. [99] (WHD)

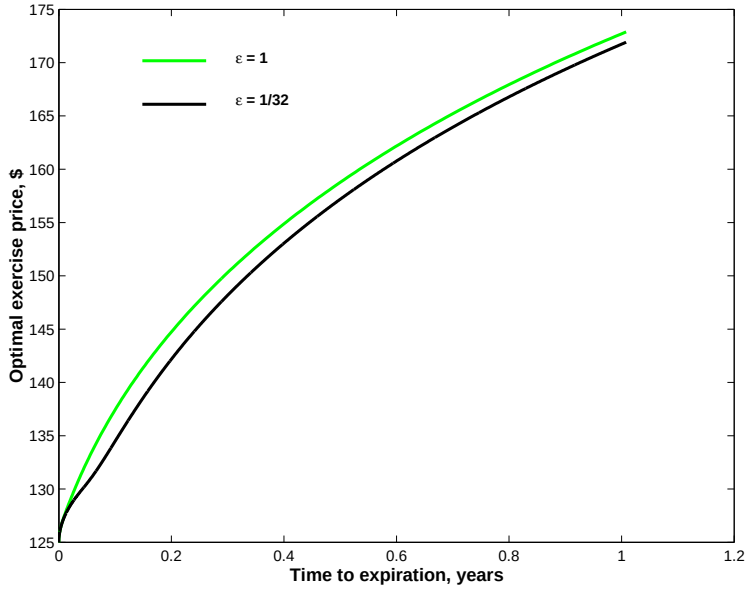

(b) Up to 1 year to expiration

Figure 7.1: Optimal exercise boundary for American call with $r = 0.1$, $q = 0.08$, $\sigma = 0.3$, and $K = \$100$.

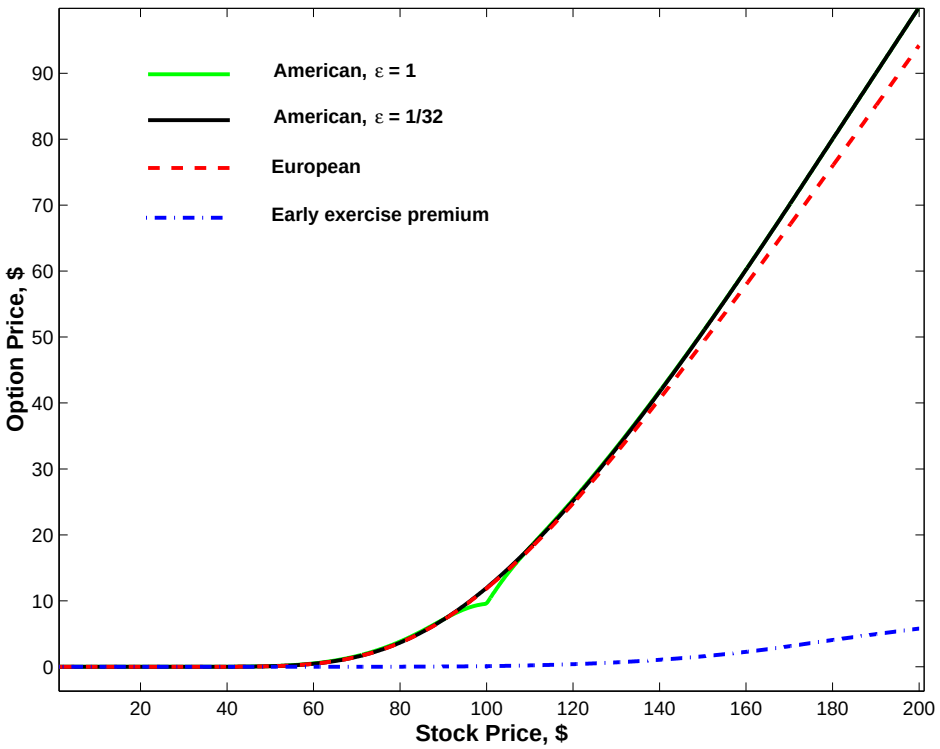

Figure 7.2: American vs. European calls with $r = 0.1$, $q = 0.08$, $\sigma = 0.3$, and $K = \$100$, $t = 1$ year from expiry.

7.5 The case $r \leq q$

In this case, $b(0^+) = 1$, and the singularity of the initial data is at the right boundary. Note that, unlike in the oxygen diffusion problem, the derivative in (7.3.7) is evaluated *at* the singularity. This means, in particular, that analytic continuation, such as Padé approximation, will not help in this case. However, we can still apply the general method, using the construction of Theorems 1 and 2. Since we still have $\phi_\epsilon \to u_0$ in the sense of distributions according to Lemma 1, we obtain a convergent method as $\epsilon \to 0$.

Note that since the denominator of (7.3.7) does not vanish initially for $r \neq q$, we do not have to use the square-root time scaling, as in the previous case. This speeds up the computations somewhat, since the time scale is shorter than in the previous case.

Results are presented in Figures 7.4 for the American put option on a non-dividend paying stock. We take the values $r = 10\%$, $K = \$100$ and $\sigma = 20\%$ for the interest rate, the strike price, and the stock volatility, respectively. The actual calculation was performed for a call with $r = 0$ and $q = 10\%$, and then the parity formula (7.3.4) was used to find the value of the put. We chose this problem because it is probably the most studied example of an American option on one asset. It is known not to admit a closed-form solution, and several approximate solutions are available [41, 56, 99]. We compare (Figure 7.3) our computations of the optimal exercise boundary for the American put to the asymptotic solutions [23] and [41] and observe good agreement close to the expiration date of the option. Note also (Figure 7.3(b)) that asymptotical formulas break down for large t, as expected. The price of both American and European options, as well as the critical stock price and the early exercise premium, are plotted in Figure 7.4; the values of the options are given 1 year before the expiration date. Here the calculated optimal exercise price is \$86.37. Note that in this case, the structure of the early exercise premium is different from the call example in the case $r > q$: here, it reaches a constant value of about 10% of the option price soon after the option becomes in the money.

The convergence of the calculated solutions to the "exact" solution (here, the one computed using $\epsilon = 1/128$) is shown in Figure 7.5 (top curve). Note that the initial data not only contain a δ-function in this case, but are also incompatible with the boundary condition at $b(\tau)$, so the initial singularity is stronger than in the case $r > q$. However, the rate of convergence is still qualitatively the same, even though better approximations of the

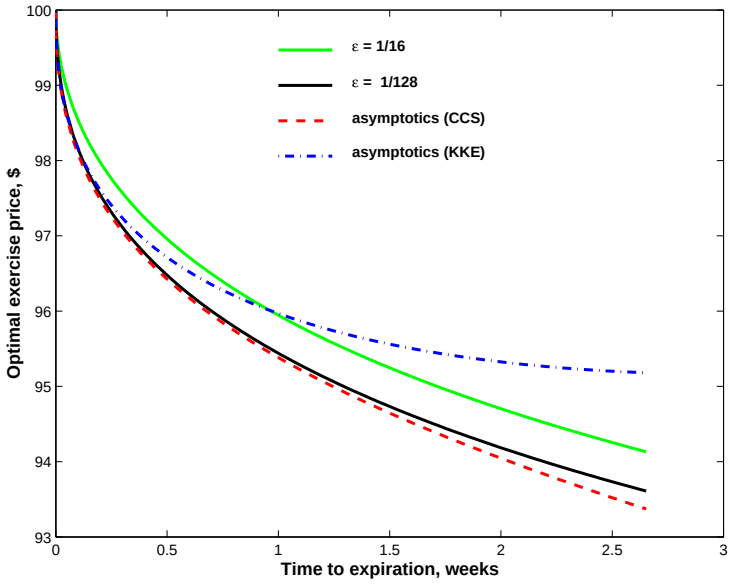

(a) Near expiry

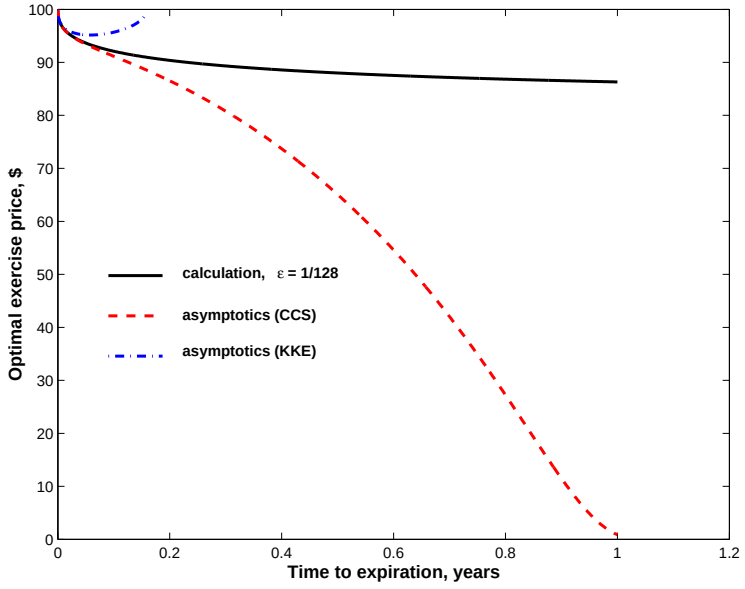

(b) Up to 1 year before expiry

Figure 7.3: Optimal exercise price for American put with $r = 0.1$, $\sigma = 0.2$, and $K = \$100$; calculations with $\epsilon = 1/16, 1/128$ compared to asymptotic formulas [41] (KKE) and [23] (CCS) .

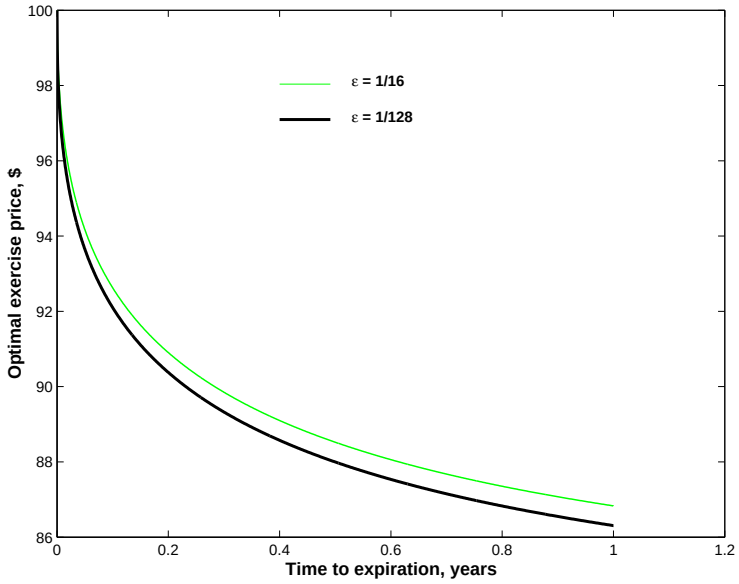

(a) Optimal exercise boundary

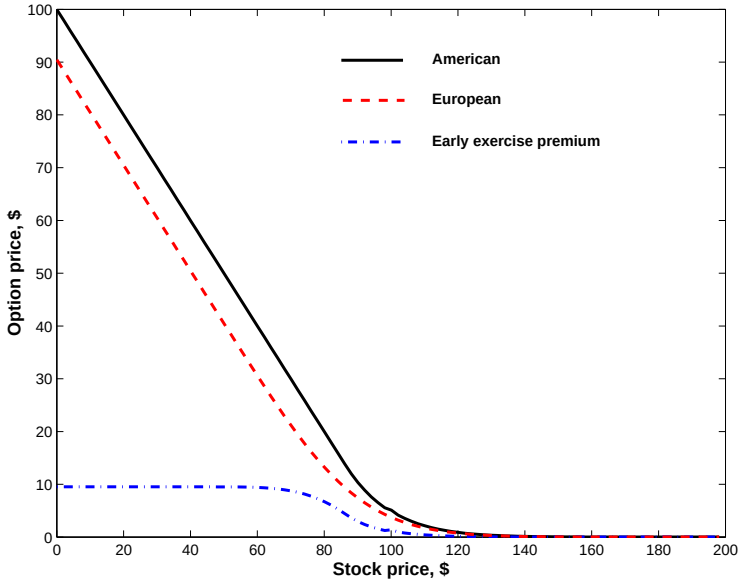

(b) American and European option prices

Figure 7.4: American vs. European puts with $r = 0.1$, $\sigma = 0.2$, and $K = \$100$, $t = 1$ year from expiry and optimal exercise boundary.

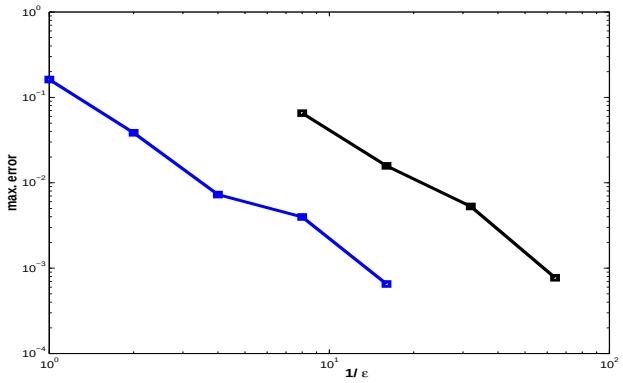

Figure 7.5: Convergence rates as $\epsilon \to 0$ for $r \leq q$ (top curve) and $r > q$ (bottom curve)

δ-function are required (i.e., smaller ϵ's in (3.4.2)) to achieve comparable accuracy levels. However, adaptive domain decomposition, with nodes initially clustered at the right end and spreading out as t increases, offsets the additional time requirement: a calculation with three correct digits in the option price takes only 4 minutes on a 700 MHz PC.

7.6 Further examples

In the preceding sections of this chapter, we presented our mathematical framework as it applies to the pricing of American options on a single stock paying a continuous dividend yield. The same approach can be used to treat more general problems which have a similar structure. One example is index options. Here the underlying is not a single stock, but an index, such as S&P 500 or FTSE 100 or Nikkei 225. Another example is foreign exchange options, i.e., options to buy or sell foreign currency at a specified exchange rate. In this case, the role of the continuous dividend yield is played by the foreign interest rate. We perform calculations for several options of these types.

Our first example is an index option on the S&P 100. This is the oldest index op-

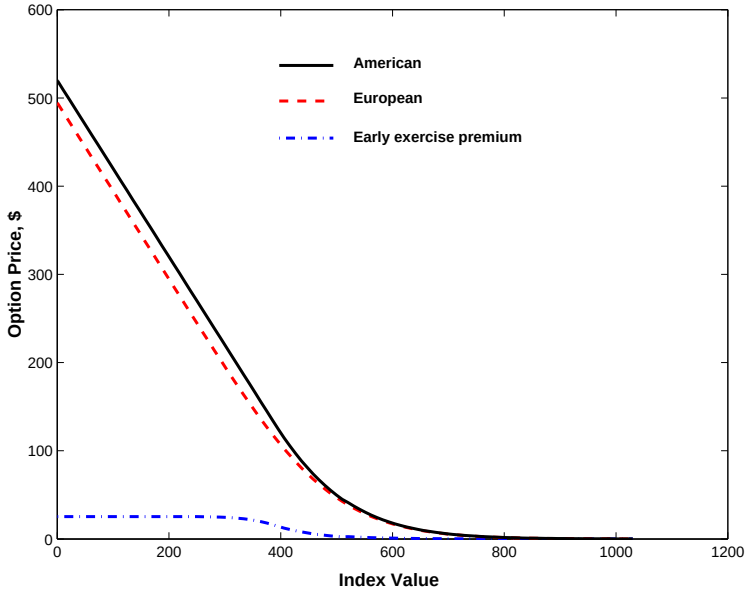

(a) American vs. European options

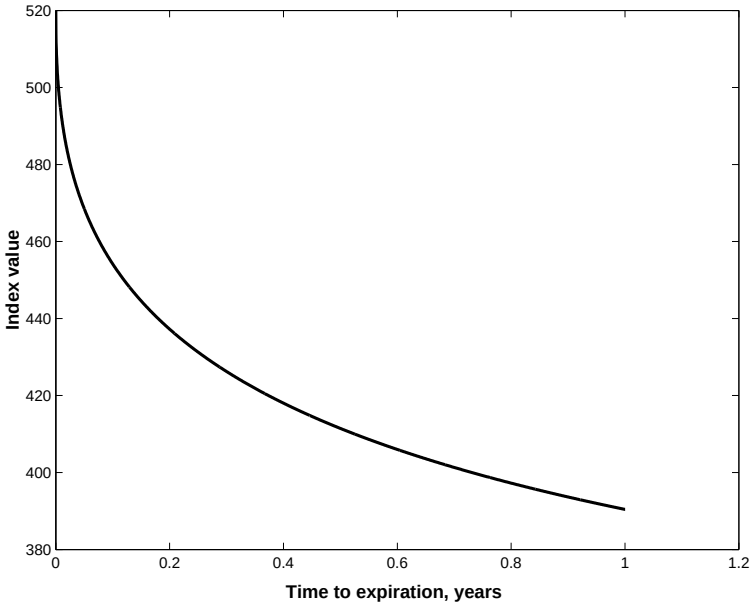

(b) Optimal exercise price

Figure 7.6: American S&P 100 put with $r = 0.05$, $\sigma = 0.25$ and $K = \$520$, 1 year from expiry.

tion traded on the Chicago Board of Options Exchange and the options written on it are American-style; therefore they are suitable for our analysis. We present numerical results for put options only, neglecting any dividend streams paid out by the constituents of the index. On May 9, 2002, the S&P 100 closed at 531.69, and we take a slightly in-the-money put with strike price $K = \$520$. We take the interest rate equal to the yield on a 10-year treasury bond, or 5%, and the volatility equal to the value of the market volatility index, or 25%.[3] We plot the results in Figure 7.6(a) for the value of the option and early exercise premium and Figure 7.6(b) for the optimal exercise boundary. The calculated value of the index, at which early exercise is optimal one year before expiration is 390.40.

Our two final examples deal with call options to buy two different currencies for US dollars. We choose the euro and the Japanese yen. The fundamental difference is in the interest rate that can be earned on these currencies: in the euro zone, it is about 3.3% and in Japan, 0.8%. Here we take one-week short rates, the analog of which in the US is currently 1.78%. Identifying $q = r_f$ for the foreign interest rate, we see that the dollar-euro call satisfies $r < r_f$, while the dollar-yen call satisfies $r > r_f$, so we have both cases here. We take the volatilities to be 9.6% for the euro and 9% for the yen, which is consistent with the numbers in the current financial press.

Results appear in Figures 7.7 and 7.8 on pages 102 and 103. The corresponding critical exercise exchange rates one year from expiration of the option are 0.816 dollars per euro and 1.90 dollars per 100 yen, respectively. Note that the early exercise premium for the yen option is extremely small, while that for the euro option is in line with the previous model calculations.

[3]On May 9, 2002, the yield on a 10-year T-bond was 5.187%, and the volatility index VIX closed at 24.36.

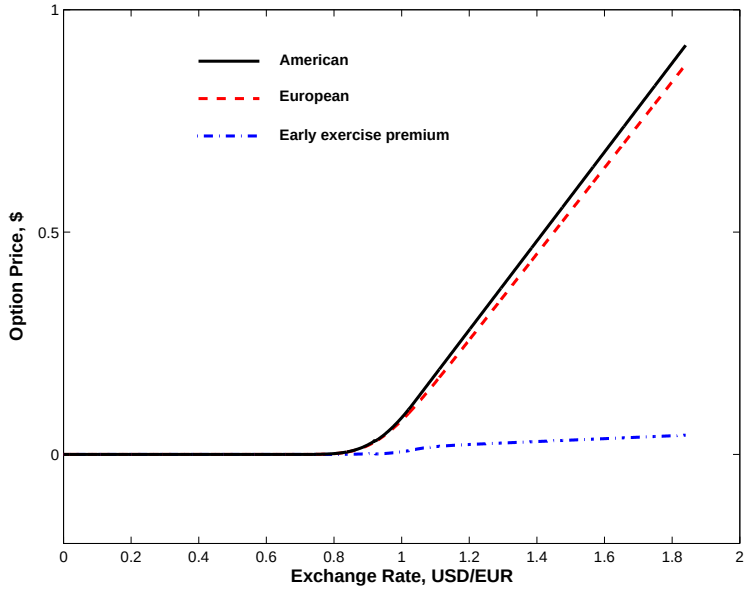

(a) American vs. European options

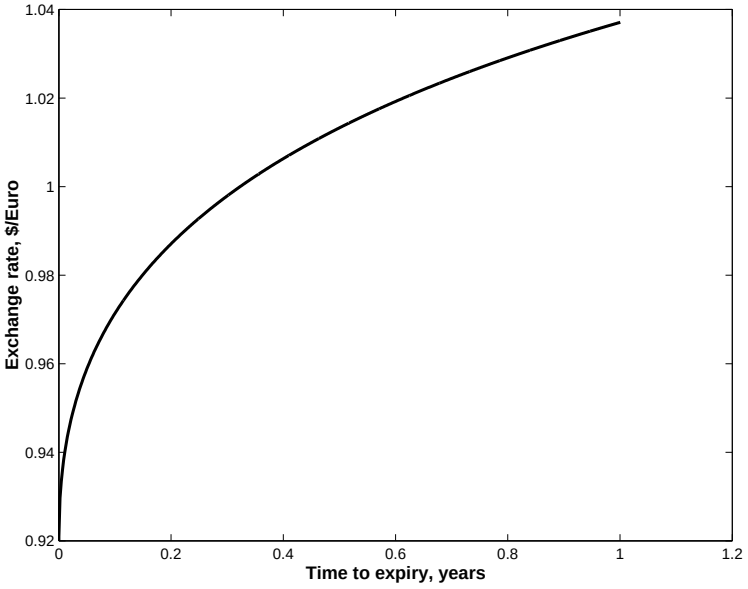

(b) Optimal exercise rate

Figure 7.7: American option to buy Euro at the exchange rate $K = 0.92$ ($ per €) within 1 year; $r = 0.018$, $r_f = 0.033$, $\sigma = 0.096$.

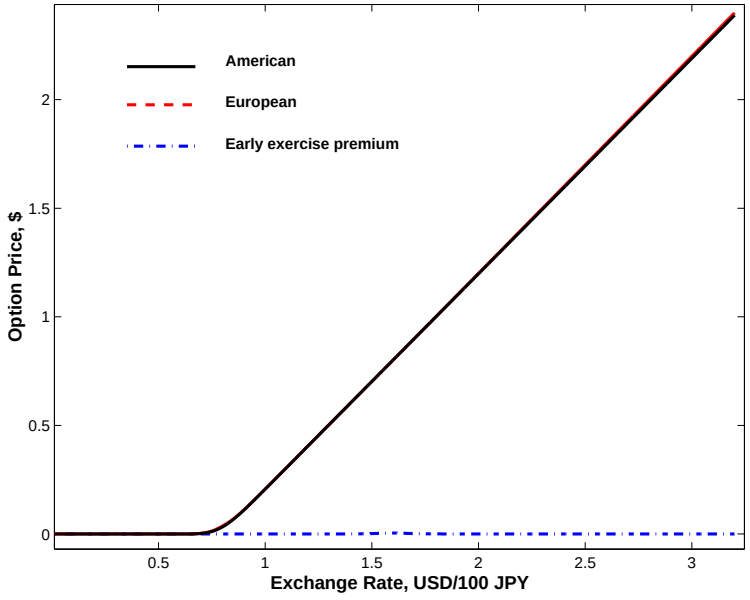

(a) American vs. European options

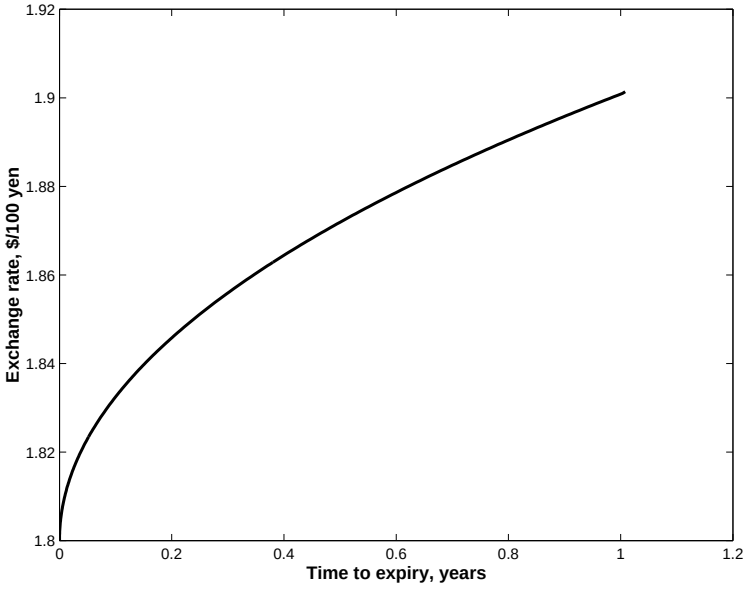

(b) Optimal exercise rate

Figure 7.8: American option to buy Japanese yen at the exchange rate $K = 0.8$ ($ per ¥ 100) within 1 year; $r = 0.018$, $r_f = 0.008$, $\sigma = 0.09$.

Chapter 8

Concluding Remarks

I hope that posterity will judge me kindly,
not only as to the things which I have explained,
but also to those which I have intentionally omitted
so as to leave to others the pleasure of discovery.
(René Descartes, 1596–1650)

8.1 Summary and conclusions

We have presented a general framework of a front-fixing method for moving boundary problems for linear parabolic equations, based on the Chebyshev expansion of solutions. Highly accurate and rapidly convergent for smooth problems, this method becomes a very powerful and robust tool in the presence of singularities, when most other techniques lose accuracy, require analytical start-off expressions (which may in many cases not exist), or, otherwise, fail altogether. The intuitively simple construction based on smooth approximations of singular initial data, introduced in this text, allows us to use the accurate spectral framework, and keep control over the convergence and the error in numerical solutions. We have proved, in the most general linear setting, the convergence of numerical solutions of approximated problems to the true solution of the original problem, as the accuracy of the approximation of the singular initial data by smooth functions increases, and have given convincing numerical evidence of the same behavior in the moving boundary case. We have provided simple modifications of the general method, relying on analytic continuation and prior integration, which allow for considerable gain in computing time for certain practical problems. We have incorporated domain decomposition into the general framework, which enhances accuracy in localized settings. The oxygen diffusion test problem was used to illustrate the power of our method in the classical framework: the theoretical predictions of quadratic convergence as

smooth data approximates singular data were verified perfectly. The approach proposed in this work, which is applicable in its full generality, compares very favorably to the existing techniques, including those which, relying on integral equation formulations, were designed specifically for the treatment of problems of a type analogous to this test problem.

In the investigation of the American option problem, we re-established an important parity result, which allowed us to formulate, classify and solve this problem from the point of view of the theory and numerical analysis of partial differential equations. Even though this approach is gaining popularity, our work is one of the very few systematic efforts to analyze this challenging finance problem from an applied mathematics angle. Our numerical method produced meaningful results both for the classical setting of one asset and for more practical examples, including index options and foreign currency options. We find the success of our general method in the treatment of these quite singular problems very encouraging indeed.

8.2 Future work

Although the general framework of the approach is established, the possibilities for further analysis and extensions are ample. We have so far focused entirely on one-phase problems, and the corresponding formulation for two-phase problems is relatively straightforward. Other boundary conditions, such as those in crystal growth models, may also be incorporated.

One important practical improvement in the accurate numerical resolution of singularities is automatic adaptive mesh refinement in space and time. This mechanism has the potential of both reducing the storage requirement and speeding up the computations. There is room for optimization in the time marching as well. Most of our computations for singular problems were performed using explicit schemes, since implicit schemes involve rather complicated nonlinear systems to be solved at each time step. We have already mentioned (see Summary in Section 2.4) the explicit methods with extended stability domains [1–3, 91] as one possible approach. Another alternative is related to the current work by O.P. Bruno and collaborators (see, e.g., [5]) on unconditionally stable explicit schemes, as it seems appropriate for the current setting.

Two- and three-dimensional problems represent another important possibility for generalization of our method. Chebyshev expansions in the radial variable, combined with peri-

odic Fourier expansions in the angular variable, are promising approaches for higher space dimensionality, especially for "star-shaped" domains (cf. [35] for fixed boundary problems and [87] for several moving boundary problems). Domain decomposition with careful patching should provide viable extensions to those domains, which can be split into several pieces of desired form. On the practical side, the partial differential equation approach is usually considered to be too cumbersome even for two-dimensional versions of the American option problem, e.g., when there are multiple assets, or one of the parameters, such as volatility or interest rate, follows its own stochastic process (see, e.g., [104]). We believe our methods have a potential to lead a change in this area, to allow for (significantly more accurate) differential equation treatments of finance problems of arbitrary space dimensionality.

Bibliography

[1] Abdulle A., "Fourth order Chebyshev methods with recurrence relation," *SIAM J. Sci. Comput.,* Vol. 6, pp. 2041–2054, 2002.

[2] Abdulle A. and Medovikov A. A., "Second order Chebyshev methods based on orthogonal polynomials," *Numer. Math.,* Vol. 90, Iss. 1, pp. 1–18, 2001.

[3] Alexiades V., Amiez G. and Gremaud P.-A., "Super-time-stepping acceleration of explicit schemes for parabolic problems," *Commun. Num. Meth. En.,* Vol. 12, Iss. 1, pp. 31–42, 1996.

[4] Alexiades V. and Solomon A. D., "Mathematical Modeling of Melting and Freezing Processes," *Washington DC: Hemisphere Publ. Co.,* 1993.

[5] Amundsen D. and Bruno O., "On explicit unconditionally-stable time stepping," in preparation.

[6] Atthey D. R., "A finite difference scheme for melting problems," *J. Inst. Maths. Applics.,* Vol. 13, pp. 353–366, 1974.

[7] Avellaneda M. and Laurence P., "Quantitative Modeling of Derivative Securities: From Theory to Practice," *CRC Press,* 1999.

[8] Bachelier L., "Théorie de la spéculation," *Ann. Sci. Ecole Norm. Sup.,* No. 17, pp. 21–86, 1900.

[9] Berger A. E., Ciment M. and Rogers J.C.W., "Numerical solution of a diffusion consumption problem with a free boundary," *SIAM J. Numer. Anal.,* Vol. 12, No. 4, pp. 646–672, 1975.

[10] Bjerksund P. and Stensland G., "American exchange options and a put-call transformation: a note," *Journal of Business, Finance and Accounting,* Vol. 20, pp. 760–764, 1993.

[11] Black F. and Scholes M., "The pricing of options and corporate liabilities," *Journal of Political Economy,* Vol. 81, pp. 637–659, 1973.

[12] Boley B. A., "A method of heat conduction analysis of melting and solidification problems," *J. Math. Phys.,* Vol. 40, pp. 300–313, 1961.

[13] Bonnerot R. and Jamet P., "A second order finite element method for the one dimensional Stefan problem," *Int. J. Numer. Meth. Eng.,* Vol. 8, pp. 811-820, 1974.

[14] Bonnerot R. and Jamet P., "A third order accurate discontinuous finite element method for the one dimensional Stefan problem," *J. Comput. Phys.,* Vol. 32, pp. 145–167, 1979.

[15] Bossaerts P.L., private communication.

[16] Boyd J. P., "Chebyshev and Fourier Spectral Methods," *New York: Dover,* 1998 (2nd ed.).

[17] Brattkus K. and Meiron D. I., "Numerical simulations of unsteady crystal growth," *SIAM J. Appl. Math.,* Vol. 52, No. 5, pp. 1303–1320, 1992.

[18] Brennan M. and Schwartz E., "The valuation of American put options," *Journal of Finance,* Vol. 32, pp. 449–462, 1977.

[19] Broadie M. and Detemple J. B., "Recent advances in numerical methods for pricing Derivative Securities," *CIRANO Scientific Publications,* May 1996.

[20] Canuto C., Hussaini M. Y., Quarteroni A. and Zang T. A. "Spectral Methods in Fluid Dynamics," *Berlin, Heidelberg: Springer-Verlag,* 1988.

[21] Carr P. and Chesney M., "American Put Call Symmetry," working paper, Morgan Stanley & Groupe H.E.C., 1996.

[22] Chen S., Merriman B., Osher S., Smereka P., "A simple level set method for solving Stefan problems," *J. Comput. Phys.,* Vol. 135(1), pp. 8–29, 1997.

[23] Chen X., Chadam J. and Stamicar R., "The optimal exercise boundary for American put options: analytic and numerical approximations," preprint, 2000.

[24] Chernous'ko F. L., "Solution of nonlinear heat-conduction problems in a medium with phase transitions," *Int. Chem. Eng.,* Vol. 10, No. 1, pp. 42–48, 1970 – translated from Черноусько Ф.Л., "Решение нелинейных задач теплопроводности в среде с фазовыми переходами," *Журн. Прикл. Мех. и Техн. Физ.,* т. 10, N. 2, pp. 6–14, 1969.

[25] Coddington E. A. and Levinson N., "Theory of Ordinary Differential Equations," *New York: McGraw-Hill,* 1955.

[26] Courtault J.-M., Kabanov Y., Bru B., Crépel P., Lebon I. and Le Marchand A., "Louis Bachelier. On the centenary of *Théorie de la Spéculation*," *Math. Fin.,* Vol. 10, No. 3, pp. 341–353, 2000.

[27] Crank J., "Free and Moving Boundary Problems," *New York: Clarendon Press,* 1984.

[28] Crank J. and Crowley A. B., "Isotherm migration along orthogonal flow lines in two dimensions," *Int. J. Heat Mass Transfer,* Vol. 21, pp. 393–398, 1978.

[29] Crank J. and Gupta R. S., "A moving boundary problem arising from the diffusion of oxygen in absorbing tissue," *J. Inst. Maths Applics,* Vol. 10, pp. 19–33, 1972.

[30] Crank J. and Gupta R. S., "A method for solving moving boundary problems in heat flow using cubic splines or polynomials," *J. Inst. Maths Applics,* Vol. 10, pp. 296–304, 1972.

[31] Crank J. and Gupta R. S., "Isotherm migration in two dimensions," *Int. J. Heat Mass Transfer,* Vol. 18, pp. 1101–1107, 1975.

[32] Crowley A. B., " On the weak solution of moving boundary problems," *J. Inst. Maths Applics.,* Vol. 24, pp. 43–57, 1979.

[33] Cryer C. W., "The solution of a quadratic programming problem using systematic overrelaxation," *SIAM Journal of Control,* Vol. 9, pp. 385–392, 1971.

[34] Dahmardah H. O. and Mayers D. F., "A Fourier-series solution of the Crank-Gupta equation," *IMA Journal of Numerical Analysis,* Vol. 3, pp. 81–85, 1983.

[35] Dew P. M. and Scraton R. E., "The solution of the heat equation in two space variables using Chebyshev series," *J. Inst. Maths Applics.,* Vol. 11, pp. 231–240, 1973.

[36] Dewynne J. N., Howison S. D., Rupf I. and Wilmott P., "Some mathematical results in the pricing of American options," *Euro. Jnl. Applied Mathematics,* Vol. 4, pp. 381–398, 1993.

[37] Douglas J. and Gallie T. M., "On the numerical integration of a parabolic differential equation subject to a moving boundary condition," *Duke Math. J.,* Vol. 22, pp. 557-570, 1955.

[38] Duvaut G. and Lions J. L., "Inequalities in Mechanics and Physics," *Berlin-Heidelberg-New York: Springer,* 1976 – translated from "Les inéquations en mécanique et en physique," *Paris: Dunod,* 1972.

[39] Elliott C. M. and Ockendon J. R., "Weak and Variational Methods for Moving Boundary Problems," *London: Pitman,* 1982.

[40] Evans II G. W., Isaacson E. and Donald J. K. L, "Stefan-like problems," *Quart. Appl. Math.,* Vol. 8, pp. 185–193, 1950.

[41] Evans J. D., Kuske R. A. and Keller J. B., "American options with dividends near expiry," *Mathematical Finance,* to appear.

[42] Ferris D. H. and Hill S., "On the numerical solution of a one-dimensional diffusion problem with a moving boundary," *NPL Report NAC 45,* 1974.

[43] Friedman A., "Partial Differential Equations of Parabolic Type," *New Jersey: Prentice Hall,* 1964.

[44] Friedman A., "Variational Principles and Free-Boundary Problems," *New York: Wiley,* 1982.

[45] Furzeland R. M., "A comparative study of numerical methods for moving boundary problems," *J. Inst. Maths Applics,* Vol. 26, pp. 411–429, 1980.

[46] Geske R. and Johnson H., "The American put valued analytically," *Journal of Finance,* Vol. 39, pp. 1511–1524, 1984.

[47] Goodman T. R., "The heat-balance integral and its application to problems involving a change of phase," *Trans. ASME,* Vol. 80, pp. 335-342, 1958.

[48] Goodman J. and Ostrov D. N., "On the early exercise boundary of the American put option," preprint, 2000.

[49] Gottlieb D. and Orszag S. A., "Numerical Analysis of Spectral Methods: Theory and Applications," *Philadelphia: SIAM-CBMS,* 1977.

[50] Gupta R. S. and Kumar D., "Complete numerical solution of the oxygen diffusion problem involving a moving boundary," *Comput. Meth. Appl. Mech. Eng.,* Vol. 29, pp. 233–239, 1981.

[51] Hansen E. and Hougaard P., "On a moving boundary problem from biomechanics," *J. Inst. Maths Applics,* Vol. 13, pp. 385–398, 1974.

[52] Hull J., "Options, Futures and Other Derivatives," *New Jersey: Prentice Hall*, 2000 (4th ed.).

[53] Jaillet P., Lamberton D. and Lapeyre B., "Variational inequalities and the pricing of American options," *Acta Applicandae Mathematicae,* Vol. 21, pp. 263–289, 1990.

[54] Kamenomostskaja S. L., "On the Stefan problem," *Mat. Sb.,* Vol. 53(95), pp. 498–514, (in Russian) – Каменомостская С.Л., "О задаче Стефана," *Математический Сборник,* Т. 53(95), N. 4, 1961.

[55] Karatzas I. and Shreve S. E., "Methods of Mathematical Finance," *New York: Springer,* 1998.

[56] Kim I. J., "The analytic valuation of American options,", *Review of Financial Studies,* Vol. 3,pp. 547–572, 1990.

[57] Knibb D. and Scraton R. E., "On the solution of parabolic partial differential equations in Chebyshev series," *Computer Journal,* Vol. 14, pp. 428–432, 1971.

[58] Knibb D. and Scraton R. E., "A collocation method for the numerical solution of non-linear parabolic partial differential equations," *J. Inst. Maths Applics.,* Vol. 22, pp. 305–315, 1978.

[59] Koo M.-H. and Leap D. I., "Modeling three-dimensional groundwater flows by the body-fitted Coordinate (BFC) method: II. Free and moving boundary problems," *Transport in Porous Media,"* Vol. 30, pp. 345–362, 1998.

[60] Kuske R. A. and Keller J. B., "Optimal exercise boundary for an American put option," *Applied Mathematical Finance,"* Vol. 5, pp. 107-116, 1998.

[61] Lamé G. and Clapeyron B. P. E., "Mémoire sur la solidification par refroidissement d'un globe solide," *Ann. Chem. Phys.,* Vol. 47, pp. 250–256, 1831.

[62] Landau H. G., "Heat conduction in a melting solid," *Quart. Appl. Math.,* Vol. 8, pp. 81–94, 1950.

[63] Lazaridis A., "A numerical solution of the multidimensional solidification (or melting) problem," *Int. J. Heat Mass Transfer,* Vol. 13, pp. 1459–1477, 1970.

[64] Li-Shang J., "Existence and differentiability of the solution of a two-phase Stefan problem for quasilinear parabolic equations," *Acta Mathematica Sinica,* Vol. 15, pp. 749–764, 1965.

[65] Little T., Pant V. and Hou C., "A new integral representation of the early exercise boundary for American put options," preprint, 1998.

[66] Longstaff F. A. and Schwartz E. S., "Valuing American options by simulation: a simple least-squares approach," *Review of Financial Studies,* Vol. 14, No. 1, pp. 113–147, 2001.

[67] McDonald R. L. and Schroder M. D., "A parity result for American options," *Journal of Computational Finance,* Vol. 1, No. 3, pp. 5–13, 1998.

[68] McKean H. P., Jr., "Appendix: A free boundary problem for the heat equation arising from a problem in mathematical economics," *Industrial Management Review,* Vol. 6, pp. 32–39, 1965.

[69] Meirmanov A. M., "The Stefan Problem," *Berlin; New York: Walter de Gruyter,* 1992 – translated from Мейрманов А.М., "Задача Стефана," *Новосибирск: Наука,* 1986.

[70] Merton R., "Theory of rational option pricing," *Bell Journal of Economics and Management Science,* Vol. 4, pp. 141–183, 1973.

[71] Meyer G. H., "One-dimensional parabolic free boundary problems," *SIAM Review,* Vol. 19, No. 1, pp. 17–34, 1977.

[72] Meyer G. H., "An alternating direction method for multidimesional parabolic free surface problems," *Int. J. Num. Meth. Eng.,* Vol. 11, pp. 741–752, 1977.

[73] Meyer G. H., "An application of the method of lines to multidimensional free boundary problems," *J. Inst. Maths Applics.,* Vol. 20, pp. 317–329, 1977.

[74] Miller J. V., Morton K. W. and Baines M. J., "A finite element moving boundary computation with an adaptive mesh," *J. Inst. Maths Applics.,* Vol. 22, pp. 467–477, 1978.

[75] Mitrović D. and Žubrinić D., "Fundamentals of Applied Functional Analysis," *Pitman Mons. and Survs. in Pure and Appl. Math.,* Vol. 91, Longman, 1998.

[76] Moiseenko B. D. and Samarskii A. A., "An economic continuous calculation scheme for the Stefan multidimensional problem," *U.S.S.R. Comput. Math. and Math. Phys.,* Vol. 5, No. 5, pp. 43–58 – translated from Моисеенко Б.Д., Самарский А.А., "Экономичная схема сквозного счета для многомерной задачи Стефана," *Журн. выч. мат. и мат. физ.,* т. 5, N. 5, pp. 816–827, 1965.

[77] Murray W. D. and Landis F., "Numerical and machine solutions of transient heat-conduction problems involving melting or freezing. Part I – method of analysis and sample solutions," *J. Heat Transfer, Trans. ASME,* Vol. 81, pp. 106–112, 1959.

[78] Musiela M. and Rutkowski M., "Martingale Methods in Financial Modelling," *Berlin; New York : Springer,* 1998.

[79] Neftci S., "Introduction to Mathematics of Financial Derivatives," *New York: Academic Press,* 1996.

[80] Ockendon J. R. and Hodgkins W. R. (eds.) "Moving Boundary Problems in Heat Flow and Diffusion," *Oxford: Clarendon Press,* 1975.

[81] Oleinik O. A., "A method of solution of the general Stefan problem," *Soviet Math. Dokl.,* Vol. 1, pp. 1350–1354 – translated from Олейник О.А., "Об одном методе решения общей задачи Стефана," *Доклады АН СССР,* т. 135, стр. 1054–1057, 1960.

[82] Revuz D. and Yor M., "Continuous Martingales and Brownian Motion," *Berlin, New York: Springer-Verlag,* 1994 (2nd ed.).

[83] Rogers L. C. G. and Talay D. (eds.), "Numerical Methods in Finance ," *Cambridge University Press,* 1997.

[84] Royden H. L., "Real Analysis," *New York: Macmillan,* 1988 (3rd ed.).

[85] Rubinshtein L. I., "The Stefan Problem," *Transl. Math. Mon.,* Vol. 27, Providence, 1971 – translated from Рубинштейн Л.И., "Проблема Стефана," *Рига: Звайгзне,* 1967.

[86] Sackett G. G., "Numerical solution of a parabolic free boundary problem arising in statistical decision theory," *Math. Comp.,* Vol. 25, No. 115, pp. 425–434, 1971.

[87] Saitoh T., "Numerical method for multi-dimesional freezing problems in arbitrary domains," *Journal of Heat Transfer,* Vol. 100, pp. 294–299, 1978.

[88] Schatz A., "Free boundary problems of Stefan type with prescribed flux," *J. Math. Anal. Appl.,* Vol. 28, pp. 569–580, 1969.

[89] Sethian J. A. and Strain J., "Crystal growth and dendritic solidification," *J. Comput. Phys.,* Vol. 98, pp. 231–253, 1992.

[90] Shastri S. S. and Allen R. M., "Method of lines and enthalpy method for solving moving boundary problems," *Int. Comm. Heat Mass Transfer,* Vol. 25, No. 4, pp. 531–540, 1998.

[91] Sommeijer B. P., Shampine L. F. and Verwer J. G., "RKC: an explicit solver for parabolic PDEs," *J. Comput. Appl. Math,* Vol. 88, pp. 316–326, 1998.

[92] Spall R., "Spectral collocation methods for one-dimensional phase-change problems," *Int. J. Heat Mass Transfer,* Vol. 38, No. 15, pp. 2743–2748, 1995.

[93] Stefan J., "Über einige Probleme der Theorie der Wärmeleitung," *S.-B. Wien. Akad. Mat. Natur.,* Vol. 98, pp. 173–484, 1889.

[94] Stefan J., "Über die Theorie der Eisbildung insbesondere über die Eisbildung im Polarmeere," *S.-B. Wien. Akad. Mat. Natur.,* Vol. 98, pp. 965–983, 1889.

[95] Tarzia D. A. "A Bibliography on moving-free boundary problems for the heat-diffusion equation. The Stefan and Related Problems," *MAT-Serie A, Universidad Austral,* #2, 2000.

[96] Thompson J. F., Warsi Z. U. and Mastin C. W., "Boundary-fitted coordinate systems for numerical solution of partial differential equations - a review," *J. Comput. Phys.,* Vol. 47, pp. 1–108, 1982.

[97] Van Moerbke P., "On optimal stopping and free boundary problems," *Archive of Rational Mechanics and Analysis,* Vol. 60, pp. 101–148, 1976.

[98] Voller V. R. and Cross M., "Accurate solutions of moving boundary problems using the enthalpy method," *Int. J. Heat Mass Transfer,* Vol. 24, pp. 545–556, 1981.

[99] Wilmott P., Howison S. and Dewynne J., "The Mathematics of Financial Derivatives. A Student Introduction," *Cambridge University Press,* 1997.

[100] Wilmott P., "Derivatives: The Theory and Practice of Financial Engineering," *John Wiley & Sons,* 1998.

[101] Zerroukat M. and Chatwin C. R., "Computational Moving Boundary Problems," *New York: Wiley,* 1994.

[102] Zerroukat M. and Chatwin C. R., "Explicit variable time-step method for implicit moving boundary problems," *Comm. Num. Meth. Eng.,* Vol. 10, No. 3, pp. 227-235, 1994.

[103] Zorich V. A., "Mathematical Analysis," Vol. 2, *Moscow: MCNMO,* (2nd ed.) (in Russian) – Зорич В.А., "Математический анализ," т. 2, *Москва: МЦНМО,* изд. 2, 1998.

[104] Zvan R., Forsyth P. A. and Vetzal K. R., "Penalty methods for American options with stochastic volatility," *J. Comput. Appl. Math.,* Vol. 91, pp. 199–218, 1998.